Detecting Sybil Attack by Using Received Signal Strength in Manets

K. Kayalvizhi[1], N. Senthilkumar [2], G. Arulkumaran [3]
[1] PG Scholar, Vivekanandha College of Engineering for Women.
[2,3] Assistant Professor, Vivekanandha College of Engineering for Women
Tiruchengode, India
Kayalvizhi07@gmail.com

Abstract— **Fully self-organized mobile ad hoc networks (MANETs) represent complex spread systems that may also be part of a huge complex system, such as a complex system-of-systems used for crisis management operations. Due to the complex nature of MANETs and its resource constraint nodes, there has always been a need to develop lightweight security solutions. Since MANETs require a unique discrete and persistent identity per node in order for their security protocols to be viable, Sybil attacks pose a serious threat to such networks. A Sybil attacker can either create more than one identity on a single physical device in order to launch a synchronized attack on the network or can switch identities in order to weaken the detection process, thereby promoting lack of responsibility in the network. In this research, we propose a lightweight scheme to detect the new identities of Sybil attackers without using centralized trusted third party or any additional hardware, such as directional antennae or a geographical positioning system. Through the help of wide simulations and real-world test bed experiments, we are able to demonstrate that our proposed scheme detects Sybil identities with good precision even in the presence of mobility.**

Keywords – Sybil attacks, Mobile Adhoc Network, Detection.

I. INTRODUCTION

The Mobile ad hoc networks (MANETs) have attracted a lot of attentions due to their interesting and promising functionalities including mobile safety, traffic congestion avoidance, and location based services. This project focus on safety driving application, where each vehicle periodically broadcasts messages including its current position, direction and velocity, as well as road information. Privacy is an important issue in MANETs. As the wireless communication channel is a shared medium, exchanging messages without any security protection over the air can easily leak the information that users may want to keep private. Pseudonym based schemes have been proposed to preserve the location privacy of mobile. However, those schemes require the mobile to store a large number of pseudonyms and certifications, and do not support some important secure functionality such as authentication and integrity.

The centralized key management has some disadvantages. For instance, the system maintenance is not flexible. Another issue regarding the centralized key management is that many existing schemes assume a tamper-proof device being installed in each vehicle. The tamper-proof device normally costs several thousand dollars. The framework to be developed in this paper does not require the expensive tamper-proof device. Here the technique used and develop a secure distributed key management framework. In my framework, the road side units are responsible for secure group private keys distribution in a localized manner. When a vehicle approaches an, it gets the group private key from the RSU dynamically. All mobile which get the group private key from the same RSU form a group. A new issue induced by the distributed key management framework is that compromised RSUs may misbehave in the key distribution procedure.

SCOPE:

A compromised may deliver other mobile group private keys to its accomplice. Then, the accomplice can send messages under the name of other mobile. Therefore develop security protocols for the distributed key management framework, which are capable of detecting the compromised RSUs and their collusion with the

malicious mobile if any. Computation overhead is another critical issue in MANETs. In the safety driving application, mobile broadcast safety messages. Since the group signature is expensive, the computation overhead of each vehicle will become intolerable when the density of mobile is high the authors propose a promising protocol which let mobile verify messages cooperatively by employing probabilistic verification.

However, in order to guarantee efficient cooperation, mobile have to verify at least twenty-five messages within 300ms which is still a heavy computation burden for the on-board unit (OBU) installed on a vehicle. In addition, the impact of packet loss at the medium access control (MAC) layer on security performance is not investigated. In this proposal recommend a more efficient and practical Cooperative message authentication protocol (CMAP) with an assumption that each safety message carries the location information of the sender vehicle (which can be generated by a global positioning system (GPS) device).

SYBIL ATTACKS

Ad hoc network is composed of mobile, wireless devices, referred to as nodes those communicate only over a shared broadcast channel. An advantage of such a network is that no fixed infrastructure is required: a network for routing data can be formed from whatever nodes are available. Nodes forward messages for each other to provide connectivity to nodes outside direct broadcast range. Each node needs a unique address to participate in the routing. Often addresses are assigned as an IP addresses or a unique media access channel (MAC) address. Because all communications are conducted over the broadcast channel, nothing but these identifiers is available to determine what nodes are present in the network.

DETECTING THE SYBIL ATTACK

In the mobile environment, a single entity impersonating multiple identities has an important constraint that can be detected: because all identities are part of the same physical device, they must move in unison, while independent nodes are free to move at will. As nodes move geographically, all the Sybil identities will appear or disappear simultaneously as the attacker moves in and out of range. Assuming an attacker uses a single-channel radio, multiple Sybil identities must transmit serially, whereas multiple independent nodes can transmit in parallel. The identities established by a Sybil attacker whether represented by IP addresses, MAC addresses, or public keys differ from those of an honest node in several ways. Because the resources of a single node are used to simulate multiple identities, any particular assumed identity is resource constrained in computation, storage, or bandwidth.

II. DETECTION OF SYBIL IDENTITIES

A. Attack model

There are two flavors of Sybil attacks. In the first one, an attacker creates new identity while discarding its previously created one; hence only one identity of the attacker is up at a time in the network. This is also called a join-and-leave or whitewashing attack and the motivation is to clean-out any bad history of malicious activities. This attack potentially promotes lack of accountability in the network. In the second type of Sybil attack, an attacker concurrently uses all its identities for an attack, called simultaneous Sybil attack. The motivations of this attack is to cause disruption in the network or try to gain more resources, information, access, etc. than that of a single node deserves in a network.

In our scheme, we will consider both types of Sybil attacks. The strategy of our detection mechanism is to detect every new identity created by a Sybil attacker; it does not matter if the intention of the attacker is to use that identity for whitewashing or simultaneous Sybil attacks. Hence, in this paper, we will refer to the new Sybil identity and whitewash identity (WID) interchangeably.

We assume that the attacker joins the network with its single identity, and that malicious nodes do not collude with one another. We also assume that nodes do not increase or decrease their transmit power. The attackers can get identities by two ways. First, they can fabricate identities (for example, creating an arbitrary identifier). Second, they can use stolen identities, i.e., spoof the identities of legitimate nodes (masquerading) in the network. We assume the first case where nodes can create arbitrary identifiers because in MANETs, there are no restrictions on identity creation.

B. Signal Strength Based Analysis

The distinction between a new legitimate node and a new Sybil identity can be made based on their neighborhood joining behavior. For example, new legitimate nodes become neighbors as soon as they enter inside the radio range of other nodes; hence their *first* RSS at the receiver node will be low enough. In contrast a Sybil attacker, which is already a neighbor, will cause its new identity to appear abruptly in the neighborhood. When the Sybil attacker creates new identity, the signal strength of that identity will be high enough to be distinguished from the newly joined neighbor. In order to analyze the difference between a legitimate newcomer and Sybil identity entrance behavior, we setup some experiments in the following. Before we start, it is important to explain how each node collects and maintains the RSS values of the neighboring nodes.

Each node maintains a list of neighbors in the form<Address, Rss-List <time, rss>>, as shown in Table I, and records the RSS values of any directly received or overheard frames of 802.11 protocol, i.e., RTS, CTS, DATA, and ACK messages. In other words, each node will capture and store the signal strength of the transmissions received from its neighboring nodes. This can be performed when a node either takes part in the communication directly with other nodes acting as a source or a destination or when a node does not take part in the direct communication. In the latter case it will capture the signal strength values of other communicating parties through overhearing the control frames. Each RSS- List in front of the corresponding address contains R_n RSS values of recently received frames along with their time of reception, T_n . Where n is the number of elements in the RSS - List that can be increased or decreased depending upon the memory requirements of a node. In our simulation, we used n to be five elements; however, for real-world scenarios, it should be greater than that because of the time varying nature of RSS.

III. PROPOSED SYSTEM

The proposed system considers both types of Sybil attacks. The strategy of our detection mechanism is to detect every new identity created by a Sybil attacker; it does not matter if the intention of the attacker is to use that identity for whitewashing or simultaneous Sybil attacks. Hence, in this paper, I will refer to the new Sybil identity and whitewash identity (WID) interchangeably. I assume that the attacker joins the network with its single identity, and that malicious nodes do not collude with one another. I also assume that nodes do not increase or decrease their transmit power. The attackers can get identities by two ways. First, they can fabricate identities (for example, creating an arbitrary identifier). Second, they can use stolen identities, i.e., spoof the identities of legitimate nodes (masquerading) in the network. I assume the first case where nodes can create arbitrary identifiers because in MANETs, there are no restrictions on identity creation.

In the following experiment, we plot the RSS of nodes in order to determine and visualize the behavior of the new legitimate nodes and the Sybil attackers' new identities.

Table 1 Neighbor list based on RSS

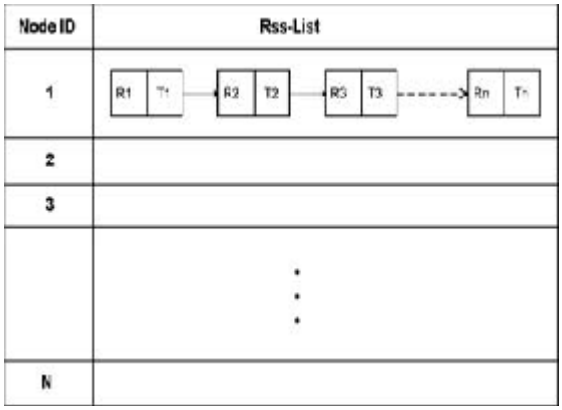

Attack Model

There are two flavors of Sybil attacks. In the first one, an attacker creates new identity while discarding its previously created one; hence only one identity of the attacker is up at a time in the network. This is also called a join-and-leave or whitewashing attack and the motivation is to clean-out any bad history of malicious activities. This attack potentially promotes lack of accountability in the network. In the second type of Sybil attack, an attacker concurrently uses all its identities for an attack, called simultaneous Sybil attack. The motivations of this attack is to cause disruption in the network or try to gain more resources, information, access, etc. than that of a single node deserves in a network. In our scheme, we will consider both types of Sybil attacks. The strategy of my detection mechanism is to detect every new identity created by a Sybil attacker; it does not matter if the intention of the attacker is to use that identity for whitewashing or simultaneous Sybil attacks.

1) *Experiment 1:* This experiment is designed to allow us to compare the behavior of new legitimate nodes with new Sybil identities. As shown in Fig. 1(a), When a new node *B* enters into another node *A*'s neighborhood or radio range, node *B* gradually enters over time. This is the natural behavior of nodes entering into one another's radio ranges and becoming neighbors in mobile environments. Due to this natural behavior of entrance and exit, when node *A* stays static and node *B* entering into *A*'s radio range with speed *s*, node *A* will observe its RSS continuously increasing. When *A* plots *B*'s RSS readings, *B* moves toward *A* and then ultimately goes out of range on the other side, assuming that *B* is continually communicating with another node *C* or *A*. In graphical form, the RSS of *B* will produce more or less a complete elliptic curve, as shown in Fig. 2. The diagram shows RSS plots for several arbitrary nodes in a random mobile scenario (this is taken from our simulation work presented in Section VI). The interesting characteristic of these plots is that the curve for each legitimate new node starts from the smallest readable RSS value (in an ideal situation), in this case it is good identity (GID) 17 indicating that GID 17 entered into 36 node's radio range normally. Whereas Sybil identities start from higher RSS values, such as WID 6 and 8 indicating that WID 6 and WID 8 did not enter normally into radio ranges of node 36 and node 21, respectively. So it can be deduced that these identities are the whitewashed one and their previous identities were roaming deep inside the radio ranges of the receivers, i.e., 36 and 21.

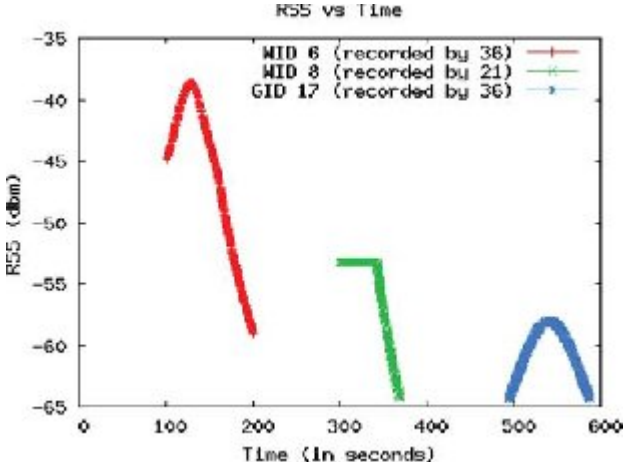

Fig. 1. Plots of three arbitrary nodes' RSS values.

This smallest readable RSS value could be used as a de- tection threshold; however mobility and velocity make things more complicated. For example, the common questions which may arise are, when *A* will receive *B*'s first RSS value and at that particular moment, what would be the location of *B* inside *A*'s radio range? The answer to both of these questions is that it depends on the speed and transmission rate of node *B*. Node with lower transmission rates can penetrate more into the radio ranges before their presence being acknowledged. In other words, the greater the transmission rate of the nodes the sooner (and close to the boundary of radio range) their presence will be acknowledged and vice versa. The greater the speed of *B*, the farther it will penetrate into the radio range of *A* before *A* acknowledges the presence of *B*. In order to refine our detection threshold, we conduct further experiments for speed.

We do not conduct experiment for transmission rate because our aim here is to demonstrate, at what distance node *B* is first acknowledged. This could potentially be affected by speed and transmission rate. We can get our aim by using speed and keeping transmission rate constant (or vice versa).

2) *Experiment 2:* We conducted this experiment in order to establish how far node *B* penetrates into node *A*'s radio range before *A* acknowledges *B*'s presence. For this purpose, we simulate the same scenario as shown in Fig. 1(a) using NS-2.30. First, *A* establishes a connection with *B*, where both the nodes are static. Then, *B* starts moving in the outward direction at a speed of 2 m/s speed until it goes out of range. After taking a pause, node *B* starts moving toward its original location with four different speeds, i.e., 2, 4, 10, and 15 m/s. The resulting RSS values received at node *A* can be seen in Fig. 3.

It is evident from the graphs that the greater the incoming speed of *B*, the greater the first RSS value of *B* that will be received by *A*. In other words, as the incoming speed of *B* increases, it penetrates deeper into *A*'s radio range before *A* acknowledges its presence. Hence, the first presence or RSS signal varies with speed for constant packet transmission rate.

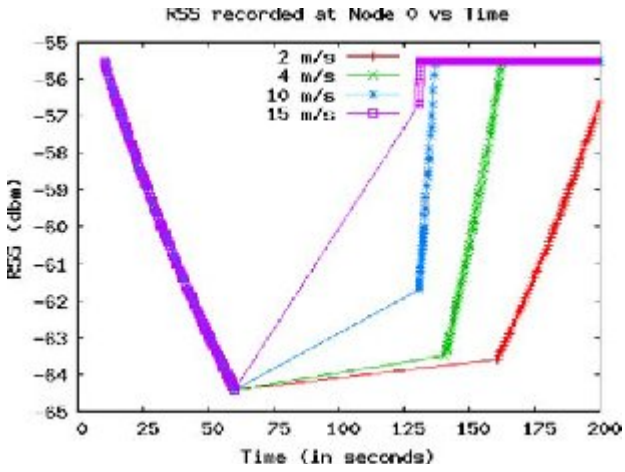

Fig. 2. Determining node presence with respect to different speeds.

IV. TUNING THE THRESHOLD

The main difference we found between the results obtained from our simulations and from our test bed experiments is the variation in RSS values. As RSS varies, for a node *B* at a fixed distance *d* from a node *A*, the receiving node *A* can receive multiple different RSS values in the fluctuation range $[-v, +v]$ (assuming $+v$ is greater than $-v$) and hence these values do not represent an *exact* indication of distance. The detection threshold will be affected when it works based on a single RSS value. For example, node *A* can receive RSS from *B* at any particular time while *B* is a good node just outside the white zone of *A* with $+v$ variance, the position of *B* can be shown in Fig. 13(a). As a result, due to the $+v$ variation in the RSS, *A* will consider *B* to be a new identity emerged in its white zone, and hence node *B* will incorrectly be detected as a Sybil identity. As shown in Fig. 13(b), another case can occur when node *B* is a whitewasher in the white zone near the boundary performs a whitewash, however, due to the variations in signal strength node *A* might receive RSS with $-v$ variation, considering it a signal coming from its gray zone and hence will consider *B* as a good node. One way of mitigating the effect of this variation is to base our detection on an average RSS across *n* values (moving average), instead of basing our detection on a single RSS value. Before we tune the threshold, it is important to determine the real –world fluctuation in RSS. For this purpose, we conducted a test bed experiment using Sun SPOT.

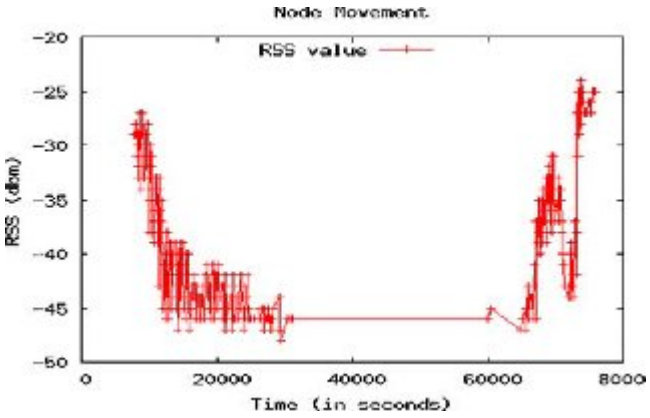

Fig. 3. Using robot, node movement with same in/out speed.

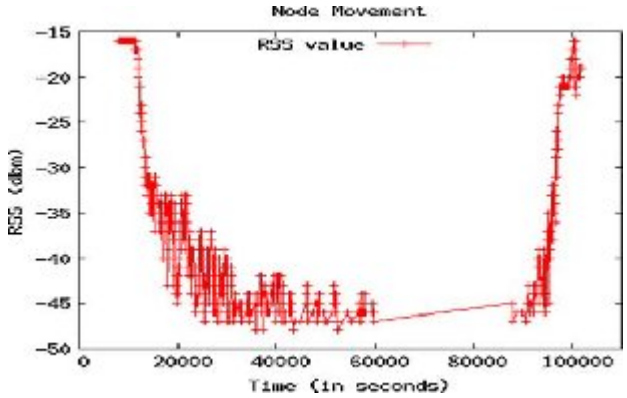

Fig.4. Using robot, node movement with different in/out speed.

We will tune our detection threshold based on the speed and variation of the RSS values. This threshold logically partitions the radio range into white and gray zones: greater (or equal) signal strength than the threshold means the signal is emanating from the white zone and from the gray zone otherwise. Let node *B* be approaching node *A*'s radio range with velocity *s* (m s−1), assuming that *d*b is the boundary of *A*'s radio range (in meters), _*t* is the time (in seconds) between two packet transmissions and *dv* is the inaccuracy in distance caused by *v* (in meters), where *v* is the variation in the RSS in the range of [−*v*, +*v*]. We assume for the sake of simplicity that just before the boundary, *B* transmits a packet which is not captured by *A*.

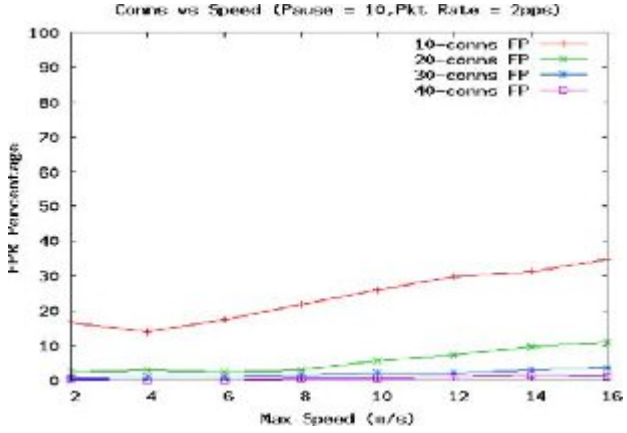

Fig.5. False positives with various speeds and connections.

So the next transmitted packet of *B* that *A* will capture as a first acknowledgment of *B* will become the worst case white zone, can be calculated as follows:

$$ZW = (db + dv) + (s \times \_t). \quad (1)$$

The value of *dv* and *s* will be negative when node *B* is moving toward node *A* and positive otherwise. From Appendix we can know the value of *db* is approximately 10m and variance *v* at the boundary is 2.24 dbm which is the two standard deviation (SD), shown in Table V. Now in order to find out *dv*, ~~we~~ do the following computations The power received at any distance *d* is inversely proportional to the *m*th power of the distance [25], that is where *Pd* is the received power at distance *d* and in free space anzd in line-of-sight conditions, the path loss exponent *m* is 2.

IV. SIMULATION SETUP AND EVALUATION

In order to implement and evaluate our scheme, we use Network Simulator NS-2.30 using the parameters listed in Table II. The *UB−THRESHOLD* is the averaged RSS value (in Watts) of several scenarios when a transmitter is moving with 10 m/s speed; lower speeds thresholds will improve detection accuracy, as discussed in Section III-C. The *TIME−THRESHOLD* is the average (maximum) time in which a node should listen from another node, otherwise that identity will be considered as out of range or previous identity of a whitewasher. Shorter time intervals will increase identity revalidations in the network; whereas lengthy intervals will increase table sizes in network nodes. The *LIST−SIZE* is the maximum RSS records retained for an identity or address. We used 5 as an arbitrary number of records per identity; however, it can be increased depending upon the memory capacity of nodes. In this simulation study our aim is to establish the detection percentage of our proposed scheme in different scenarios. As we discussed above, there are some attributes of the network that are mainly responsible for affecting the accuracy of our Sybil attack detection scheme. These attributes are number network connections, node density and transmission rate. In each of our scenario we take speed as our main attribute.

All of the results we present here have been calculated as an average of 25 different random scenarios (or simulation runs). In the following subsections, we will discuss our metrics and will analyze our simulation results that are based on a
variety of node speeds, packet transmission rates, connections and node densities.

A. Metrics

We use two main metrics in order to determine the detection accuracy of our scheme in different environments, i.e., true positive rate (TPR) and false positive rate. True positive means a malicious node is correctly detected and false positive means a good or legitimate node is incorrectly detected as a malicious.

B. Analysis

As shown in figure data connections in the network are inversely proportional to the false positives of our scheme. For detection, movement sensing or the reception of frequent RSS values are important. In order to obtain RSS values from a node, that node should be involved in some form of communication, for example by acting as a source, forwarder, or destination. The more frequently a node sends or receives packets, the more efficiently a neighboring node will detect
it in the event that it tries to create its Sybil identity. Fewer connections in a network imply fewer source and destination nodes, and greater difficulty for a node to distinguish other nodes' positions (i.e., their position as being either in a gray or white zone). Consequently a greater number of false positives will result. However, connections have no apparent effect on the true positives and for most of our experiments the true positives remained around the 90% level, as depicted

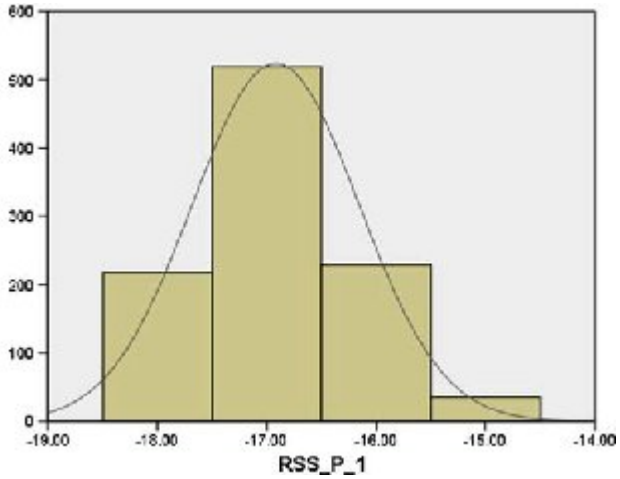

Fig. 6. Data distribution for 1-ft distance.

V. CONCLUSION

In this paper, we proposed an RSS-based detection mechanism to safeguard the network against Sybil attacks scheme worked on the MAC layer using the 802.11 protocol without the need for any extra hardware. We demonstrated through various experiments that a detection threshold exists for the distinction of legitimate new nodes and new malicious identities. We confirmed this distinction rationale through simulations and through the use of a real-world test bed of Sun SPOT sensors. We also showed the various factors affecting the detection accuracy, such as network connections, packet transmission rates, node density, and node speed. The simulation results showed that our scheme works better even in mobile environments and can detect both join-and-leave and simultaneous Sybil attackers with a high degree of accuracy.

REFERENCES

[1] I. Chlamtac, M. Conti, and J. J.-N. Liu, "Mobile ad hoc networking: Imperatives and challenges," *Ad Hoc Netw.*, vol. 1, no. 1, pp. 13 64, 2003.

[2] J. R. Douceur, "The Sybil attack," presented at the Revised Papers from the First Int. Workshop on Peer-to-Peer Systems, 2002, pp. 251–260.

[3] J. Newsome, E. Shi, D. Song, and A. Perrig, "The Sybil attack in sensor networks: Analysis and defences," presented at the 3rd Int. Symp. Information Processing in Sensor Networks (IPSN), 2004, pp. 259–268.

[4] B. Parno and A. Perrig, "Challenges in securing vehicular networks," in *Proc. 4th Workshop HotNets*, 2005, pp. 1–6.

[5] K. Hoeper and G. Gong, "Bootstrapping security in mobile ad hoc networks using identity-based schemes," in *Security in Distributed and Networking Systems* (Computer and Network Security). Singapore: World Scientific, 2007.

[6] S. Hashmi and J. Brooke, "Toward Sybil resistant authentication in mobile ad hoc networks," in *Proc. 4th Int. Conf. Emerging Security Inform., Syst. Technol.*, 2010, pp. 17–24.

[7] Y. Chen, J. Yang, W. Trappe, and R. P. Martin, "Detecting and localizing identity-based attacks in wireless and sensor networks," *IEEE Trans. Veh. Technol.*, vol. 59, no. 5, pp. 2418–2434, Jun. 2010.

[8] M. S. Bouassida, G. Guette, M. Shawky, and B. Ducourthial, "Sybil nodes detection based on received signal strength variations within VANET," *Int. J. Netw. Security*, vol. 8, pp. 322 333, May 2009.

[9] B. Xiao, B. Yu, and C. Gao, "Detection and localization of Sybil nodes in VANETs," presented at the Proc. 2006 Workshop on Dependability Issues in Wireless Ad Hoc Networks and Sensor Networks, 2006, pp. 1–8.

[10] T. Suen and A. Yasinsac, "Ad hoc network security: Peer identification and authentication using signal properties," presented at the Proc. 6th Annual IEEE SMC Information Assurance Workshop (IAW), New York, Jun. 2005, pp. 432 to 433.

MAC Layer Control to Achieve High Network Perfomance Using Replication

R.Prabu[#1],K.Malathi[#2],S.Vivekpandian[#3]
Assitant Professor[#1,#2,#3],Department of ComputerScience
R.V.S Educational Trust's Group of Institutions,Dindugul,TamilNadu.
praburk@gmail.com[#1],nimal.cse@gmail[#2].com,vivekpandian01@gmail.com[#3]

Abstract—**Various demands may oblige speedy data trade in Wireless Local Area Networks (WLANS) nowadays. An executor delineation is the EAST (Experimental Advanced Superconducting Tokamak) wander where physical science investigators need to transport huge examination data using the TCP (Transmission Control Protocol). In any case, the high debate level and the high disappointment rate in remote frameworks have an exceptional impact on the TCP execution. To alleviate this issue, this paper proposes a MAC layer obstructing control framework to oversee remote group adversity due to slips. Our framework is executed at the nearby remote centers subordinate upon the IEEE 802.11 DCF framework yet without any adjustment to the TCP layer. We first propose the prospect of the mac layer stopping up window in which the mac layer will send all the bundles in a window when it gets access to the remote channel. By then we allow our stopping up control framework to adjust its MAC obstructing window considering the clash degree and the cluster mishap rate at the mac layer. By performing remote blockage control at the mac layer, our framework can allay the effect of remote bunch hardship on TCP, and in this way improve the TCP execution. The diversion besides test conclusions exhibit that our instrument can achieve favored execution over the ordinary MAC layer segments in WLANS**

Keywords- Distributed algorithm, IEEE 80211WLAN,MAClayer congestion control, TCP performance.

I. INTRODUCTION

IEEE 802.11 based WLANS (Wireless Local Area Networks) are getting to be progressively pervasive as of late on the grounds that numerous provisions can utilize them to enter Internet. For instance, the EAST (Experimental Advanced Superconducting Tokamak) office at the ASIPP (Ins), Hefei, China, utilizes a PC framework with high velocity systems to backing the material science research exercises in acquirin titute of Plasma Physics under the Chinese Academy of Science and investigating enormous measure of symptomatic information. As of late, more material science analysts are utilizing WLANS to help their exploration provisions because of their pervasive accommodation.Unfortunately, the analysts are not content with the throughput and postponement execution when exchanging gigantic mass information. This is on the grounds that the TCP (Transmission Control Protocol) at the transport layer accepts that every parcel misfortune is because of clogging and accordingly diminishes its blockage window at every event of bundle misfortune. In an environment of high misfortune because of high cycle blunder rate at the more level layers, the throughput and equitability execution might corrupt rapidly notwithstanding the dispute nature of WLANS transmission process.

In this paper, we will mull over a clogging control technique at the MAC-layer (rather than the Transport Layer) to determination the throughput corruption issue in a high lapse the earth. Our strategy will alter the blockage window consistent with the MAC layer delay and the bundle misfortune rate. Since the MAC layer can get the remote channel status specifically, performing clogging control at the MAC layer could be more productive. In the interim, so as to be versatile, our component receives a conveyed calculation where each remote customer upholds its blockage window and performs the MAC layer clogging control, without the requirement to adjust any AP (Access Point) capacities. Our calculation intends to enhance the reasonableness and throughput execution for WLANS particularly for EAST information.

The commitments of our paper upgraded blockage control at the MAC layer by taking the MAC layer parcel misfortune rate and deferral into attention. Through the configuration standards to be examined, our sub-optimal calculation can enhance the execution all the more rapidly. An appropriated operation that makes the calculation versatile to the system size; to our best information, we are the first to propose a blockage control calculation in the MAC layer and which can run in a conveyed way around all hubs. It is inviting to (good with) both the TCP and the IEEE 802.11 MAC conventions.

II. RELATED WORK

Various results have been proposed to manage TCP's poor throughput execution in WLANS. We order these methodologies into three classifications consistent with their convention layers: the TCP layer systems, the cross-layer strategy including the TCP layer and MAC layer, and the MAC layer strategies.

The greater part of the components handles this issue just at the TCP layer. TCP Westwood is a finish to-end transport layer result that uses the ACK landing rate to gauge the transfer speed, and afterward sets a fitting blockage window as per the assessed data transmission after three double ACKs are accepted. In spite of the fact that this operation reduces the impact of remote drops and enhances the channel use, the principle inconvenience is the wavering in the estimation of the accessible transmission capacity. BIC-TCP embraces a parallel pursuit system to forcefully expand the clogging window when the distinction between the

present blockage window and the greatest window is extensive. Then again, it is challenging to gauge the most extreme permitted window (which is evolving ceaselessly). Quick TCP consolidates multiplicative increment if the cushion involved by the association at the bottleneck is far not exactly some predefined limit, and switch to direct build in the event that it is close. At that point, FAST tries to uphold the cradle inhabitance around and decreases sending rate if postponement is further expanded. Hypothetical dissection and investigations indicate that defer based methodologies are superior to unadulterated misfortune based methodologies in numerous execution measures, for example, accomplishing higher usage, less self-incited parcel misfortunes, speedier meeting pace, and additionally better RTT reasonableness and stabilization. Be that as it may, past work likewise uncovers that postpone based methodologies will most likely be unable to get a decent amount when they are contending with misfortune based methodologies like standard TCP.

A few instruments have received a cross-layer methodology to enhance TCP's execution. The MCP (Mobile-host-Centric Protocol) moves the control focus to the portable have, and joins together the MAC layer and TCP layer to gauge the remote channel status, (for example, dispute and touch blunder). It can modify the TCP layer clogging window dependent upon the channel states to enhance the exactness of blockage control. The ACK-delay instrument is an incorporated component which can defer the TCP ACKs at the MAC layer of an AP. This component can enhance channel usage and conform TCP's clogging window dependent upon the MAC layer blockage status. The above systems all arrangement with remote parcel misfortune through movements in the TCP layer yet it might be much better when we can deal with it specifically where it happens (the MAC layer).

There are various studies where just the MAC layer capacities are changed to enhance the channel use and to handle MAC layer clogging. The result in changes the conflict window and AIFS (Arbitration Inter Frame Spacing) to enhance equitability. The model in derives a hypothetical upper bound of the throughput, and gives a system to accomplish the upper bound by giving a dynamical clogging window change calculation. The result in conforms the conflict window dependent upon distinctive discord levels to enhance MAC layer execution. Be that as it may, their primary thought of lessening the dispute window size of a hub in awful situations really expands the impact likelihood. The MAC layer blockage by conforming the edge size. In light of diverse touch failure rates. The point when the spot slip rate is low, the parcel length will be expanded; overall, and the bundle length will be diminished. The thought is to land at an optimal parcel measure that is typically challenging to acquire. The MAC layer resolution clogging by expanding the remote asset through the utilization of different channels.

In our past work, we have proposed the MACC (MAC layer Congestion Control) convention which is a MAC layer blockage control component to manage remote bundle misfortune. On the other hand, this instrument is AP-driven (i.e., it is an incorporated calculation) and not adaptable in light of the fact that the AP need to administer the windows of every versatile stations and to perform the blockage control component.

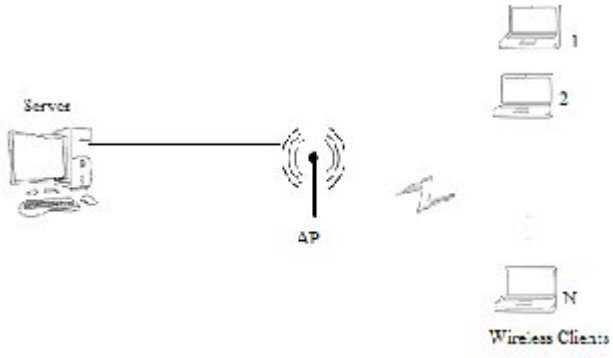

Figure 1 Network Model

To propose an appropriated MAC layer blockage control component, in which every remote customer can execute autonomously, while obliging no adjustment to the AP. By conforming its blockage window dependent upon the MAC layer bundle misfortune rate and postponement, the remote customers can bring about a significant improvement utilization of the remote channel, and hence moderate the effect of remote drops and enhance the execution

III. SYSTEM MODEL AND OPERATION

Figure 1 shows the general system setup utilized within the EAST office. After the server saves the exploratory information (transported through a spine) and the diagnose information (transported from remote stations), the researchers might utilize their laptops to acquire (download) these information through the APs (Access Points).For straightforwardness and demonstrating examination, one and only AP is indicated *N* researchers (remote customers). These clients can additionally transfer their handled information once more to the server through the opposite way.

FTP (File Transportation Protocol) is the provision layer convention the researchers generally use to transport monstrous measure of information. FTP depends on TCP New Reno in the transport layer underneath to give a consistent association between the sender (e.g., server sending information) and the remote customer recipient. Further down the convention building design, the IEEE 802.11[15] is the MAC (Medium Access Control) layer convention utilized within the WLAN that empowers one-jump correspondence with the AP or alternate remote customers.

In the MAC layer, the IEEE 802.11 WLAN utilizes an obligatory conflict based channel access capacity called the DCF (Distributed Coordination Function). The DCF receives the CSMA/CA (Carrier Sense Multiple Access with Collision Avoidance) process and utilization the twofold exponential backoff calculation for every crash. In DCF, all remote stations with the same conflict parameter qualities have an equivalent chance to gain entrance to the transmission medium. Over a sufficiently long interim, this outcomes in station-based reasonable access which is additionally alluded as MAC layer reasonable access. In any case, this system couldn't guarantee honesty, and it likewise lessens the channel usage for the accompanying explanations.
In 802.11 DCF, before sending parcels, a hub need to screen the channel, and afterward trade RTS and CTS bundles with the collector. The parcels might be sent just if these methods are great. The transmission succeeds when the compared ACK is gained; overall, the sender need to fight the channel again with the dispute window multiplied. In the event that the channel experiences a few issues, for example, high conflict or high touch failure rate, then the channel use is decreased because of retransmission. Note that the amount of contending stations likewise has an extraordinary impact on the channel usage of IEEE 802.11 MAC convention. There is additionally an equitability issue if the remote hubs are in diverse conditions in light of the fact that the hubs with a higher bit blunder rate might endure a higher parcel misfortune rate; they will be in the backoff state more frequently than those with an easier bit mistake rate. This expedites a bigger backoff window for the hubs in terrible conditions. So the hubs in better conditions can get more opportunities to gain entrance to the channel, bringing about the shamefulness issue in WLAN.

TCP uses four algorithms for congestion control: slow start, congestion avoidance, fast retransmission and fast recovery. Slow start allows fast detection and utilization of available network bandwidth by doubling its congestion window in one RTT (Round Trip Time) every time a data packet in a window is acknowledged. When the congestion window exceeds a threshold, congestion avoidance kicks in by increasing the congestion window by 1 after one RTT if there is no packet loss. It is used to slow the rate increase in order to avoid congestion that would deplete network buffers. Packet loss is assumed to happen when duplicated ACKs are received. Then TCP will halve its congestion window, and perform a fast retransmission. This is the Fast Recovery phase. If an ACK times out, it will reduce congestion window to 1 MSS and then perform a Slow Start. Note that the principal assumption of TCP is that every packet loss is due to congestion whose mechanism has been summarized above. Unfortunately, this is not true in wireless networks because the chance to lose packets due to packet errors has become high. This can cause performance degradation through windowing operation because TCP cannot distinguish packet loss due to congestion from loss due to packet errors. This is the subject of our congestion control algorithm proposed in the next section to combat these errors.

IV. THE DISTRIBUTED CONGESTION CONTROL ALGORITHM

In this paper, the main focus is to justify for the configuration of our appropriated MAC calculation, accompanied by an exact depiction. The check might originate from the execution assessment later. In the event that a sender is permitted to send all the parcels in a blockage window when it gets access to the remote channel, we can enhance the bundle triumph rate and the channel use. This is in light of the fact that hub necessities to perform one backoff just, which are autonomous of what number of bundles, are lost inside a window. This thusly would decrease the MAC layer holding up time, and the MAC layer queuing length, and in the end might alleviate system clogging. Since IEEE 802.11 utilization the DCF instrument condensed above, one can see that when the controversy level is low, there are less system assets needed to perform the backoff and screen operations. Consequently, if one can build the blockage window at the same conflict level, more throughputs could be accomplished by conferring the same measure of assets. The point when the controversy is direct not immersed, a few hubs might not have information to send now and again. Thus, it is better to screen and perform backoff systems as DCF component typically does.

One can get an optimal decency and throughput execution if every hub can fight the channel dependent upon the discord level. The point when the system is immersed (i.e., when all hubs have information to send), DCF performs crudely in light of its lower great transmission rate and huge backoff time. In this circumstance, one can enhance the fruitful transmission rate by expanding the clogging window. Around distinctive administration restrains, a round-robin administration around all hubs gives off an impression of being an optimal decision to acquire both high throughput and honesty execution. From the basis examined above, one can see that the new component ought to be made versatile to the system progressions to enhance its throughput and equitability. Hence, we propose the accompanying systems to relieve system clogging to attain an optimal result rapidly.

A. The Algorithm

Since the IEEE 802.11 MAC sends one and only bundle after the RTS/CTS, we propose the accompanying improvements in place for a hub to send all bundles inside a clogging window.

1) RTS/CTS operations: A hub is obliged to support the clogging window of each one focus to focus association. To update the AP of the clogging window, a sending hub adjusts the NAV field in its RTS outline. In the event that the hub is a getting hub, it utilizes the CTS outline. The AP can then appropriate or send the parcels dependent upon the blockage window data it appropriates.

2) Incorporation of the MAC layer defer: This might permit a close hub to alter its MAC layer blockage window dependent upon the MAC layer postpone notwithstanding its parcel misfortune rate. By overseeing the remote channel, a hub can see all the bundles not having a place with itself. It will record the MAC layer deferral of each of these parcels from the time a parcel is sent until the relating ACK is gained. In the event that the relating ACK is not accepted in a given time, that bundle is disregarded. The point when a hub needs to send its parcels, it will first figure the normal MAC deferral of all others bundles followed and also the normal postponement of its own bundles. At that point it utilizes the accompanying methodology to alter its clogging window (M_cwnd) under two separate situations.

<u>No Packet Loss</u>

The point when there is no bundle misfortune, the blockage window is upgraded as per

_ (+= -) (1)

where M-delayis the MAC layer delay, which is the normal postponements of all its bundles (from inside one window), and aver_delay is the normal postponement of all its neighbor hubs that a remote customer can listen. Here, deferral is measured from the time a bundle is sent until the time the comparing ACK is gained. Comparison (1) originates from the observation/rationale that when there is no bundles misfortune, the channel is most likely sit without moving. So one may as well send more bundles without any additional backoff. Nonetheless, transmitting more bundles for one association may build the deferral and hence cause timeout in different associations. Subsequently, one may as well diminishing its clogging window at whatever point its MAC layer postponement drops once again to underneath the normal deferral. Then again, transmitting a window of bundles for one association may expand the deferral for others, particularly when the window is enormous. Subsequently, we pick a limit w=4 /3+4, past which the blockage window won't increase by 1 for a fruitful transmission yet just changes consistent with the deferral proportion. That is

_ (+= -) (1a)

<u>On a Packet Loss</u>

The point when a parcel misfortune happens, we will conform the following blockage window consistent with

$$M\_cwnd = (1+p) * M\_cwnd \qquad (2)$$

where p is the MAC layer bundle slip rate characterized to be the degree between the amount of Acks not appropriated and the aggregate number of information parcel conveyed in a window.

Mathematical statement (2) hails from the thought that there will be p * M-cwnd packet lost throughout a clogging window. These lost bundles must be retransmitted in addition to any new parcels in the new window. This will enhance the throughput and the equitability on the grounds that we can utilize a substantial window to enhance the impeded throughput execution for parcel lapse to achieve the normal system execution. The point when the retransmitted bundles are appropriated adequately in the first retransmission, we may as well uproot the interim augmentation added to the blockage window. This is to avert inadvertent interferences that may drop bundles. In the event that the channel is not debased constantly, it might not take long for the blockage window to recuperate the lost parcels and afterward return once again to its unique worth for typical operation

B. Discussion

Our component tries to manage remote parcel misfortune at the MAC layer which is not because of clogging, and in this manner might be outlandish to perform blockage control system as TCP does. Yet we can't overlook the bundle misfortune really because of MAC layer retransmission either since the remote parcel failure will expand the MAC layer holding up time, which will thusly irritate blockage.

Note that no adjustment of the AP is needed, however this unpretentious improvement has made our instrument conveyed since it can now be actualized effortlessly in every remote customer freely. The characteristic likewise makes our system component adaptable.

V. PERFOMANCE EVALUATIONS

We utilize Qualnet 3.7 recreation to look at the execution of our enhanced system with the default instrument (IEEE 802.11g) and MACC under different situations. The MACC is a calculation that likewise embraces a MAC layer clogging control strategy yet with an incorporated operation at the AP, and it just acknowledges MAC layer parcel lapse. To approve our new system further, we have additionally actualized the component and assessed its execution in the Red Hat9.0 Linux Operating System. The items, execution results also their dialogs are furnished in a later area. The accompanying are the meanings of the execution measures used to assess our calculation:

1) End-to-end throughput: this is the measure of activity (measured in bundles) for every unit time. This is measured by the amount of parcels effectively appropriated at the recipient over the mimicked time.
2) Average finish to end postponement: End to end deferral is the time interim between the time when one parcel was sent by the sender and the time when the parcels was accepted by the recipient. At that point the normal is gotten from just those parcels gained.
3) Delay difference: The fluctuation is the desire of the square of the deviation of a closure to end delay from its group mean quality.
4) Number of TCP timeouts: this number is measured at the TCP sender.

We utilize the system arrangement as a part of Fig. 1 where the wired line data transfer capacity is 100mbps, and the remote transfer speed is54mbps. A spread deferral of 45ms is utilized. We have acquired numerous recreation hurries to study the impact of distinctive parameters on different execution measures. The predominant 4subsections underneath are dependent upon reenactment and Section V-E is dependent upon a life-test. In our execution figures to be examined, "default", "MACC" and "enhanced" speak to the default IEEE 802.11g system, the MACC component, and our enhanced instrument, individually.

A. Effect of Contention Level

In this first aggregation of recreations, we shift the amount of remote hubs from 5 to 40. The hubs are circulated equitably around the AP, and have a consistent parcel slip rate of P=0.2.

Fig. 2 shows that the throughputs of all instruments are a diminishing capacity of the amount of hubs not surprisingly from the increment in controversy level. Whatsoever levels, our enhanced calculation is the best and the default is the most noticeably bad. Both our instrument and MACC can enhance the channel usage by changing the amount of bundles sent dependent upon the parcel misfortune rate and in this manner enhance the system throughput when contrasted with the default calculation. Be that as it may, it is fascinating to see that the MACC execution corrupts extraordinarily past N=25 hubs.

This could be illustrated as accompanies.

With an expanding number of remote hubs, clogging sets in when the expansive measure of dispute causes more impact and squanders the transmission capacity. What's more, the throughput execution diminishes on the grounds that more assets of a hub must be committed on the reckoning.

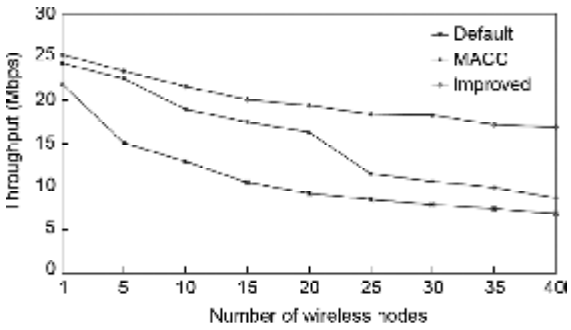

Figure 2 Throughput examination with distinctive stream numbers

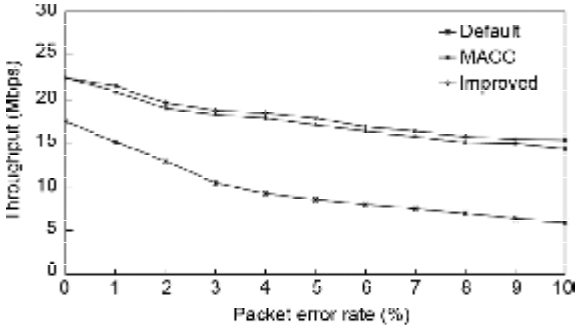

Figure 3 Throughput correlation in diverse bundle lapse rate

Its throughput practically drops to the level of the default calculation. Because of the low reckoning unpredictability of our conveyed instrument, its execution is stable concerning an expanding number of remote hubs.

B. Effect of Bit Error Rate

In this second situation, we change the parcel lapse rate p from 0.01 to 0.1 while settling the amount of hubs at *N*=20 .The bundle mistake rate expands, the execution of the default system corrupts extraordinarily, while our component and MACC diminish only a smidge. This is on the grounds that these two components utilize a bigger blockage window, and thusly for every transmission, there will be a few parcels transmitted effectively. Since certain fruitful transmission level can now be administered, the channel use and additionally the generally arrange throughput might be enhanced in the vicinity of high bundle slip rate. These two calculations are hence more powerful to bundle mistakes.

C. Similarity

Since we can't ensure that each remote hub receives our component, we might perceive how our improved instrument and the default system can coincide. We test it by running two reproductions to check their similarity. In the first recreation, each of the twelve hubs utilize the default system; and in the second, we let six remote hubs (Node Ids 1 to 6) utilize the default MAC layer component, while the other six (Node Ids 7 to 12) utilize our instrument. Fig. 4 shows that in the first recreation (the white section on the left under every Node ID), the total throughput is 10.3mbps, while in the second reproduction (the right segment), it is 13.1 Mbps. We have likewise figured the honesty list ($\sum$ $)^2/($ n$\sum$ $)$and throughput of hub *i*, the qualities of the two reproductions are 0.72 and 0.94.the effects indicate that not just the enhanced calculation has no effect to the default additionally has given some execution pick up. Furthermore, they have attained about the same throughput execution, proposing the calculation has an impact on reasonableness. As an alternate fascinating perception, different (Nodes Ids 1 to 6) not executing the enhanced calculation additionally profit by enhancing their throughput. Basically, our system could be perfect with the default MAC 802.11 component.

D. Effect of our Mechanism on TCP

By using the proposed idea it is deliberately compound the system environment by expanding the amount of hubs N=40 to in the first recreation, and by expanding the bundle lapse rate to P=0.1in the second reenactment while keeping N=40. The Table analyzes the normal defer and number of TCP timeouts. One can see that both MACC and our system can diminish the normal close to end defer by enhancing the MAC layer transmission proficiency at the expenditure of a bigger postponement difference. Nonetheless, since our instrument was planned with the thought of the effect of MAC layer defer on TCP execution, our calculation can change the MAC layer blockage limit, and subsequently enormously diminishing the amount of TCP timeouts.

E. CONCLUSION

In this paper, we have proposed another MAC layer blockage control instrument by altering the clogging window as per the parcel misfortune and MAC layer delay. By enhancing the channel use and expanding clogging window for feeble hubs, our instrument can enhance the throughput execution and decency execution essentially. Recreation and introductory examination outcomes indicate that our instrument can enhance the throughput and equitability execution of WLANs fundamentally.

REFERENCES

[1] C. Casetti et al., "TCPWestwood: Bandwidth estimation for enhancedtransport over wireless links," in Proc. 7th ACM Annu. Int. Conf. MobileComputing and Networking, Rome, Italy, 2001, pp. 287–297.

[2] D.Wei, C. Jin, S. Low, and S. Hedge, "FAST TCP:Motivation, architecture,algorithm and performance," IEEE/ACM Trans. Netw., vol. 4,no. 6, pp. 1246–1259, 2006.

[3] J. Freitag, N. L. S. da Fonseca, and J. F. de Rezende, "Tuning of 802.11e
network parameters," IEEE Commun. Lett., pp. 611–613, Aug.

[4] L. Xu, K. Harfoush, and I. Rhee, "Binary increase congestion control(BIC) for fast long-distance networks," in Proc. 23rd IEEE INFOCOM,Hong Kong, China, 2004, pp. 2514–2524

[5] Y. Shu, L. Zhang, W. Zhao, H. Chen, and J. Luo, "P2P-based datasystem for the east experiment," IEEE Trans. Nucl. Sci., vol. 53, no. 3,pp. 694–699, Jun. 2006

[6] Y. Shu, L. Zhang, W. Zhao, H. Chen, and J. Luo, "P2P-based datasystem for the east experiment," IEEE Trans. Nucl. Sci., vol. 53, no. 3,pp. 694–699, Jun. 2006.

Single Cylinder Four Stroke Spark Ignition Engine - Thermodynamic Simulation Model

Bridjesh.P[1], Sushma.P[2]
[1]Department of Mechanical Engineering, Bhajarang Engineering College,Ayathur,Tiruvellore Dist. Chennai,
[2]Department of Mechanical Engineering, SA Engineering College, Veeraraghavapuram, Thiruverkadu Post,
Chennai - 600 077, Tamilnadu, India
e-mail: meetbridjesh@gmail.com, meetshushma@gmail.com

Abstract: - The performance of an engine whose basic design parameters are known can be predicted with the assistance of simulation programs. A thermodynamic model for the simulation of a single cylinder spark ignition engine running on Iso-octane fuel is presented. The simulation consists of compression, combustion and expansion processes. The model is based on the classical two-zone approach, wherein parameters like heat transfer from the cylinder, blow-by energy loss and heat release rate are also considered. The general fuel is specified by way of its C-H-O-N values. Curve-fit coefficients are then employed to simulate air and fuel data along with fuel-air composition and practical chemical equilibrium routines. The calculated data is then used to plot the various thermodynamic parameters with respect to crank angle. Simulation program is usable to set for varies compression ratios, engine speed, and engine sizes.

Key words: Spark Ignition (SI) engine, Simulation model, Thermodynamic Modeling of Engines.

I. INTRODUCTION

The thermodynamic simulation model of spark ignition (SI) engines are one of the most effective tools for the analysis of engine performance, parametric examinations and assistance to new developments. Researchers have been spending essential effort to improve the performance of SI engines and about internal combustion engines (ICE). Generally, engine simulations are practice in two ways, which are fluid dynamic based and thermodynamic based models. Thermodynamic cycle models are based on the thermodynamic analysis of the content of cylinder during the engine cycle. In these models, the first law of thermodynamics is applied to open system of air-fuel and residual gas mixture into the manifolds and cylinders and it is zero dimensioned. Therefore, the equations leading the model are made of basic differential equalities [4, 6, and 8].

The present trend is towards the development of comprehensive 3-D models, which describes the functioning of engines at a very high level of detail and accuracy; however, these require substantial computational power. There are several instances where theoretical methods, which are based on a limited set of experimental data, are preferred. From these considerations, the need for a simple, fast and accurate engine simulation model is quite evident.

Nomenclature

A	area exposed to heat transfer (m^2)	b	bore of cylinder (m)
c_p	specific heat at constant pressure	C	blow-by coefficient (s^{-1})
E	total energy (kJ)	ΔG	Standard-state Gibbs free energy
h	specific enthalpy (kJ. kg^{-1})	K	Equilibrium constant
m	mass (kg)	N_u	Nusselt number
p	pressure (Pa)	Q	heat transfer (kJ)
r	compression ratio		

In this paper a two-zone, Zero-dimensional model was used to simulate the engine operations. The most important assumptions were, a) The working medium was considered, in general, to be a mixture of 10 species (CO_2, H_2O, N_2, O_2, CO, H_2, H, O, OH, NO) and fuel vapor. b) All 10 species were considered as ideal gases. And c) The fuel is limited to C-H-O-N species.

II. THERMODYNAMIC MODEL

For the present study, a Zero-dimensional combustion model is employed. The combustion chamber is divided into two zones consisting of unburned gas (mixture of fuel, air and residuals) and burned gas (mixture of 10 product species), each under uniform composition. This model assumes that at any instant of time during the combustion, the cylinder volume is divided into burned and unburned zones by an infinitesimally thin flame-front with a spherical shape. The burned gases are assumed to be in chemical equilibrium during combustion. A Wiebe function specifies the fuel burn rate and controls the rate at which mixtures from the unburned zone is converted to the burned zone. Mass and energy conservation relations and equations of state form the principle governing equations. Also considering crank angle as the independent variable, thus form the base of our thermodynamic model.

A. Mass and Energy Balance

The equation of state for an ideal gas is

$$PV = mRT \tag{1}$$

The rate of change of mass within any open system is the net flux of mass across the system boundaries. Hence for a control volume enclosing the air-fuel mixture, we have

$$m = \sum_k \dot{m}_k \tag{2}$$

The first law of thermodynamics to an open system yields the energy equation as

$$E = Q - W + \sum_k \dot{m}_k \, h_k \tag{3}$$

Equations (2) and (3) can be written as

$$\frac{dm}{d\theta} = \sum_k \frac{dm_k}{d\theta} \tag{4}$$

$$\frac{d(mu)}{d\theta} = \frac{dQ}{d\theta} - p\frac{dV}{d\theta} + \sum_k h_k \frac{d\dot{m}_k}{d\theta} \tag{5}$$

B. Air and Combustion Products Data

Colin R. Ferguson and Kirkpatrick [4] proposed the following expressions that were curve-fitted to polynomials by minimizing the least squares error. The function will employ for any given species is

$$\frac{c_p}{R} = a_1 + a_2 T + a_3 T^2 + a_4 T^3 + a_5 T^4 \tag{6}$$

$$\frac{h}{RT} = a_1 + \frac{a_2}{2} T + \frac{a_3}{3} T^2 + \frac{a_4}{4} T^3 + \frac{a_5}{5} T^4 + \frac{a_6}{T} \tag{7}$$

$$\frac{s}{R} = a_1 \ln T + a_2 T + \frac{a_3}{2} T^2 + \frac{a_4}{3} T^3 + \frac{a_5}{4} T^4 + a_7 \quad (8)$$

where c_p is the specific heat at constant pressure, h is the specific enthalpy and s is the specific entropy.

The coefficients a_1 to a_7 are calculated over two different temperature ranges: 1) 300 <T< 1000 K; and 2) 1000 <T< 5000 K and can be sourced from [6, 8].

The most combustion models are based on the assumption that the burned mixture is in equilibrium [6]. The following are species of interest during combustion: CO_2, H_2O, N_2, O_2, CO, H_2, H, O, OH and NO [4].

C. Fuel Data

Heywood [6] has represented the thermodynamic properties of fuels (in vapor phase).

$$\frac{c_p}{R} = a_1 + a_2 T + a_3 T^2 + a_4 T^3 + a_5 \frac{1}{T^2} \quad (9)$$

$$\frac{h}{RT} = a_1 + \frac{a_2}{2} T + \frac{a_3}{3} T^2 + \frac{a_4}{4} T^3 - a_5 \frac{1}{T^2} + \frac{a_6}{T} \quad (10)$$

$$\frac{s}{R} = a_1 \ln T + a_2 T + \frac{a_3}{2} T^2 + \frac{a_4}{3} T^3 - \frac{a_5}{2} \frac{1}{T^2} + a_7 \quad (11)$$

The following relation is proposed for deriving the properties like specific heats and enthalpies for various species, with ξ referring to the property and x is the burnt mass fraction.

$$\xi_{mixture} = \sum_{k=1}^{N} x_k \xi_k \quad (12)$$

D. Equivalence Ratio

When modeling with a single fuel, the equivalence ratio is given by [4]

$$\phi = \left(\frac{F}{Air} \right)_{Act} / \left(\frac{F}{Air} \right)_{st} \quad (13)$$

where subscript Act. refers to actual and St. refers to stoichiometric.

E. Practical Chemical Equilibrium

Under the assumption of atmospheric air composition (21%v Oxygen and 79%v Nitrogen), and provided ϕ < 3, the only species that are important because of dissociation are O, H, OH, and NO [4]. The combustion reaction thus becomes

$$\varepsilon\phi C_\alpha H_\beta O_\gamma N_\delta + 0.21 O_2 + 0.79 N_2 \rightarrow x_1 CO_2 + x_2 H_2 O + x_3 N_2 + x_4 O_2 + x_5 CO + x_6 H_2 + x_7 H + x_8 O + x_9 OH + x_{10} NO \quad (14)$$

where x_1 to x_{10} represents mole fractions of the products.

The atom balance for the various elements gives

$$C : \varepsilon\phi\alpha = (x_1 + x_5)N \qquad (15)$$

$$H : \varepsilon\phi\beta = (2y_2 + 2y_6 + y_7 + y_9)N \qquad (16)$$

$$O : \varepsilon\phi\gamma + 0.42 = \begin{pmatrix} 2y_1 + y_2 + 2y_4 + y_5 \\ + y_8 + y_9 + y_{10} \end{pmatrix} N \qquad (17)$$

$$N : \varepsilon\phi\delta + 1.58 = (2y_3 + y_{10})N \qquad (18)$$

where $N = \sum_{i=1}^{10} x_i$ is the total number of moles. The constraint that the mole fraction of all the products adds up to unity requires that

$$\sum_{i=1}^{10} x_i = 1 \qquad (19)$$

To solve for the unknowns, we need equations that are provided by the criteria of equilibrium among the products, which are expressed by the following hypothetical relations

$$\frac{1}{2}H_2 \leftrightarrow H \qquad K_1 = \frac{x_7 P^{0.5}}{x_6^{0.5}} \qquad (20)$$

$$\frac{1}{2}O_2 \leftrightarrow O \qquad K_2 = \frac{x_8 P^{0.5}}{x_4^{0.5}} \qquad (21)$$

$$\frac{1}{2}H_2 + \frac{1}{2}O_2 \leftrightarrow OH \qquad K_3 = \frac{x_9}{x_4^{0.5} x_6^{0.5}} \qquad (22)$$

$$\frac{1}{2}O_2 + \frac{1}{2}N_2 \leftrightarrow NO \qquad K_4 = \frac{x_{10}}{x_4^{0.5} x_3^{0.5}} \qquad (23)$$

$$H_2 + \frac{1}{2}O_2 \leftrightarrow H_2O \qquad K_5 = \frac{x_2}{x_4^{0.5} x_6^{0.5}} \qquad (24)$$

$$CO + \frac{1}{2}O_2 \leftrightarrow CO_2 \qquad K_6 = \frac{x_1}{x_5 x_4^{0.5} P^{0.5}} \qquad (25)$$

The equilibrium constant K, for the above are determined from the Gibbs free energy as

$$-\frac{\Delta G}{RT} = \ln K_p \qquad (26)$$

where ΔG is the standard-state Gibbs free energy. The values of the equilibrium constants can be obtained from [4, 18]

F. Thermal Properties

We consider the unburned and burnt mixture zones as separate open systems. Therefore, the specific internal energy, u and specific volume, v is expressed as

$$u = \frac{U}{m} = xu_b + (1-x)u_u \tag{27}$$

$$v = \frac{V}{m} = xv_b + (1-x)v_u \tag{28}$$

subscripts b and u refers to burnt gas and unburned gas respectively.

Assuming that the pressures of burnt and unburned gases are equal, v_b and v_u are functions of T_b, T_u and p . Hence

$$\frac{dv_b}{d\theta} = \frac{\partial v_b}{\partial T_b}\frac{dT_b}{d\theta} + \frac{\partial v_b}{\partial p}\frac{dp}{d\theta} \tag{29}$$

$$\frac{dv_u}{d\theta} = \frac{\partial v_u}{\partial T_u}\frac{dT_u}{d\theta} + \frac{\partial v_u}{\partial p}\frac{dp}{d\theta} \tag{30}$$

Substituting the logarithmic derivatives into the Eq. (29) and Eq. (30) yields

$$\frac{dv_b}{d\theta} = \frac{v_b}{T_b}\frac{\partial \ln v_b}{\partial \ln T_b}\frac{dT_b}{d\theta} + \frac{v_b}{p}\frac{\partial \ln v_b}{\partial \ln p}\frac{dp}{d\theta} \tag{31}$$

$$\frac{dv_u}{d\theta} = \frac{v_u}{T_u}\frac{\partial \ln v_u}{\partial \ln T_u}\frac{dT_u}{d\theta} + \frac{v_u}{p}\frac{\partial \ln v_u}{\partial \ln p}\frac{dp}{d\theta} \tag{32}$$

Similarly, the internal energies of both the burnt and unburned gases, under the same pressure condition and including the logarithmic derivatives can be written as

$$\frac{du_b}{d\theta} = \left(c_{pb} - \frac{pv_b}{T_b}\frac{\partial \ln v_b}{\partial \ln T_b}\right)\frac{dT_b}{d\theta} - v_b\left(\frac{\partial \ln v_b}{\partial \ln T_b} + \frac{\partial \ln v_b}{\partial \ln p}\right)\frac{dp}{d\theta} \tag{33}$$

$$\frac{du_u}{d\theta} = \left(c_{pu} - \frac{pv_u}{T_u}\frac{\partial \ln v_u}{\partial \ln T_u}\right)\frac{dT_u}{d\theta} - v_u\left(\frac{\partial \ln v_u}{\partial \ln T_u} + \frac{\partial \ln v_u}{\partial \ln p}\right)\frac{dp}{d\theta} \tag{34}$$

G. Mass in Control Volume

The mass at any angle is

$$m = m_1 \exp\left[-C(\theta - \theta_1)/\omega\right] \tag{35}$$

where C is the blow-by constant. The initial mass m_1 at $\theta = \theta_1$ (start of compression) is specified from knowledge of the volumetric efficiency and residual fraction.

The volume of the cylinder at any crank angle instant is given by [4]

$$V = V_c\left\{1+\frac{r-1}{2}\left\{\begin{matrix}1-\cos\theta+\\ \frac{1}{\varepsilon}\left[1-\left(1-\varepsilon^2\sin^2\theta\right)^{0.5}\right]\end{matrix}\right\}\right\} \quad (36)$$

V_c is clearance volume, r is the compression ratio and

$$\varepsilon = \frac{stroke}{2 * lengthofco\ nnectingro\ d}$$

H. Fuel Burning Rate Model

The Wiebe function represents the mass fraction burned, x_b versus crank angle and defined as [6]

$$x_b(\theta) = 1-\exp\left[-a\left(\frac{\theta-\theta_s}{\theta_d}\right)^n\right] \quad (37)$$

where θ = crank angle, θ_s = start of heat release, θ_d = duration of heat release, n = Wiebe form factor and a = Wiebe efficiency factor. The parameters a and n are adjustable parameters used to fit experimental data. The present simulation uses a =5 and n =3, these values have been reported in [6].

I. Heat Transfer Model

Heat transfer into the system is expressed in terms of heat loss from the burned and unburned gas respectively.

$$\frac{dQ}{d\theta} = \frac{-Q_l}{\omega} = \frac{-Q_b - Q_u}{\omega} \quad (38)$$

To express the heat loss in terms of temperature requires the introduction of a heat transfer coefficient h,

$$Q_b = hA_b\left(T_b - T_w\right) \quad (39)$$

$$Q_u = hA_u\left(T_u - T_w\right) \quad (40)$$

where A_b and A_u are the areas of burned and unburned gas in contact with the cylinder walls at temperature T_w. We have the following relations to calculate the areas of A_b and A_u

$$A_b = \left(\frac{\pi b^2}{2}+\frac{4V}{b}\right)x^{0.5} \quad (41)$$

$$A_u = \left(\frac{\pi b^2}{2}+\frac{4V}{b}\right)1-x^{0.5} \quad (42)$$

The fraction of cylinder area contacted by burned gas is assumed to be proportional to the square root of the mass fraction burned to reflect the fact, because of the density difference between burned and unburned gas, the

burned gas occupies a larger volume fraction of the cylinder than the unburned gas. We assumed that $h_u = h_b = h$ = constant in this paper.

This simulation model has the convenience to adapt the heat transfer correlation proposed by Woschni [7].

J. Blow-by Energy Loss

Enthalpy loss due to blow-by is expressed as [4]

$$h_l = (1 - x^2)h_u + x^2 h_b \qquad (43)$$

Early in the combustion process, unburned gas leaks past the rings. Late in the combustion process, burned gas leaks past in the rings. The above indicates that more leaking is due to the unburned gas compared with the burnt gas in the early stage of combustion.

K. Principle Governing Equations

Differentiating (28) with respect to crank angle and incorporating (31) and (32), we have

$$\frac{1}{m}\frac{dV}{d\theta}+\frac{VC}{m\omega}=x\frac{v_b}{T_b}\frac{\partial \ln v_b}{\partial \ln T_b}\frac{dT_b}{d\theta}+(1-x)\frac{v_u}{T_u}\frac{\partial \ln v_u}{\partial \ln T_u}\frac{dT_u}{d\theta}+\left[x\frac{v_b}{p}\frac{\partial \ln v_b}{\partial \ln p}+(1-x)\frac{v_u}{p}\frac{\partial \ln v_u}{\partial \ln p}\right]\frac{dp}{d\theta}+(v_b-v_u)\frac{dx}{d\theta} \qquad (44)$$

Expressing the heat loss of burnt and unburned gases as a function of the rate of change of specific entropy gives

$$-Q_b = m\omega x T_b \frac{ds_b}{d\theta} \qquad (45)$$

$$-Q_u = m\omega(1-x)T_u \frac{ds_u}{d\theta} \qquad (46)$$

Where

$$\frac{ds_b}{d\theta} = \left(\frac{c_{pb}}{T_b}\right)\frac{dT_b}{d\theta} - \frac{v_b}{T_b}\frac{\partial \ln v_b}{\partial \ln T_b}\frac{dp}{d\theta} \qquad (47)$$

$$\frac{ds_u}{d\theta} = \left(\frac{c_{pu}}{T_u}\right)\frac{dT_u}{d\theta} - \frac{v_u}{T_u}\frac{\partial \ln v_u}{\partial \ln T_u}\frac{dp}{d\theta} \qquad (48)$$

Expressing the heat loss of burnt and unburned gases as a function of the rate of change of specific entropy by combining (39)-(42) and (45)-(48)

$$c_{pb} = \frac{dT_b}{d\theta} - v_b \frac{\partial \ln v_b}{\partial \ln T_b}\frac{dp}{d\theta} = \frac{-hA_b(T_b - T_w)}{m\omega x} \qquad (49)$$

$$c_{pu} = \frac{dT_u}{d\theta} - v_u \frac{\partial \ln v_u}{\partial \ln T_u}\frac{dp}{d\theta} = \frac{-hA_u(T_u - T_w)}{m\omega(1-x)} \qquad (50)$$

Differentiating Equations (36) and (37) and incorporating with Equations (4), (27), (28), (31)-(34) and (38)-(43) into Equation (5), we have the following relations [4]

$$\frac{dp}{d\theta} = \frac{A + B + C}{D + E} \tag{51}$$

$$\frac{dT_b}{d\theta} = \frac{-hA_b\left(T_b - T_w\right)}{m\omega c_{pb} x} + \frac{v_b}{c_{pb}} \frac{\partial \ln v_b}{\partial \ln T_b} \frac{dp}{d\theta} +$$

$$\frac{h_u - h_b}{x c_{pb}} \left[\frac{dx}{d\theta} - \left(x - x^2\right) \frac{C}{\omega} \right] \tag{52}$$

$$\frac{dT_u}{d\theta} = \frac{-hA_u\left(T_u - T_w\right)}{m\omega c_{pb}\left(1 - x\right)} + \frac{v_u}{c_{pu}} \frac{\partial \ln v_u}{\partial \ln T_u} \frac{dp}{d\theta} \tag{53}$$

Where

$$A = \frac{1}{m}\left(\frac{dV}{d\theta} + \frac{VC}{\omega} \right) \tag{54}$$

$$B = \frac{h}{m\omega} \left[\begin{array}{l} \dfrac{v_b}{c_{pb}} \dfrac{\partial \ln v_b}{\partial \ln T_b} \dfrac{A_b\left(T_b - T_w\right)}{T_b} + \\ \dfrac{v_u}{c_{pu}} \dfrac{\partial \ln v_u}{\partial \ln T_u} \dfrac{A_u\left(T_u - T_w\right)}{T_u} \end{array} \right] \tag{55}$$

$$C = -\left(v_b - v_u\right) \frac{dx}{d\theta} - v_b \frac{\partial \ln v_b}{\partial \ln T_b} \frac{h_u - h_b}{c_{pb} T_b} \left[\frac{dx}{d\theta} - \frac{\left(x - x^2\right) C}{\omega} \right]$$

(56)

$$D = x\left[\frac{{v_b}^2}{c_{pb} T_b} \left(\frac{\partial \ln v_b}{\partial \ln T_b} \right)^2 + \frac{v_b}{p} \frac{\partial \ln v_b}{\partial \ln p} \right] \tag{57}$$

$$E = \left(1 - x\right)\left[\frac{{v_u}^2}{c_{pu} T_u} \left(\frac{\partial \ln v_u}{\partial \ln T_u} \right)^2 + \frac{v_u}{p} \frac{\partial \ln v_u}{\partial \ln p} \right] \tag{58}$$

Equations (54)-(58) are functions of θ, p , T_b and T_u respectively.

III. RESULTS

The results obtained from the thermodynamic simulation model are presented. We simulate Pressure, Temperature, Work, Heat Transfer and Heat flux for a single cylinder; four stroke SI engine running on Isooctane (C_8H_{18}). We have assumed a bore of 0.1m, stroke of 0.15m. The engine is assumed to operate at 2000 rpm, with an equivalence ratio of 0.8.

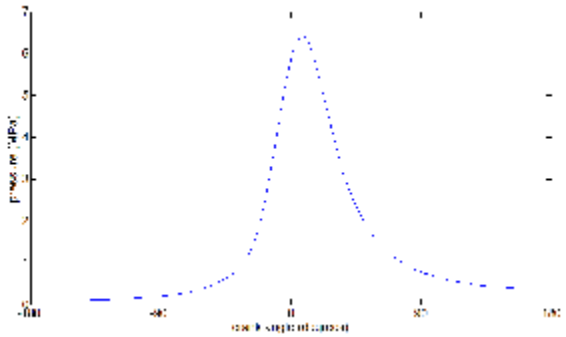

Figure 1: Pressure v/s Crank Angle

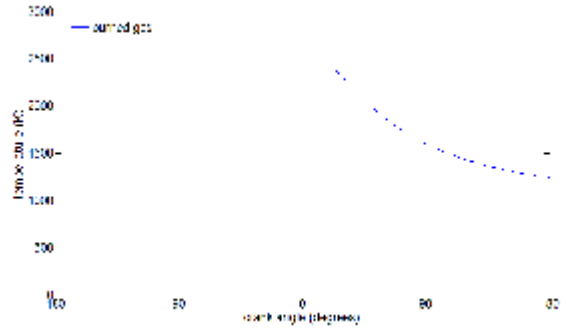

Figure 2: Temperature v/s Crank Angle

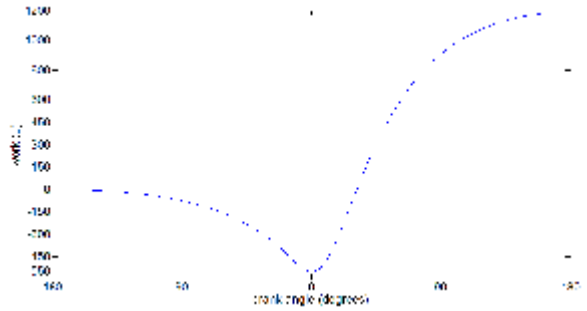

Figure 3: Work v/s Crank Angle

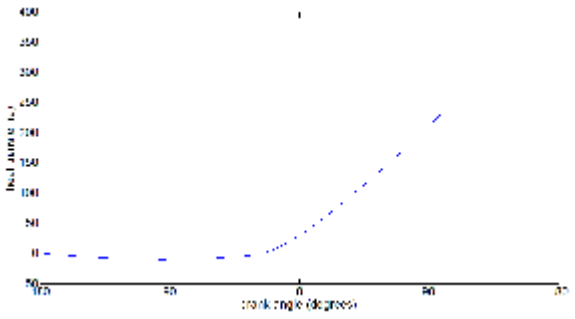

Figure 4: Heat Transfer v/s Crank Angle

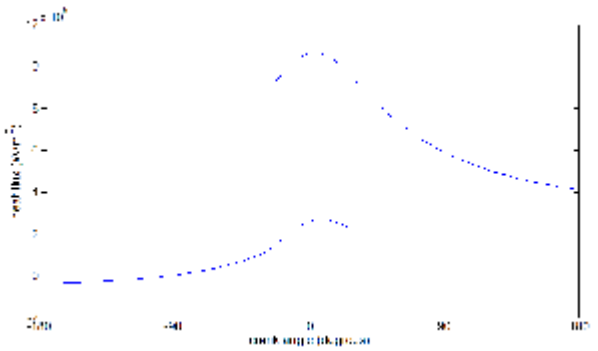

Figure 5: Heat Flux v/s Crank Angle

IV. CONCLUSION

A thermodynamic simulation model has been developed to simulate a single cylinder 4-stroke cycle of a spark ignition engine fuelled with Isooctane. The program written from this simulation model can be used to assist in the design of a spark ignition engine for alternative fuels as well. The results obtained can be used as a first-degree approximation and is useful in numerous engineering applications including general design predictions.

REFERENCES

[1] G. H. Abd Alla, "Computer simulation of a four stroke spark ignition engine" En. Convers. Mng., vol. 43, 2002, pp. 1043-1061.
[2] D. R. Buttsworth, "Spark Ignition Internal Combustion Engine Modelling using Matlab", Faculty of Engineering & Surveying Technical Reports, University of Southern Queensland, 2002.
[3] S. H. Chan and J. Zhu, "Modelling of engine in-cylinder thermodynamics under high values of ignition retard", Int. J. Therm. Sci., vol. 40, 1999, pp. 94-103.

[4] C. R. Ferguson, Internal Combustion Engines, Applied Thermosciences. New York: John Wiley and Sons, 1986.

[5] M. Grill, M. Chiodi. H. Berner and M. Bargende, "Calculating the Thermodynamic Properties of Burnt Gas and Vapor Fuel for User-Defined Fuels", MTZ 05|2007, 2007, pp. 398.

[6] J. B. Heywood, Internal Combustion Engine Fundamentals. New York: McGraw-Hill, 1988.

[7] G. Woschni, "A Universally Applicable Equation for the Instantaneous Heat Transfer Coefficient in the Internal Combustion Engine", SAE Paper 670931, 1967.

[8] Sundeep Ramachandran, "Rapid Thermodynamic Simulation Model of an Internal Combustion Engine on Alternate Fuels", IMES, Vol II, 2009.

[9] Ismet Sezer, and Atilla Bilgin, "Mathematical analysis of spark ignition engine operation via the combination of the first and second laws of thermodynamics", the royal Society, 2008.

[10] Perihan Sekmen., and Yakup Sekmen, "Mathematical Modelling Of a SI Engine Cycle with Actual Air-Fuel Cycle Analysis", Mathematical and Computational Applications, Vol 12, No. 3, pp 161-171, 2007.

[11] MaherA. R. Sadiq AL-BAGHDADI., "A Simulation Model for a Single Cylinder Four-Stroke Spark Ignition Engine Fuelled with Alternative Fuels", Turkish J. Eng. Env. Sci. 30 (2006), 331 – 350.

[12] I. Arsie, C. Pianese and G. Rizzo, "Models for the Prediction of Performance and Emissions in a Spark Ignition Engine – A Sequentially Structured Approach", SAE Paper 980779, 1998.

[13] "CHEMKIN Thermodynamic Database", Sandia Report SAND87-8215 B, 1991.

[14] M. Grill, M. Chiodi. H. Berner and M. Bargende, "Calculating the Thermodynamic Properties of Burnt Gas and Vapor Fuel for User-Defined Fuels", MTZ 05|2007, 2007, pp. 398.

[15] B. J. McBride, S. Gordon and M.A. Reno, "Coefficients for Calculating Thermodynamic and Transport Properties of Individual Species", NASA Technical Memorandum 4513, 1993.

[16] C. Olikara and G. L. Borman, "Calculating Properties of Equilibrium Combustion Products with Some Application to I.C. Engines", SAE Paper 750468, 1975.

[17] E. Sher and Y. Hacohen, "On the Modelling of a SI 4-Stroke Cycle Engine Fuelled with Hydrogen-Enriched Gasoline", Int. J. Hydrogen Energy, vol. 12, 1987, pp. 773-781.

[18] "JANAF Thermochemical Tables", United States National Bureau of Standards Publications NSRDS-NBS 37, 1971.

[19] Shahrir Abdullah, Wendy Hardyono Kurniawan and Azhari Shamsudeen, "Numerical Analysis of the Combustion Process in a Compressed Natural Gas Direct Injection Engine", Journal of Applied Fluid Mechanics, Vol. 1, No. 2, pp. 65-86, 2008.

[20] Emel Evren Selamet, Ahmet Selamet, James M. Novak, "Predicting chemical species in spark-ignition engines", Elsevier Ltd., Energy 29 (2004) 449–465.

A Framework for Method Level Clone Breakthrough On Web Pages Using Metrics

K.Nirmalrajan[1], V.UdhayaKumar [2]
[1] M.Tech I Yr., Dept. of IT, [2] Asst., Prof., Dept. of CSE, Prist University
Pondicherry – 605 007, India.
nirmalrajank@gmail.com[1], Udhaya_kurinji@yahoo.com [2]

Abstract— **As the use of the web pages are increasing nowadays to a huge amount, some of the data that are present in the web pages can be characterized so that the work of the programmer is reduced. Many web applications use a mixture of HTML and scripting language code as the front-end to business services, where scripts can run on both the client and server side. Thus code duplication occurs frequently during the development and evolution of web applications. This ad-hoc but pathological form of reuse consists in copying, and eventually modifying, a block of existing code that implements a piece of required functionality. Duplicated blocks are named clones and the act of copying, including slight modifications, is called cloning. When entire functions are copied rather than fragments, duplicated functions are called function clones. In this paper we propose a model that identifies all the function clones that are present in the web pages.**

I. INTRODUCTION

Code duplication occurs frequently during the development and evolution of large software systems. This ad-hoc form of reuse consists in copying, and eventually modifying, a block of existing code that implements a piece of required functionality. Duplicated blocks are named clones and the act of copying, including slight modifications, is called cloning. When entire functions are copied rather than fragments, duplicated functions are called function clones.A code fragment that has identical or similar code fragment(s) to it in the source code,in general, terms as code clone. A copied fragment can be used with or without minor modifications in a system by the developer. If there is no modifications or the modifications are within a certain level in the copied fragment then the original and copied fragments are called code clones and they form a clone pair as shown in fig1.1

Metrics-based techniques are related to hashing algorithms For each fragment of a program the values of a number of metrics is calculated, which are subsequently used to find similar fragments.

- Clone Pair:

A pair of code portions/fragments is called a clone pair if there exists a clone-relation between them, i.e., a clone pair is a pair of code portions/fragments which are identical or similar to each other.

- Clone Class:

A clone class is the maximal set of code portions/fragments in which any two of the code portions/fragments hold a clone-relation, i.e., form a clone pair.

- Clone Class Family:

The group of all clone classes that have the same domain is called a clone class family . Such a clone class family is also termed super clone.

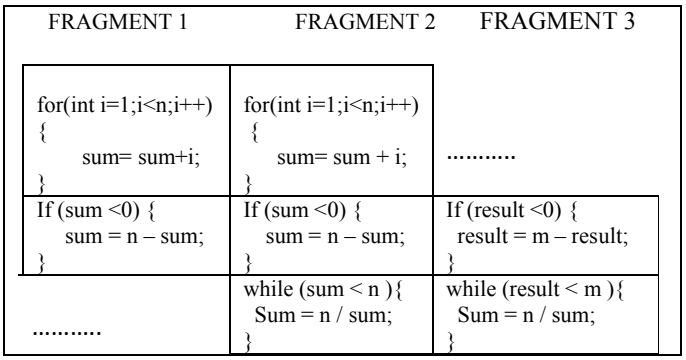

Fig: 1.1 Clone Pair and Clone Class

A. Different Types Of Clones

The cloning is performed based on to main constraints which is the textual similarity and the functional similarity.

- *Type I Clones:*

In *Type I* clones, a copied code fragment is the same as the original. However, there might be some variations in whitespace (blanks, new line(s), tabs etc.), comments and/or layouts. *Type I* is widely known as *Exact clones*.

- *Type II Clones:*

A *Type II* clone is a code fragment that is the same as the original except for some possible variations about the corresponding names of user-defined identifiers (name of variables, constants, class, methods and so on), types, layout and comments. The reserved words and the sentence structures are essentially the same as the original one. We see that the two code segments change a lot in their shape, variable names and value assignments. However, the syntactic structure is still similar in both segments.

- *Type III Clones:*

In *Type III* clones, the copied fragment is further modified with statement(s) changed, added and/or deleted. This copied fragments with one statement inserted is called *Type III* code clone of the original with a gap of one statement inserted.

- *Type IV Clones:*

Type IV clones are the results of semantic similarity between two or more code fragments. In this type of clones, the cloned fragment is not necessarily copied from the original. Two code fragments may be developed by two different programmers to implement the same kind of logic making the code fragments similar in their functionality. Functional similarity reflects the degree to which the components act alike, i.e., captures similar functional properties and similarity assessment methods rely on matching of pre/post-conditions.

II. **RELATED WORK**

In the existing system we use a tool called as the dup tool. The Dup tool[5] uses a line-by-line parameterized match to identify code portions that differ in semantic substitution of variable and constant names. This tool do not easily scale up because it is expensive. A string matching algorithm is also applied by the Duploc tool[4]. It offers a clickable matrix display that allows users to visually inspect the source code that produced the match. Like our semi automated approach, automatic clone detection and visual exploration of code are combined to guide refactoring. Here a viewing tool is presented that identifies exact repetitions of text using fingerprints, which are short strings used in place of larger data objects for more efficient comparisons. Sif is based on the same approach. CCFinder concatenates the tokens of a single file into a single token sequence, skipping whitespaces and applying transformation rules, such as replacement of variables with special tokens.

From all the substrings in the transformed token sequence, equivalent pairs are detected as clone pairs. Since this tool uses line by line parameterized match, this tool does not easily scale up because this is expensive.

III. PROPOSED SYSTEM

Our aim is to create a tool in JAVA which is used to find the potential function clones in HTML pages. The main aim is to identify all the various types of clones. Recently, clone identification has been proposed for static web documents, written in HTML. However, modern web applications are a mixture of HTML and scripting language code, where scripts can run as event handlers on the client-side or perform HTTP processing on the server-side. Scripts come embedded in client pages, i.e., documents available to browsers, as the content of the script HTML element, or they are retrieved from include files(containing pure scripting code with no HTML) using the src attribute (of the script HTML element) in every client page that needs them. The vast majority of client scripts are written with JavaScript. On the server side, the enabling technologies are more varied depending more on the vendors than on standards. A major approach to server-side processing of HTTP requests is using server pages, i.e., documents containing HTML annotated with server-side interpreted scripts. Many scripting languages are supported and representative examples are Java Server Pages (JSP), Microsoft's Active Server Pages (ASP), and PHP. The main advantages of this system is that it can detect the function clones which is present in the web pages with the help of the java script.

Our approach uses as input the report of potential cloned functions as a guide to the visual inspection of code. The goal of this stage is to check whether homonym script functions can be actually considered clones, and to identify the opportunities of refactoring

The first level, *Identical*, holds when the two functions are exactly equal, because no changes have been applied after the copy. This is the simplest occurrence of function cloning: it does not matter which of the copies will be taken off to eliminate duplication.

The second level, *Nearly-identical*, occurs when the two functions differ for modifications which have no effect on output or application state.

Analogously to the first level, any of the cloned functions can be removed during refactoring, but you need to choose which copy will be discarded. Changes to indentation, comments, and blank lines surely fall in this class.

The third level, *Similar*, takes place when two script functions have common characteristics, such as same code structure and same expressions, but refactoring will require changes to unify the functions. This may happen when the two function clones have different output statements or work on different inputs.

The fourth level, *Distinct*, occurs when two script functions, albeit homonym, differ so much in what they do (and then in how they do it) that any refactoring for eliminating duplication would not make sense.

IV.DESIGN OF ARCHITECTURE

The architecture consists of four modules as shown in fig 1.2 are:

1. Transformation
2. Clone Detection
3. Clone Extraction
4. Clone Documentation

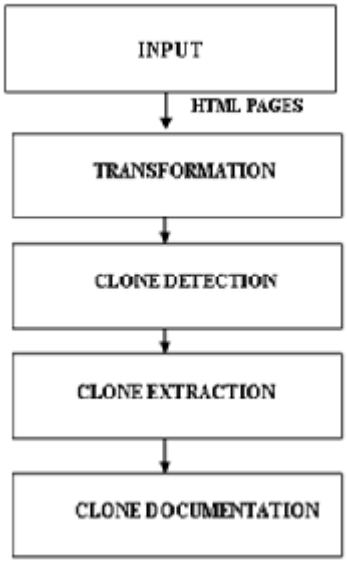

Fig:1.2 PROPOSAL MODULES

1. *Transformation*

The comparison units of the source code are transformed to another intermediate internal representation for ease of comparison or for extracting comparable properties. This transformation is just removing the whitespace and comments to very complex representation and/or extensive source code transformations.

- Pretty printing of source code:

Pretty printing is a simple way of reorganizing the source code to a standard form. By applying pretty printing, source code of different layouts can be transformed to a common standard form. Pretty printing is normally used by the text-based clone detection approaches to avoid the false positives that occur due to the different layouts of the similar code segments. Cordy et al. use an *extractor* to generate separate pretty-printed text file for each of the potential clones obtained using an island grammar.

- Removal of comments:

Most of the approaches ignore/remove comments from the source code before performing the actual comparison. Marcus & Maletic search for similarities of concepts extracted from comments and source code elements. Mayrand et al., on the other hand, use metrics to measure the amount of comments and use that metric as a measuring metrics to find clones.

- Removal of whitespace:

Almost all the approaches (except line-based approaches) disregard whitespace. Line-based approaches remove all whitespace except line breaks. Davey et al use the indentation pattern of pretty printed source text as one of the features for their attribute vector. Mayrand et al. use layout metrics like *number of non-blank lines*.

- Transformation of program elements:

In addition to identifier normalizations, several other transformation rules may be applied to the source code elements. In this way, different variants of the same syntactic element may treat as similar to find clones.

2. *Clone Detection*

The transformed code is next input to a suitable comparison algorithm where transformed comparison units are compared to each other to find a match. Using the order of the comparison units, adjacent similar units are summed up to form larger units. For fixed granularity clones, all the comparison units that belong to a source unit are aggregated. For free granularity clones, on the other hand, aggregation is continued as long as the aggregated sum is above a given threshold for the number of aggregated comparison units. This makes sure that

the aggregation is continued until the largest possible group of comparison units is found. The output is a list of matches with respect to the transformed code. These matches are either already in the clone pair candidates or have to aggregate to form clone pair candidates. Each clone pair is normally represented with the location information of the matched fragments in the transformed code.

3. Clone Extraction

In this phase, false positive clones are filtered out with manual analysis and/or a visualization tool.

- Manual Analysis

After extracting the original source code, raw code of the clones of the clone pairs are subject to the manual analysis. In this phase, false positive clones are filtered out.

- Visualization

The obtained clone pair list can be used to visualize the clones with a visualization tool. A visualization tool can speed up the process of manual analysis for removing false positives or other associated analysis.

4. Clone Documentation

After the clones are being detected and are extracted, then finally the clones that are extracted are identified and all the clones are documented according to their respective types for the further purpose.

V. CONCLUSION

The model proposed here outlines an algorithm capable of detecting all four clone types. By this identification the line of code of the program is being reduced which reduces the complexity for the programmer. Here we present a semi automated approach for identifying function clones embedded in HTML scripting of web applications. A list of potential cloned script functions is automatically produced by a tool, while classification of suspect clones is performed through visual inspection of source code. We took the chance to remove function clones in the web application for which there were more duplicates. However, that we found a high number of function clones does not mean that we were able to identify most of code duplication. In fact, our approach looks for clones at the function level but it does not detect duplicated code at lower granularity levels. Our approach might be refined, by developing specific redesign patterns for web applications to provide a guide to duplication removal. The automatic selection of potential clones could also be extended to other web enabling technologies, such as Java Server Pages or PHP.

REFERENCES

[1].Yue Jia, David Binkley, Mark Harman, Jens Krinke and Makoto Matsushita. KClone: A Proposed Approach to Fast Precise Code Clone Detection. International Workshop on Software Clones (IWSC) – 2009.

[2].Elmar Juergens, Florian Deissenboeck, Benjamin Hummel. Clone Detective – A Workbench for Clone Detection Research. International Conference on Software Engineering (ICSE) – 2009.

[3].S. Bellon, R. Koschke, G. Antoniol, J. Krinke, and E. Merlo.Comparison and evaluation of clone detection tools. IEEE Transactions on Software Engineering, 33(9):577–591, 2007.

[4].Ducasse, S., Rieger, M. and Demeyer, S. A Language Independent Approach for Detecting Duplicated Code. in International Conference on Software Maintenance, (Oxford, U.K., 1999).109-118.

[5]. Baker, B.S. On Finding Duplication and Near-Duplication in Large Software Systems. in SecondWorking Conference on Reverse Engineering, (Toronto, Canada, 1995). 86-95.

[6].Eytan Adar and Miryung Kim. SoftGUESS: Visualization and Exploration of Code Clones in Context. In the proceedings of the 29th International Conference on Software Engineering (ICSE'07), Tool Demo, pp.762-766, Minneapolis, MN, USA, May 2007 .

[7].Brenda S. Baker. Finding Clones with Dup: Analysis of an Experiment. *IEEE* Transactions on Software Engineering, Vol. 33(9): 608-621, September 2007.

[8].Lerina Aversano, Luigi Cerulo, and Massimiliano Di Penta. How Clones are Maintained: An Empirical Study. In Proceedings of the 11th European Conference on Software Maintenance and Reengineering (CSMR'07), pp. 81-90, Amsterdam, the Netherlands, March 2007.

Role of Surface Modified Nano Calcium Carbonate as Filler and Linseed Oil as an Extender in the Vulcanization of Acrylonitrile Butadiene Rubber (NBR) Nanocomposites

Kumarjyoti Roy, Md. Najib Alam, Subhas Chandra Debnath*

Department of Chemistry, University of Kalyani, Kalyani, Nadia 741235(W.B), India

*Corresponding author. Tel.: +91-33-2582-8750(O) [Ext. 305]

Fax: 91-33-2582-8282

E-Mail address: debnathsubhas@yahoo.com

Abstract—**The present study mainly focuses on the effect of surface modified nano calcium carbonate ($CaCO_3$) as filler and linseed oil as extender on the cure, mechanical and thermal properties of acrylonitrile butadiene rubber (NBR) nanocomposites. The surface modification of nano $CaCO_3$ is confirmed using Fourier transform infrared (FTIR) spectra. Only surface modified nano $CaCO_3$ is able to give little enhancement in the cure and mechanical properties of NBR nanocomposites in comparison to unmodified nano $CaCO_3$. But the incorporation of surface modified nano $CaCO_3$ along with linseed oil as an extender provides greater amount of enhancement in cure, mechanical and properties of NBR nanocomposites in comparison to unmodified nano $CaCO_3$ at same phr (Parts per hundred parts of rubber) level. The incredible improvement in the properties of NBR nanocomposites is the part of great interest for rubber researcher regarding the application of surface modified nano $CaCO_3$ as filler along with linseed oil as extender for NBR nanocomposites.**

Keywords-Surface modification, linseed oil, cure characteristics, mechanical properties.

I. INTRODUCTION

In practical application, rubbers are mostly applied with reinforcing fillers not only enhanced mechanical properties of rubber but also reducing the cost of the final product in industry, which is commercially interesting. Among the different types of filler, Carbon black (CB) is most widely used and the oldest filler in rubber materials. Since, the source of CB is petroleum, the preparation and processing of CB is hazardous. Carbon black not only causes pollution but also imparts black coloration in the rubber materials. Thus, the use of nano $CaCO_3$ as filler is an interesting way to substitute carbon black in rubber compounding [1-5]. Nano $CaCO_3$ is also important from environment point of view due to its low level of toxicity and less polluting nature [6].

Among the various types of rubber, the excellent oil and fuel resistance properties of NBR are utilized in many industry such as belts, hoses, O rings etc. Homogeneous dispersion of nano $CaCO_3$ within the rubber matrix is mandatory to achieve proper enhancement in NBR nanocomposites. Now, due to its hydrophilic nature a problem arises in the uniform dispersion of nano $CaCO_3$ within the rubber matrix [5]. Thus, surface modification of nano $CaCO_3$ by hydrophobic species is necessary for the wide use of nano $CaCO_3$ as filler in rubber industry. In this respect, application of stearic acid as surface modifier for nano $CaCO_3$ is an interesting way [4].

To accomplish far better dispersion of nano $CaCO_3$ within the rubber matrix linseed oil has been used as extender for styrene-butadiene rubber (SBR), natural rubber (NR) [1, 7]. Linseed oil is an important extender for rubber industry due to higher linoleic concentration [1]. With our best knowledge till now no vast study has been reported regarding the application of surface modified nano $CaCO_3$ as filler in combination with linseed oil as extender on the properties of NBR. The present work aims to examine the effect of surface modified nano $CaCO_3$ and linseed oil on the cure, mechanical and thermal properties of NBR nanocomposites.

II. EXPERIMENTAL SETUP

A. Materials and physical measurements

Acrylonitrile butadiene rubber (NBR KNB 35L) is supplied by Shilton Rubber Industries, Liluah. Zinc oxide (Merck), stearic acid (Loba Chemie, India), sulfur (Loba Chemie, India), tetra benzyl thiuram disulfide (TBzTD) (Apollo tyre, Ltd. India), calcium chloride (Merck), poly(ethylene glycol) (PEG; molecular weight 6000), potassium bicarbonate (Merck) and toluene (Merck) are used as received. Nano $CaCO_3$ is synthesized using the procedure given by Mishra et al. [1].

X-ray diffraction (XRD) pattern of nano $CaCO_3$ is recorded on a Xpertpro-Panalytical X-ray diffractometer. FTIR spectra (ν_{max} in cm^{-1}) of surface modified nano $CaCO_3$ are recorded on a Perkin-Elmer L 120-000A spectrometer (ν_{max} in cm^{-1}) on KBr disks. The cure characteristics of the different stocks are obtained using the Monsanto Rheometer R-100 at 3 degree arc for 160 ^oC. The stocks are cured under pressure at 160 ^oC for optimum cure time (t_{90}), keeping vulcanizates for 24 hrs at ambient temperature before measuring the modulus at 100% (M_{100}) elongation, tensile strength (T.S.) and elongation at break (E.B. in %) according to ASTM D 412-51 T using dumbbell shaped test pieces in an Amsler (Sweden) tensile tester. Hardness (shore A) of the vulcanizates is measured by a Hirosima Hardness Tester as per ASTM D 1415-56T. Thermogravimetric analysis (TGA) is carried out in order to study the thermal behavior of NBR vulcanizates. TGA scans are performed using a TA instrument (Q 5000) under nitrogen flow from 20 ^oC to 800 ^oC with a heating rate of 10 ^oC/min.

B. Synthesis of $CaCO_3$ nanoparticles

Nano $CaCO_3$ is synthesized by a procedure given by Mishra et al. [1]. At first, 110 g of calcium chloride is dissolved in 100 ml of distilled water. Then, 248 g of PEG is dissolved in 100 ml of water under mildly heated condition. A complex is then prepared by the mixing of calcium chloride and PEG in a molar ratio 1: 32. A solution of K_2CO_3 is prepared by dissolving 106 ml of K_2CO_3 in 100 ml of distilled water. Then, the solution of K_2CO_3 is added to the previously prepared complex and the mixture is digested for 12 hrs. The resulting precipitate is filtered, washed with water and dried in a vacuum oven to obtain nano $CaCO_3$ nanoparticles [1].

C. Preparation of NBR composites

NBR is masticated in a two-roll mixing mill, and then Zinc oxide (ZnO) and stearic acid are added and again masticated. After that accelerator and sulfur are incorporated to the rubber matrix and the mixing is done near about for 10 minutes. At last different types of filler with and without linseed oil are added and the mixing done for sufficient time. Mixing composition of different ingredients is presented in Table 1.

III. RESULTS AND DISCUSSION

A. Nanoparticle characterization using X-Ray Diffraction (XRD) analysis

The XRD pattern of synthesized nano $CaCO_3$ is recorded in Figure 1. The detected XRD pattern is found to be similar with the earlier report [1]. The nano size of $CaCO_3$ particle is confirmed from XRD pattern using well known Scherrer equation [1, 7]. The Scherrer equation is given as:

$$d\ (Å) = K\lambda/(B \cos\theta)$$

Here, d is the particle size, K is a constant nearly about to unity, λ is 1.542, B is the integral half-width, and θ is the diffraction angle. The particle size for the synthesized nano $CaCO_3$ is found to be 40 ± 5 nm.

B. Evaluation of surface modification using FTIR analysis

The FTIR spectrum of stearic acid modified $CaCO_3$ nanoparticles is shown in Figure 2. The peak nearly 1680 cm^{-1} is due to the appearance of carboxylic salt and thus, this peak clearly indicates stearic acid is present on the surface of $CaCO_3$ nanoparticles via an ionic bond [5]. The peaks nearly at 2916 cm^{-1} and 2850 cm^{-1} characterize C-H stretching frequency [5]. The peaks nearly at 875 cm^{-1} and 711 cm^{-1} characterize the presence of long alkyl chain on the surface of nano $CaCO_3$ [5].

C. Cure characteristics of NBR vulcanizates

Cure parameters of NBR vulcanizates in presence of unmodified nano $CaCO_3$, surface modified nano $CaCO_3$ with and without linseed oil are calculated at 160 ^oC and the results are presented in Table 2. The highest value of maximum rheometric torque (R_∞) is obtained in mix no 6 containing 4 phr surface modified nano $CaCO_3$ as filler along with linseed oil. The result indicates maximum level of interaction of rubber chain with nano filler occurs in mix no 6 due to the plasticizing effect of linseed oil [7].

The cure enhancement of NBR vulcanizates in presence of linseed oil becomes clear from the value of cure rate index (CRI). At the same level of filler loading, the value of CRI remains unchanged for NBR vulcanizates containing unmodified and surface modified nano $CaCO_3$. But the presence of linseed oil along with surface modified nano $CaCO_3$ successfully increases the value of CRI of NBR vulcanizate. This is mainly due to the homogeneous dispersion of nano $CaCO_3$ within the rubber matrix in presence of linseed oil.

Thus, for NBR nanocomposites surface modified nano $CaCO_3$ with linseed oil causes much greater cure enhancement in comparison to surface modified nano $CaCO_3$ without linseed oil.

Table 1: The formulation of studied vulcanizates in parts per hundred parts of rubber (phr)

Ingredients	Mix No					
	1	2	3	4	5	6
NBR	100	100	100	100	100	100
ZnO	5	5	5	5	5	5
Stearic acid	2	2	2	2	2	2
TBzTD	4.896	4.896	4.896	4.896	4.896	4.896
Sulfur	0.5	0.5	0.5	0.5	0.5	0.5
Unmodified nano $CaCO_3$	0	2	4	6		-
Surface modified nano $CaCO_3$	-	-	-	-	4	4
Linseed oil	-	-	-	-	-	2

Table 2: Cure characteristics of NBR vulcanizates at 160 ^oC in presence of unmodified and surface modified nano $CaCO_3$

Mix No	Maximum rheometric torque, R_∞ (dNm)	Optimum cure time, t_{90} (min)	Scorch time, t_2 (min)	Cure rate index, CRI= $100/(t_{90}-t_2)$ (min^{-1})
1	29	10	3	14.28
2	30	10	3.25	14.81
3	32.5	9.5	3.5	16.66
4	29.5	9.5	3.25	16
5	33	9.5	3.5	16.66
6	35	9	3.25	17.39

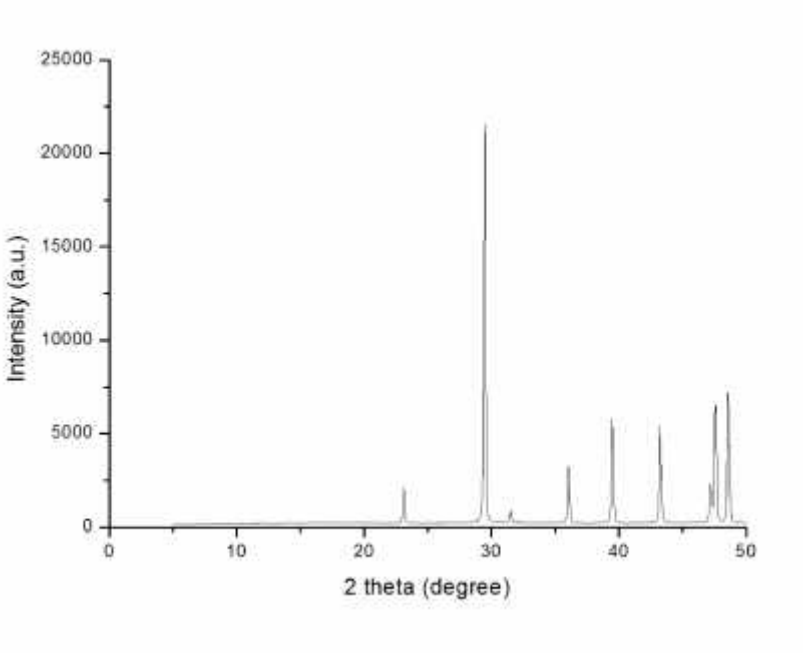

Fig 1. XRD pattern of nano $CaCO_3$

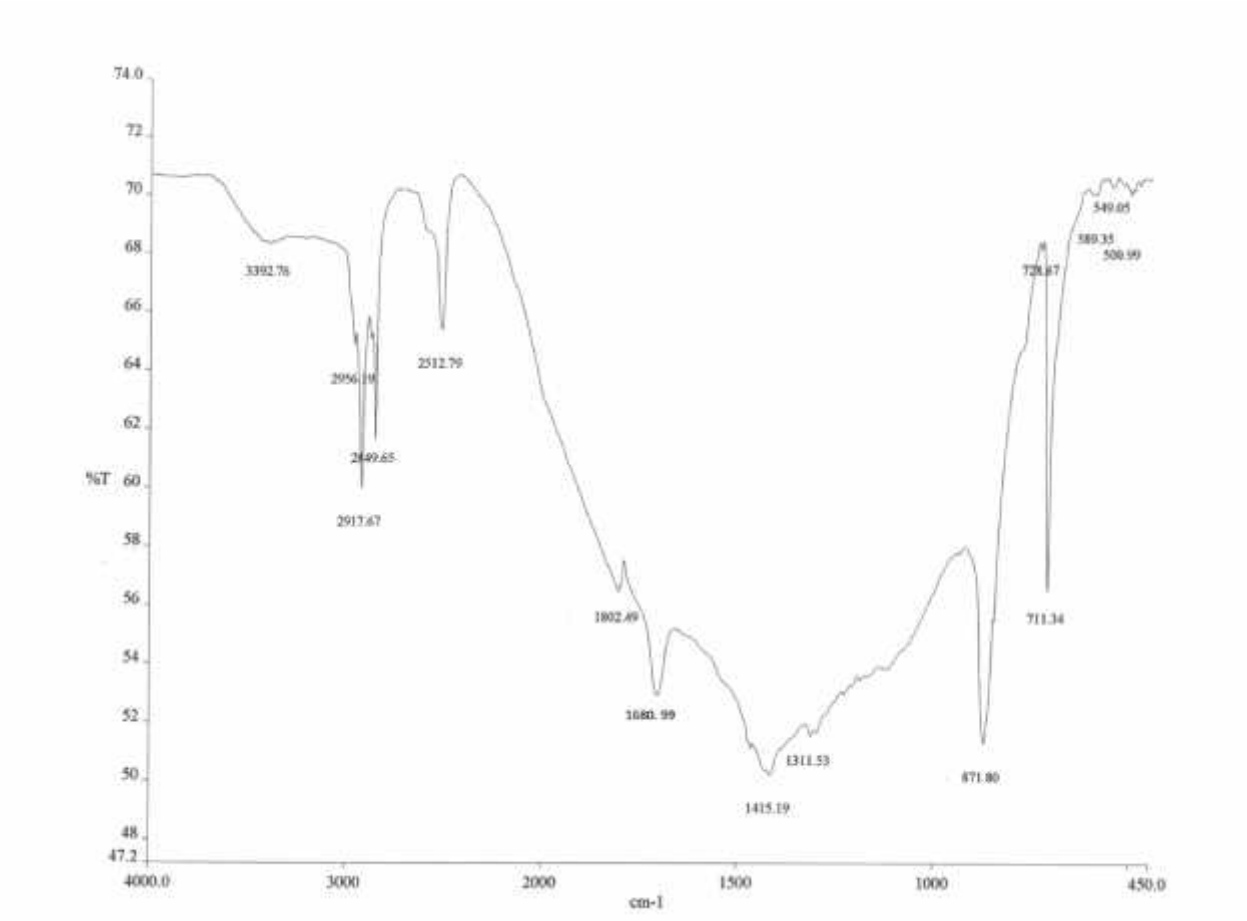

Fig 2. FTIR spectrum of stearic acid modified nano $CaCO_3$

D. Mechanical properties of NBR vulcanizates

The mechanical properties of various NBR vulcanizates (mix no 1-6) are also studied and shown in Table 3. For NBR vulcanizates, with increasing the amount of unmodified nano $CaCO_3$, the modulus value at 100% elongation (M_{100}) increases upto 4 phr filler loading. Above 4 phr filler loading, M_{100} value decreases due to agglomeration of filler particles [1, 7]. On the other hand, surface modified nano $CaCO_3$ shows an enhancement in the M_{100} value of NBR nanocomposite in comparison to unmodified nano $CaCO_3$. Further large enhancement in the M_{100} value is observed when surface modified nano $CaCO_3$ is used as filler in combination with linseed oil as extender. This is described by the better dispersion of nano filler within the rubber matrix in presence of linseed oil, which results greater interfacial interaction between nano fillers and rubber chain [7].

Like M_{100} value, the value of tensile strength also increases upto 4 phr filler loading. The variation of tensile strength of NBR vulcanizates containing different types of filler are shown in Figure 3. The presence of linseed oil plays a vital role on the improvement of tensile strength of NBR vulcanizates and 4 phr surface modified nano $CaCO_3$ along with linseed oil shows an increment by 18.30% in the value of tensile strength in comparison to 4 phr unmodified nano $CaCO_3$. The variation of elongation at break is analogous with tensile strength.

E. Swelling studies

The swelling indexes of mix no 3 (containing 4 phr unmodified nano $CaCO_3$), mix no 5 (containing 4 phr modified nano $CaCO_3$) and mix no 6 (containing 4 phr modified nano $CaCO_3$ with linseed oil) are represented in Table 4. The value of swelling index is lower for mix no 6 in comparison to other two mixes. Thus, from the values of swelling index it is clear that uniform dispersion of surface modified nano $CaCO_3$ occurs within the rubber matrix in presence of linseed oil and it results in greater amount of crosslinking of rubber for mix no 6 [1].

Table 3: Mechanical properties of NBR vulcanizates cured at 160 ^oC

Mix No	M_{100} (MPa)	T.S. (MPa)	E.B. (%)	Hardness (shore A)
1	0.956	1.861	440	56
2	1.018	2.252	450	57
3	1.058	2.617	550	58
4	1.047	2.442	500	58
5	1.074	2.890	550	58
6	1.122	3.097	600	58

Table 4: Variation in swelling index and thermal properties of NBR vulcanizates

Mix No	Swelling index (Q)	T_i (^oC)	T_{max} (^oC)
3	2.42	397	442
5	2.27	398	442
6	2.14	405	444

F. Thermal properties of NBR vulcanizates

Thermogravimetric analysis (TGA) and differential thermogravimetric analysis (DTA) curves of NBR vulcanizates (mix no 3, 5, 6) are shown in figures 4a and 4b. TGA study indicates rapid degradation region shifted towards little higher temperature for mix no 6 (containing linseed oil as extender) than other two mixes. However, only surface modified nano $CaCO_3$ without linseed oil is not able to enhance the thermal stability of NBR vulcanizate in comparison to unmodified nano $CaCO_3$.

The little thermal enhancement of mix no 6 over other two mixes (mix no 3 and 5) is confirmed from DTA analysis. The onset decomposition temperature (T_i) and the temperature at which the rate of decomposition is maximum (T_{max}) are calculated from DTA curve and represented in Table 4. Although T_{max} values are almost same for three mixes (mix no 3, 5, 6), but the T_i value of mix no 6 shifted towards higher temperature in comparison to mix no 3 and 5. This data clearly reveals the greater thermal stability of NBR nanocomposite containing modified nano $CaCO_3$ as filler along with linseed oil as extender in comparison to NBR nanocomposite containing only modified nano $CaCO_3$ or unmodified nano $CaCO_3$ as filler.

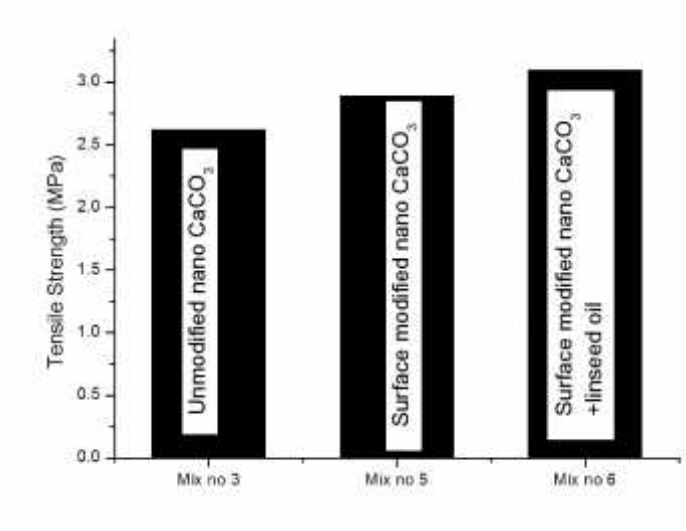

Fig 3. Variation of tensile strength of NBR nanocomposites

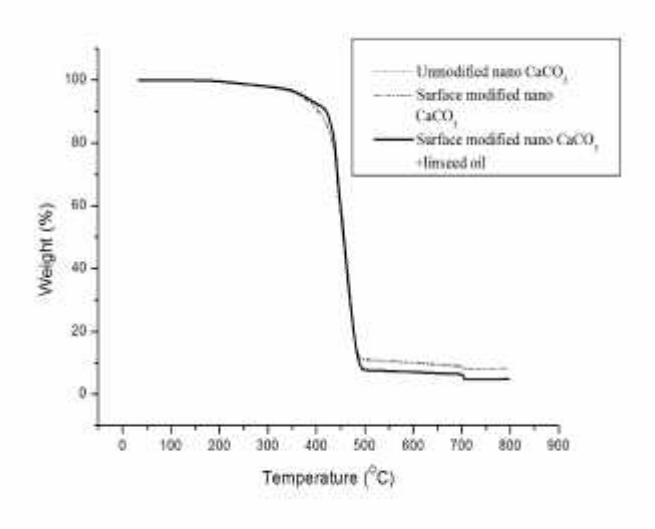

Fig 4a. TGA analysis of NBR vulcanizates

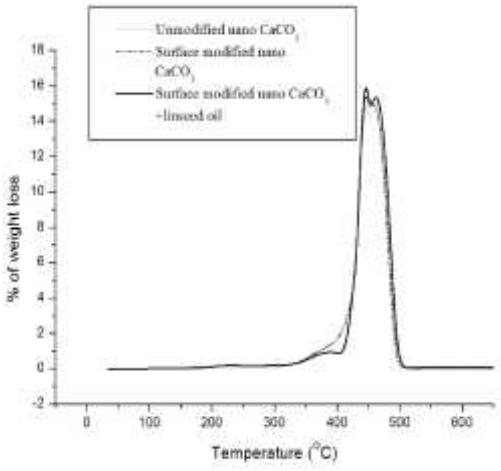

Fig 4b. DTA curve of NBR vulcanizates

IV. CONCLUSION

The present study describes the importance of linseed oil as extender for better filler dispersion in NBR nanocomposites. Only surface modified nano $CaCO_3$ provides a little enhancement in the cure and mechanical properties of NBR nanocomposites in comparison to unmodified nano $CaCO_3$. Furthermore, the presence of linseed oil along with surface modified nano $CaCO_3$ results an extraordinary improvement in the cure and mechanical properties of NBR nanocomposites. Only surface modified nano $CaCO_3$ is not able to enhance thermal stability of NBR nanocomposites, although the use of linseed oil along with surface modified filler produces little thermal stability in NBR nanocomposites. Thus, the application of nano $CaCO_3$ in combination with linseed oil will be an important approach for the industrial use of NBR nanocomposites.

V. ACKNOWLEDGEMENTS

Authors thankfully acknowledge DST-PURSE programme, Govt. of India, for financial support.

REFERENCES

[1] S. Mishra and N.G. Shimpi, "Mechanical and flame-retarding properties of styrene–butadiene rubber filled with nano-$CaCO_3$ as a filler and linseed oil as an extender", J. Appl. Polym. Sci., Vol. 98, pp. 2563-2571, 2005.

[2] S. Mishra, N. G. Shimpi and U. D. Patil, "Effect of Nano $CaCO_3$ on thermal properties of Styrene Butadiene Rubber (SBR)", J. Polym. Res.,Vol. 14, pp. 449-459, 2007.

[3] S. Mishra and N. G. Shimpi, **"**Studies on Mechanical, Thermal, and Flame Retarding Properties of Polybutadiene Rubber (PBR) Nanocomposites", Polym. Plas. Technol. Eng., Vol. 47, pp. 72-81, 2007.

[4] S. Mishra, N. G. Shimpi and A. D. Mali, "Influence of stearic acid treated nano-$CaCO_3$ on the properties of silicone nanocomposites", J. Polym. Res., Vol. 18, pp. 1715-1724, 2011.

[5] S. Mishra, N. G. Shimpi and A. D. Mali, "Investigation of photo-oxidative effect on morphology and degradation of mechanical and physical properties of nano $CaCO_3$ silicone rubber composites", Polym. Adv. Technol., Vol. 23, pp. 236-246, 2012.

[6] C. M. Deng, M. Chen, N. J. Ao, D. Yan and Z. Q. Zheng, "CaCO3/Natural Rubber Latex Nanometer Composite and Its Properties", J. Appl. Polym. Sci., Vol. 101, pp. 3442-3447, 2006.

[7] S. S. Fernandez and S. Kunchandy, "Effect of Nano $CaCO_3$ as a Filler and Linseed Oil as an Extender on the Cure and Mechanical Properties of Natural Rubber Vulcanizates", Orient. J. Chem., Vol. 29, pp. 219-226, 2013.

Fluid Flow Analysis And Velocity Distribution Along A Gas Turbine Blade Profile Using CFD Technique And Tool

Bhupendra E. Gajbhiye*, Sachin V. Bhalerao**, Amit G. Pdgelwar***
Mech Engg Dept, Jawaharlal Darda Institute of Engineering and Technology,
Yavatmal, MH, India
Mail ID: bhupendragajbhiye@gmail.com*, sv_bhalerao@rediffmail.com**, amit_padgelwar@yahoo.co.in***

Abstract—**Gas turbine blade are designed to operate at high temperature which just below material melting temperature. It always undergoes high temperature and pressures which creates stresses in the gas turbine blade material. Due to this gas turbine mostly fails before its specified time period. It also tends to damage stators in turbine engine. The working environment of gas turbine blade is very hot, aggressive and harsh for blade material. But blade metallurgy and coating always saves the blade material for long period of time. It is observed that gas turbine blade fails due to hot flowing fluid over its profile. Means flowing fluid makes impact on blade working life period and ultimately of course on rotation of blades. The actual flow of hot fluid in gas turbine blade decides the impact in blade. By simulating actual flow of hot fluid on blade can give more information about that environment and we can understand the working phenomenon. If we capable to understand the flow of hot fluid in gas turbine then we can understand root causes of gas turbine blade failure.**

In this paper we are simulating actual working condition of gas turbine blade by using CFD tool. Further nature of hot fluid flow and its effect on gas turbine blades are discussed. The various parameters are included for exact simulation of fluid flow.

Keywords: CFD (Computational Fluid Dynamics)

I. INTRODUCTION

Due to high temperature, pressure which is created by hot flowing fluid over a gas turbine blade, it tends to failure after some specific time period. There are several types of failure accurse in gas turbine blade. Few of the failures and investigations are discussed below.

When 150 MW gas turbine examined, it fails with extremely high vibrations, it is observed that all blade including stationary blades were damaged at extremely high level. Blade had completed only 1800 hours of life with intermittent mode running. More important is that there was no damage in other sections. It was pure blade failure and it is due to the crack in the securing pin hole (stress raiser) located at the root of the blade and propagated. [1]

Cooling system is installed on generator because of high increasing temperature. Employing a fan of a cooling system on the generator at the end sides of its rotor is generally preferred. In some cases, due to the fracture of blades short circuit between rotor and stator can accurse and generator tends to fail with huge financial loss. [2]

Most frequent damages in gas turbine blade are creep and stress rupture. These are accurse due to high working temperature and hot flowing fluid. But the working of gas turbine blade is based on microstructure of blade

material. During service exploration blade material microstructural degradation can accurse. Hence it is also important to perform detailed microstructural examination of gas turbine blade. For effective microstructural analysis of turbine blades after service exposure, a reliable method should be there. [3]

While designing gas turbine blade by thermal point of view, prediction of stresses and coefficient of heat transfer plays an important role. Some studies are based on an investigation of stresses and heat transfer in blades with circular cooling passages. FVM and FEM commercial codes are used for 3D-numerical conjugated simulations in CFX and ANSYS tools to find out of the heat transfer coefficients distributions along a blade and the stresses, respectively. On the stagnation point of blade leading edge coefficient of heat transfer is more because of incoming gas flow impingement. But lowest on trailing edge at pressure and suction sides because of thermal boundary layer formation. At the trailing edge near the mid-span, the maximum material temperature and the maximum thermal stress occurs. [4]

Nickel base superalloy provides strength at high temperature hence mostly used in certain applications. As blade works at high temperature it suffers service induced degradation. First stage blade of 3 MW gas turbine having material nickel-base alloy Nimonic 80A which is capable to sustain high temperature. Metallographic and microhardness test was done on blades it is tested for microstructure and microhardness with four different blade zones i.e. root, 30%, 60%, and 90% to total hot region height of blade. Creep damage is found on the basis of performed test. Considering peak loading of centrifugal force and surface (aerodynamic) loads Finite element method (FEM) analysis is conducted to predict the life of turbine blades using the Larson–Miller method. Also two heat treatment cycles are suggested and applied. The heat treatments effects on grain size, volume friction of c0 primary phase, and micro hardness are investigated. Detailed analysis results explain the root cause of failure of blade and it is loss of coating resistance at high temperature due to oxidation, corrosion, erosion and inters diffusion of coating-substrate. [5]

As gas turbine blades are subjected to high temperature working conditions cooling of blades is an important factor. There are various methods are available to perform this task, one of them is providing radial holes to high velocity cooling air throughout the blade span. Due to this blade temperature considerably reduces. Steady state thermal & structural performance on blade which has material N155 & Inconel 718 nickel-chromium alloys with four separate models which consisting of solid blade and blades with several holes (i.e. 5, 9 & 13 holes) able to find out optimum number of blades. Also found that Inconel 718 is better suited for high temperature applications. [6]

II. CAD MODELING OF GAS TURBINE BLADE

CAD modelling of gas turbine blade is an important part of entire project. Because the blade profile is very complex and it will decide the nature of the hot flowing fluid over a blade. The advanced CAD software i.e. CATIA V5R17 is selected for modeling the gas turbine blade.

A. Parameters of gas turbine blade

Various dimensions required to model gas turbine blade are obtained by Reverse Engineering Process. The gas turbine blades are taken for the reference purpose with owners [7] permission. Steel rule, Screw gauge, Micrometer, Vernier caliper etc instruments are used for taking the dimensions from actual blades. CAD model of

gas turbine blade is prepared in such a way that it should exactly represent the actual blade virtually and its profile can be taken for the further analysis.

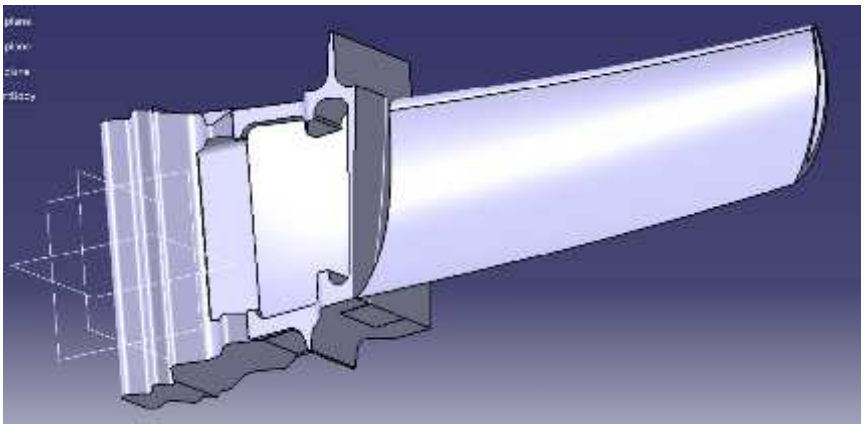

Figure 1. CAD model of first stage gas turbine Blade

B. IGES (Neutral File) format.

After creating model of gas turbine blade we need to convert it into suitable Neutral File Format. Now to perform analysis on gas turbine blade, it must be imported in FEA software. But FEA software can't work directly on CAD file. Hence the universal accepted format for exchanging such data is used which is called as neutral file format.

It is also called vendor-neutral standard format. The IGES (Initial Graphics Exchange Specification) is used to exchange geometric models between various CAD and CAE softwares. But it is able to import partial files which contain dimensions and geometry related data. We are also able to import multiple files into the same model. [8]

III. COMPUTATIONAL FLUID DYNAMICS (CFD) ANALYSIS

Here the blade assembly is considered for simulating hot fluid flow over a profile. Specific domain for this purpose is set and by applying boundary condition required results can be obtained. The prepared domain for CFD analysis is shown below figure.

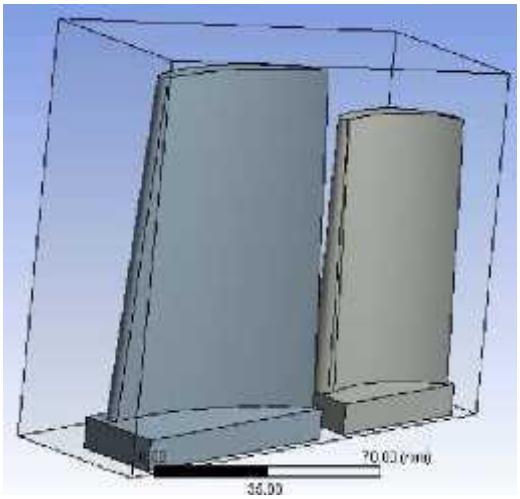

Figure 2. Blade assembly domain for CFD analysis

A. CFD Analysis.

We are using ANSYS 14.0 Fluent CFD tool for performing this analysis. [8]

Following figure shows the meshed view of considered domain. The overall domain is under the influence of hat fluid. So such kind of fluid properties is applied and behavior of fluid is checked out.

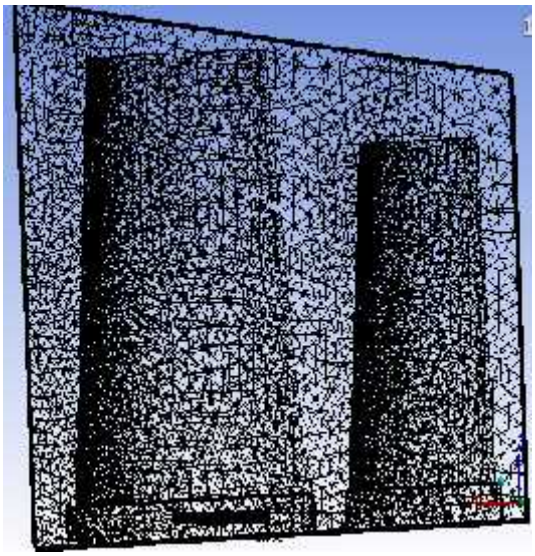

Figure 3. Meshed view of blade and vane assembly

IV. RESULTS OF CFD ANALYSIS

In this step, we will display the results of the simulation, Results calculated by performing CFD analysis are shown below.

A. Velocity Distribution along a blade profile.

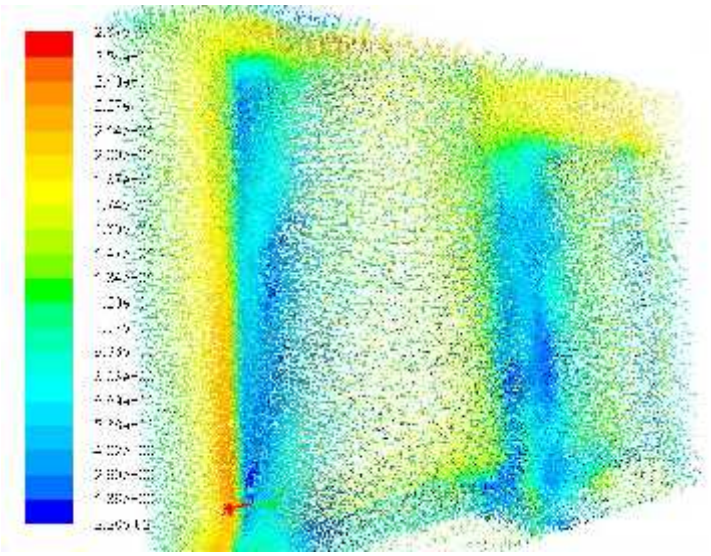

Figure 4. Velocity Counters on Blade profile.

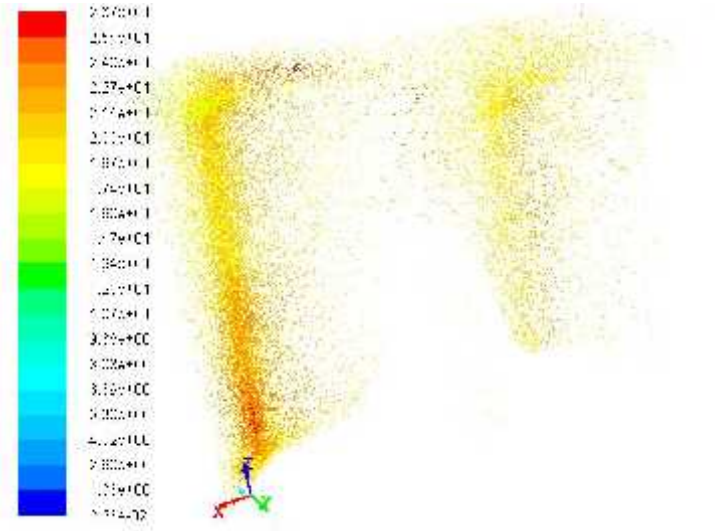

Figure 5. High Velocity points on Blade profile.

B. Temperature Distribution along a blade profile

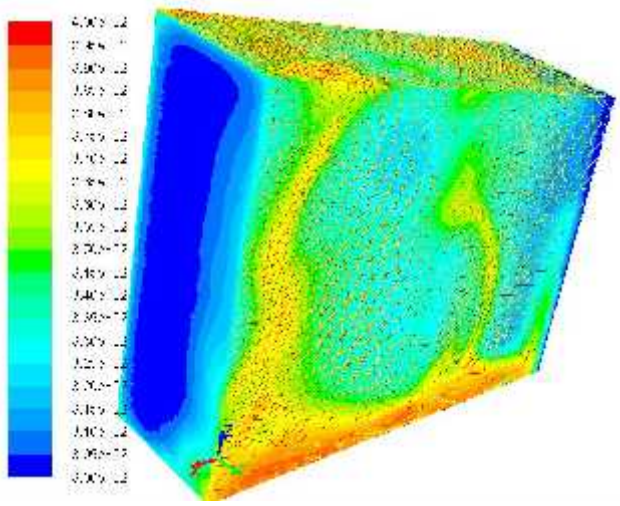

Figure 6. Temperature Counters on Blade profile

Above figures illustrates the nature of fluid flow, temperature distribution, Velocity vectors etc. By studying these results we can understand where the possible defects may accurse. The behavior of blade material at high temperature can be examined.

Following summerised results also help for studying flow of hot fluid on blade.

TABLE1 RESULTS OBTAINED BY PERFORMING CFD ANALYSIS.

Sr No	Properties	Minimum Value	Maximum Value
1	Velocity	0 m/s	25.69 m/s
2	Temperature	1000C	8000C
3	Pressure	-996.20 Pa	20.66 pa
4	Density	1.22 kg/m3	1.22 kg/m3
5	Turbulence	0.0037 m2/s2	175.36 m2/s2
5	Heat Transfer Rate	153 w	153 w

V. CONCLUSIONS

Based on the CFD analysis it is to be state that, the root cause of failure of gas turbine blade is high working temperature with high pressure difference. Results show the temperature counters on blade profile which illustrate the possible damage due to overheating.

Conducting thermal mapping CFD tool provides extensive information about failure of gas turbine blade. It gives better approximate solutions with material saving. It can be implemented where the direct contact thermal mapping techniques cannot be applied. The following observations can also conclude accordingly.

- Due to high temperature at middle and top of the blade there is always possibility of failure.
- Pressure difference affects the blade material at high temperature.
- Turbulence in hot fluid is due to pressure difference.
- CFD tools are best for thermal mapping of gas turbine blade and are also reliable.

REFERENCES

[1] J. Kubiak , G. Urquiza, J.A. Rodriguez, G. González, I. Rosales, G. Castillo, J. Nebradt, “Failure analysis of the 150MW gas turbine blades” State University of Morelos, Centro de Investigación en Ingeniería y Ciencias Aplicadas, CIICAp, Av. Universidad 1001, Col. Chamilpa, C.P. 62209, Cuernavaca, Morelos, Mexico,Accepted 12 August 2008, Available online 29 August 2008, Sciencedirect.

[2] S.E. Moussavi Torshizi, S.M. Yadavar Nikravesh, A. Jahangiri, “Failure analysis of gas turbine generator cooling fan blades”,PWUT-Power and Water University of Technology, P.O. Box 16765-1719, Tehran, Iran, Available online 24 December 2008, Sciencedirect.

[3] M. Sujata, M. Madan, K. Raghavendra, M.A. Venkataswamy, S.K. Bhaumik, “Identification of failure mechanisms in nickel base superalloy turbine blades through microstructural study”, Failure Analysis & Accident Investigation Group, Materials Science Division, National Aerospace Laboratories, Council of Scientific and Industrial Research (CSIR), Bangalore 560 017, India, Available online 26 May 2010, Sciencedirect.

[4] Kyung Min Kim, Jun Su Park, Dong Hyun Lee, Tack Woon Lee, Hyung Hee Cho, “Analysis of conjugated heat transfer, stress and failure in a gas turbine blade with circular cooling passages”, Department of Mechanical Engineering, Yonsei University, Seoul 120-749, Republic of Korea, Accepted 1 March 2011, Available online 8 March 2011, Sciencedirect.

[5] S. Kargarnejad, F. Djavanroodi, “Failure assessment of Nimonic 80A gas turbine blade”, Department of Mechanical Engineering, Urmia University of Technology, Urmia, Iran, Accepted 28 May 2012, Available online 30 August 2012, Sciencedirect.

[6] Jui-Sheng Chou, Chien-Kuo Chiu, I-Kui Huang, Kai-Ning Chi, “Failure analysis of wind turbine blade under critical wind loads”, Department of Construction Engineering, National Taiwan University of Science and Technology, 43 Sec.4, Keelung Rd., Taipei 106, aiwanm Accepted 2 August 2012, Available online 13 September 2012, Sciencedirect.

[7] R D V Prasad, G Narasa Raju, M S SSrinivasa Rao, N Vasudeva Rao, "Steady State Thermal & Structural Analysis Of Gas Turbine Blade Cooling System", Department of Mechanical Engineering, BVC Engineering College, Odalarevu, Andhra Pradesh, India. International Journal of Engineering Research & Technology (IJERT) Vol. 2 Issue 1, January- 2013.

[8] http://www.ansys.com
Ansys 14.0 workbench and Ansys 14.0 APDL Help

A Searching Strategy to Adopt Multi-Join Queries Based on Top-K Query Model

[1]M.Naveena, [2]S.Sangeetha,
[1]M.E-CSE, [2]AP-CSE
V.S.B. Engineering College,
Karur, Tamilnadu, India.
[1]naveenaskrn@gmail.com, [2]sangi.vs@gmail.com

***Abstract*—Asearch-as-you-type system determines answerson-the-fly as a user types in a keyword query, character by character. There arises a higher need to know the support search-as-you-type on data residing in a relational DBMS. The existing work on keyword query focuses on to support type of search using the native database SQL. The leverage existing database functionalities is to meet high performance requirement to achieve an interactive speed. It uses auxiliary indexes that are stored as tables to increase search performance. But the main drawbacks in existing work were that it handle search as you type for databases for single table at the same time multiple tables were not taken into consideration. The Proposed work presents a Fuzzy Multi-Join technique to support multiple tables for search as-you-type in relational databases. Further the proposal presents a Top-K Query Search model to support ranking queries for search as-you-type in relational databases Top-k join queries are generated in relational query processors.**

***Keywords*—**Search-as-you-type, Databases, SQL, Fuzzy Search.

I. INTRODUCTION

A Search-as-you-type on DBMS systems using the native query language (SQL). In other words, we want to use SQL to find answers to a search query as a user types in keywords character by character. Our goal is to utilize the built-in query engine of the database system as much as possible. In this way, we can reduce the programming efforts to support search-as-you-type.

In addition, the solution developed on one database using standard SQL techniques is portable to other databases which support the same standard. Similar observation are also made by Gravano et al. and Jestes et al. which use SQL to support similarity join in databases.

Rank-aware query processing has become a vital need for many applications. In the context of the Web, the main applications include building meta-search engines, combining ranking functions and selecting documents based on multiple criteria. Efficient rank aggregation is the key to a useful search engine. In the context of multimedia and digital libraries, an important type of query is similarity matching. Users often specify multiple features to evaluate the similarity between the query media and the stored media.

Most of these applications have queries that involve joining multiple inputs, where users are usually interested in the top-k join results based on some score function. Since most of these applications are built on top of a commercial relational database system, our goal is to support top-k join queries in relational query processors. The answer to a top-k join query is an ordered set of join results according to some provided function that combines the orders on each input.

More precisely, consider a set of relations R1 to Rm. Each tuple in Ri is associated with some score that gives it a rank within Ri. The top-k join query joins R1 to Rm and produces the results ranked on a total score. The total score is computed according to some function, f, which combines individual scores. Note that the score attached with each relation can be the value of one attribute or a value computed using a predicate on a subset of its attributes.

To increase the search performance and to achieve an interactive speed it uses auxiliary indexes stored as tables. Support both single-keyword and multi-keyword queries using the database language SQL. A higher need to know the support of search-as-you-type on data residing in a relational DBMS it uses ranking and multi-join technique.

II. RELATED WORK

ESTER further supports are designed by H. Bast et al. (2007) [1] a natural blend of such semantic queries with ordinary full-text queries. Moreover, the prefix search operation allows for a fully interactive and proactive user interface, which after every keystroke suggests to the user possible semantic interpretations of his or her query, and speculatively executes the most likely of these interpretations.

Imagine a user of a search engine is developed by I. Weber et el. (2006) [2] typing a query. Then with every letter being typed, we would like an instant display of completions of the last query word which would lead to good hits. At the same time, the best hits for any of these completions should be displayed. Known indexing data structures that apply to this problem either incur large

processing times for a substantial class of queries, or they use a lot of space. We present a new indexing data structure that uses no more space than a state-of-the-art compressed inverted index, but that yields an order of magnitude faster query processing times. Even on the large TREC Terabyte collection, which comprises over 25 million documents, we achieve, on a single machine and with the index on disk, average response times of one tenth of a second. We have built a full-edged, interactive search engine that realizes the proposed auto completion feature combined with support for proximity search, semi-structured (XML) text, sub word and phrase completion, and semantic tags.

Complete Search, an interactive search engine is developed by H. Bast (2007) [3] that offers the user a variety of complex features, which at first glance have little in common, yet are all provided via one and the same highly optimized core mechanism. This mechanism answers queries for what we call context-sensitive prefix search and completion: given a set of documents and a word range, compute all words from that range which are contained in one of the given documents, as well as those of the given documents which contain a word from the given range.

We propose a simple algorithm based on novel is designed by Y. Ma et al. (2007) [4], indexing and optimization strategies that solve this problem without relying on approximation methods or extensive parameter tuning. We show the approach efficiently handles a variety of datasets across a wide setting of similarity thresholds, with large speedups over previous state-of-the-art approaches.

A system which enables keyword-based search was developed by G. Bhalotia et al. (2002) [5] on relational databases, together with data and schema browsing. BANKS enables users to extract information in a simple manner without any knowledge of the schema or any need for writing complex queries. A user can get information by typing a few keywords, following hyperlinks, and interacting with controls on the displayed results.

III. A SEARCHING STRATEGY TO ADOPT MULTI-JOIN QUERIES BASED ON TOP-K QUERY MODEL

In top-k selection queries, the goal is to apply a scoring function on multiple attributes of the same relation to select tuples ranked on their combined score.

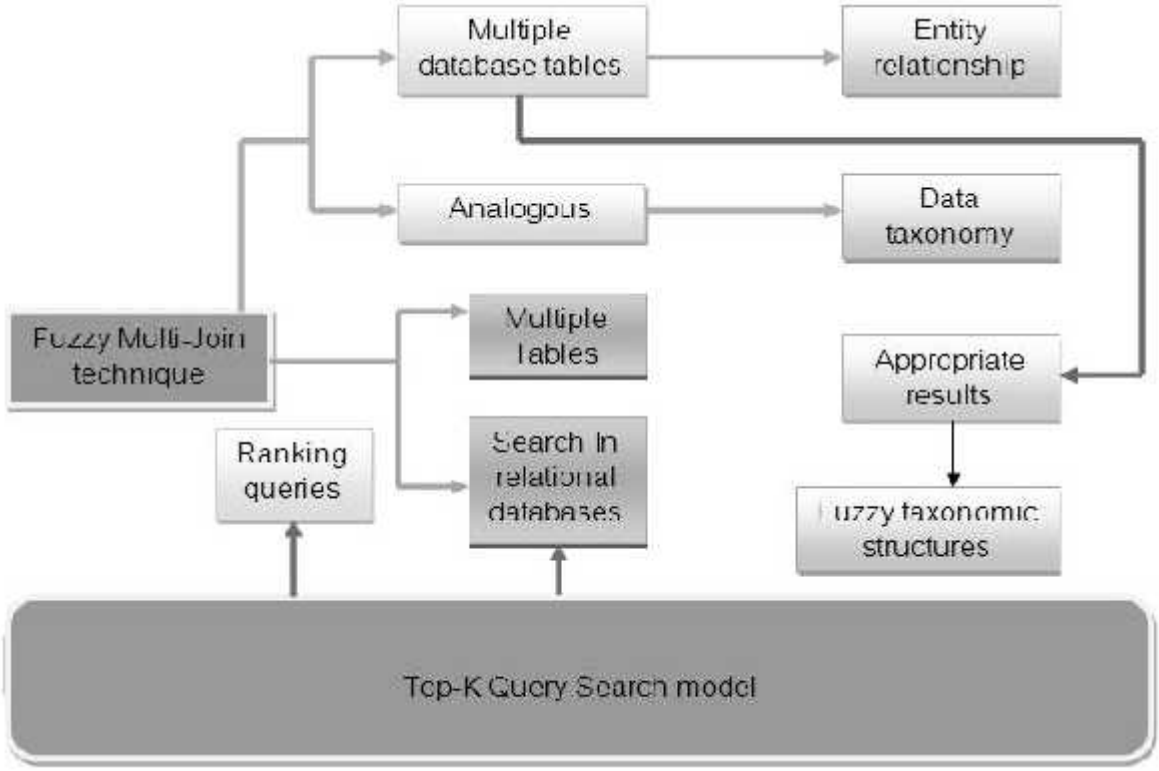

Fig. 1 Architecture Diagram of A Searching Strategy to Adopt Multi-Join Queries Based on Top-K Query Model

The problem is tackled in different contexts. In middleware environments, Fagin and Fagin et al. introduce the first efficient set of algorithms to answer ranking queries. Database objects with m attributes are viewed as m separate lists, each supports sorted and, possibly, random access to object scores. The TA algorithm assumes the availability of random access to object scores in any list besides the sorted access to each list.

- Search as you type Multiple Tables
- Fuzzy Multi-join Search
- Top K-Query Ranking
- Exact Search for Single Keywords
- Fuzzy Search for Single Keywords
- Multi-Keyword Search Updates

A. Search as you type multiple tables

Search-as-you-Type multiple tables allow to add dynamic real-time search to requested queries. Dynamically present suggestions and auto-complete queries, before user is even done typing. Use Search-as-you-Type on any text input field; integrate it with multiple databases as server interface.

SQL to find answers to a search query as user types in keywords character by character in multiple tables. Utilize built-in query engine of databases system as much as possible. Reduce programming efforts to support search-as-you-type, solution developed on one database using standard SQL techniques is portable to multiple tables as well.

B. Fuzzy multi-join search

Search as you type queries look for results from multiple tables across the databases. Fuzzy multi-join search for multiple tables uses hierarchical taxonomy (concept hierarchy) of search data to generate different search criteria at different levels in the taxonomy for databases containing multiple tables.

Fuzzy multi-join search enable to discover crisp search as you type results fuzzy generalized search rules. Search queries are mapped to form similarity queries. Similarity queries are made into multi-join search in the databases.

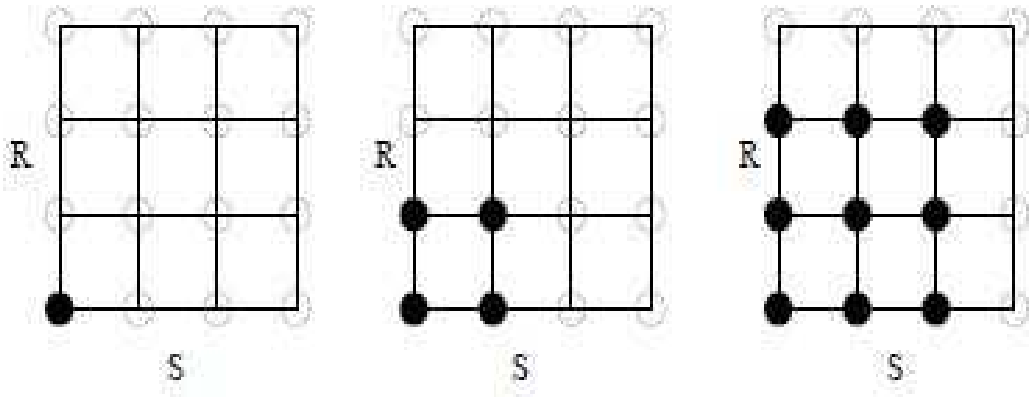

Fig. 2 Three steps in Ripple Join

Ripple join is a family of join algorithms introduced in the context of online processing of aggregation queries in a relational DBMS. Traditional join algorithms are designed to minimize the time till completion estimate of the query result is available. Ripple joins can be viewed as a generalization of nested-loops join and hash join.

In the simplest version of a two-table ripple join, one previously-unseen random tuple is retrieved from each table (e.g., R and S) at each sampling step. These new tuples are joined with the previously-seen tuples and with each other. Thus the Cartesian product R _ S is swept out as depicted in Fig 2.

The square version of ripple join draws samples from Rand S at the same rate. However, in order to provide the shortest possible condense intervals; it is often necessary to sample one relation at a higher rate. This requirement leads to the general rectangular version of the ripple join where more samples are drawn from one relation than from the other.

Variants of ripple join are:

1. Block Ripple Join, where the sample units are blocks of tuples of size b (In classic ripple join, b = 1)
2. Hash Ripple Join, where all the sampled tuples are kept in hash tables in memory. In this case, calculating the join condition of a new sampled tuple with previously sampled tuples is very fast (saving I/O).

C Ttop k-query ranking

Multi-join queries search in multiple tables are improved by ranking top k queries in search as you type multiple databases. Introduced rank-join algorithm makes use of individual orders of its inputs to produce join results ordered on a user-specified scoring function. Rank the join results progressively during the join operation. The operators are non-blocking integrated into pipelined

execution plans. Arrive optimization heuristics to integrate new join operators in practical query.

Ripple joins are designed to minimize time acceptably precise estimate of query result is available. Ripple joins viewed as generalization of nested-loops join and hash join. In a two-table ripple join one previously-unseen random tuple is retrieved from each table (e.g., R and S) at each sampling step, new tuples are joined with previously seen tuples and with each other Cartesian product RS is swept out.

More precisely, consider a set of relations R1 to Rm. Each tuple in Ri is associated with some score that gives it a rank within Ri. The top-k join query joins R1 to Rm and produces the results ranked on a total score. The total score is computed according to some function, f, that combines individual scores. Note that the score attached with each relation can be the value of one attribute or a value computed using a predicate on a subset of its attributes.

A possible SQL-like notation for expressing a top-k join query is as follows:

SELECT *FROM R1,R2,….,Rm WHERE join condition(R1,R2,….,Rm)ORDERBY f(R1:score,R2:score, …..,Rm:score)STOP AFTER k;

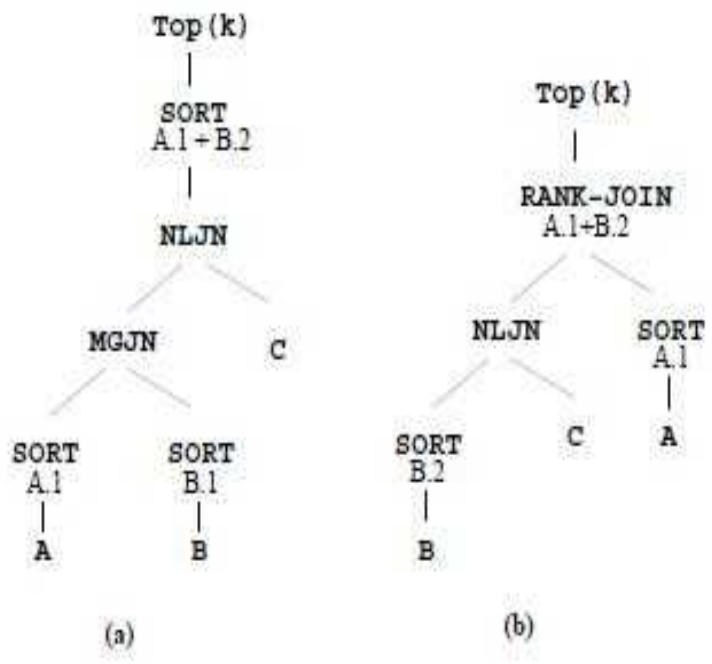

Fig.3 Alternative plans for Query Q1

Propose a new rank-join algorithm, with the desired properties, along with its correctness proof. Implement the proposed algorithm in practical pipelined rank-join operators based on ripple join, with better capabilities of preserving orders of their inputs. The new operators can be integrated in query plans as ordinary join operators and hence give the optimizer the chance to produce better execution plans. Fig 3(b) gives an example execution plan for Q1, using the proposed rank-join operator (RANK-JOIN). The plan avoids the unnecessary sort of the join results by utilizing the base table access plans that preserve interesting orders. Moreover, the plan produces the top-k results incrementally.

Propose a novel score-guided join strategy that minimizes the range of the Cartesian space that needs to be evaluated to produce the top-k ranked join results. We introduce an adaptive join strategy for joining ranked inputs from external sources, an important characteristic of the applications that use ranking.

Evaluate our proposed join operators and compare them with other approaches to join ranked inputs. The experiments validate approach and show a superior performance of algorithm over other approaches.

The algorithm takes m ranked inputs, a join condition, a monotone combining ranking function f and the number of desired ranked join results k. The algorithm reports the top k ranked join results in descending order of their combined score. **The rank-join algorithm works as follows:**

Retrieve objects from the input relations in a descending order of their individual scores. For each new retrieved tuple:

1. Generate new valid join combinations with all tuples seen so far from other relations, using some join strategy.

2. For each resulting join combination, J, compute the score J:score as

f(O1:score;O2:score; : : : ;Om:score), where Oi:score is the score of the object from the ith input in this join combination.

3. Let the object O(di) i be the last object seen from input i, where di is number of objects retrieved from that input, O(1) i be the _rst object retrieved from input i, and T be the maximum of the following m values:

   f(O(d1)1 :score;O(1)2 :score; : : : ;O(1) m :score),
   f(O(1) 1 :score;O(d2)2 :score; : : : ;O(1) m :score), : : :,
   f(O(1) 1 :score;O(1) 2 :score; : : : ;O(dm) m :score).

4. Let Lk be a list of the k join results with the maximum combined score seen so far and let scorek be the lowest score in Lk, halt when scorek>_ T.

D. Exact search for single keywords

Exact search for single keyword comprises of two methods,

1. No-Index method
2. Index method

1. No-Index method

No-Index Method support search-as-you-type to issue an SQL query that scans each record and verifies whether record is an answer to the query.

Using the LIKE predicate databases provide a LIKE predicate to allow users to perform string matching, use LIKE predicate to check whether a record contains the query, keyword introduce false positives remove these false positives by calling UDFs.

Two no-index methods need no additional space, but they are not scalable since they need to scan all records in the table.

2. Index method

Index-Based Methods build auxiliary tables as index structures to facilitate prefix search, develop a new method used in all databases, performs prefix search more efficiently.

Inverted-index table

Given a table T, assign unique ids to the keywords in table T, following their alphabetical order. Create an inverted-index table IT with records in the form (kid; rid) where kid is the id of a keyword and rid is the id of a record that contains the keyword. Given a complete keyword, we can use the inverted-index table to find records with the keyword.

(a) Keywords

kid	keyword
k_1	icde
k_2	icdt
k_3	preserving
k_4	privacy
k_5	publishing
k_6	pvldb
k_7	sigir
k_8	sigmod
k_9	vldb
k_{10}	vldbj
...	...

(b) Inverted-index Table

kid	*rid*
k_2	r_{10}
k_5	r_6
k_5	r_8
k_5	r_{10}
k_6	r_1
k_7	r_9
k_8	r_3
k_8	r_6
k_9	r_8
k_{10}	r_4
...	...

(c) Prefix Table

prefix	*lkid*	*ukid*
ic	k_1	k_2
p	k_3	k_6
pr	k_3	k_4
pri	k_4	k_4
pu	k_5	k_5
pv	k_6	k_6
pvl	k_6	k_6
sig	k_7	k_8
v	k_9	k_{10}
vl	k_9	k_{10}
...	...	...

Table.1 Inverted-index Table and Prefix Table

Prefix table

Given a table T, for all prefixes of keywords in the table, we build a prefix table PT with records in the form (p; lkid; ukid) where p is a prefix of a keyword, lkid is the smallest id of those keywords in the table T having p as a prefix, and ukid is the largest id of those keywords having p as a prefix.

Use the following SQL to answer the prefix-searchquery w:

SELECT T* FROM PT; IT; T WHERE
PT.prefix = "w" AND PT .ukid >= IT .kid AND PT.lkid>=IT.kid AND IT .rid =T.rid.

Thus, given a prefix keyword w, use the prefix table to find the range of keywords with the prefix.

E. Fuzzy search for single keywords

In fuzzy search for single keyword comprises of two methods,

1. No-Index method
2. Index method

1. No-Index method

In fuzzy search for single keyword UDFs support fuzzy search. Improve performance by doing early termination in dynamic-programming computation using edit-distance threshold, devise a new UDF. If there is a keyword in string having prefixes with an edit distance within returns true. Issue an SQL query that scans each record and calls UDF to verify the record.

2. Index method

Use the inverted-index table and prefix table to support fuzzy search-as-you-type. Given a partial keyword compute its answers in two steps .First compute its similar prefixes from the prefix table get the keyword ranges of these similar prefixes, and then compute answers based on these ranges using the inverted-index table.

Gram-based Method

There are many q-gram-based methods to support approximate string search. Given a string s, its q-grams are its substrings with length q.

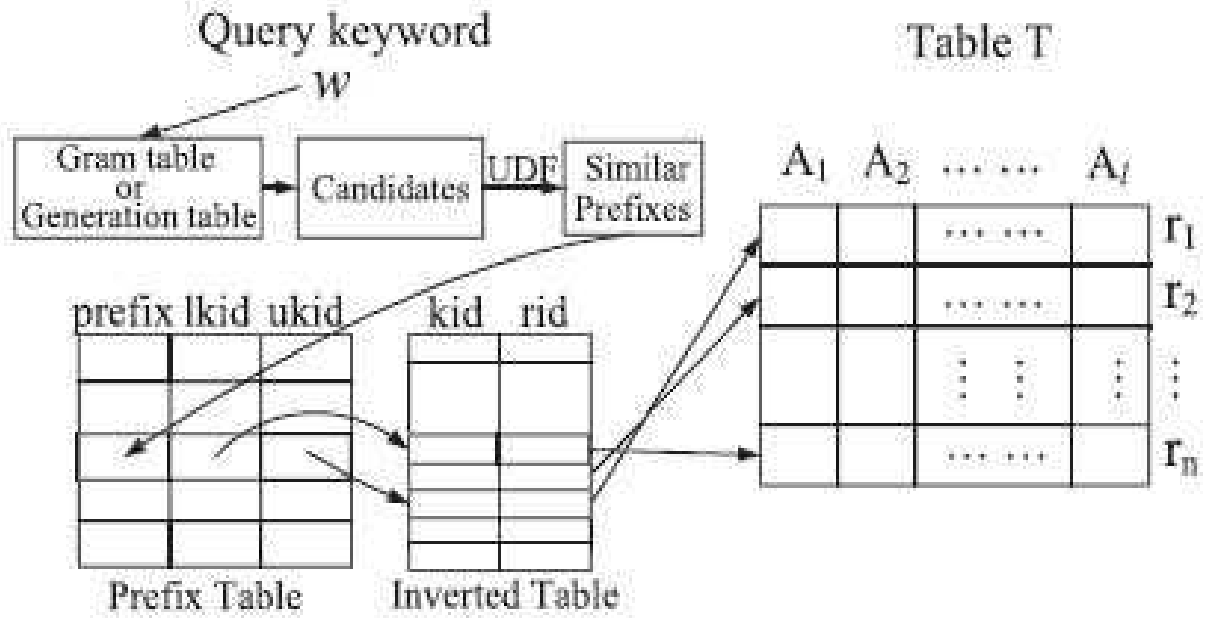

Fig.4 Use the q-gram table and the neighborhood generation table to Support fuzzy search.

To find similar prefixes of a query keyword, besides use the inverted-index table and the prefix table, also in need to create a q-gram table with records.

F. Multi-keyword search updates

Multi-keyword Search updates is given a multi-keyword query Q with m keywords, using the "INTERSECT" Operator first compute records for each keyword and then use INTERSECT operator to join these records for different keywords to compute answers. Using Full-text Indexes first use full-text indexes to find records matching the first complete keywords and then use proposed methods to find records matching the last prefix keyword. Two methods cannot use pre-computed results lead to low performance.

Word-Level Incremental Computation use previously computed results to incrementally answer a query. Assuming a user has typed in a query with keywords create a temporary table to cache the record ids of query. If the user types in a new keyword and submits a new query with keywords use temporary table to incrementally answer the new query. Exact search focus on the method that uses the prefix table and inverted-index table. Fuzzy search consider character level incremental method. Fuzzy search consider character level incremental method, the user arbitrarily modifies the query, can easily extend this method to answer new query.

IV. PERFORMANCE RESULTS AND DISCUSSION

We use a simple ranking query that joins four tables on the non-key attribute JC and retrieves the join results ordered on a simple function. The function combines individual scores which in this case a weighted sum of the scores (wi is the weight associated with input i). Only the top k results are retrieved by the query.

Performance measurement metrics are given below,

- ✓ Number of Tables
- ✓ Number of letters in keyword
- ✓ Query Time
- ✓ Number of answers
- ✓ Number of records

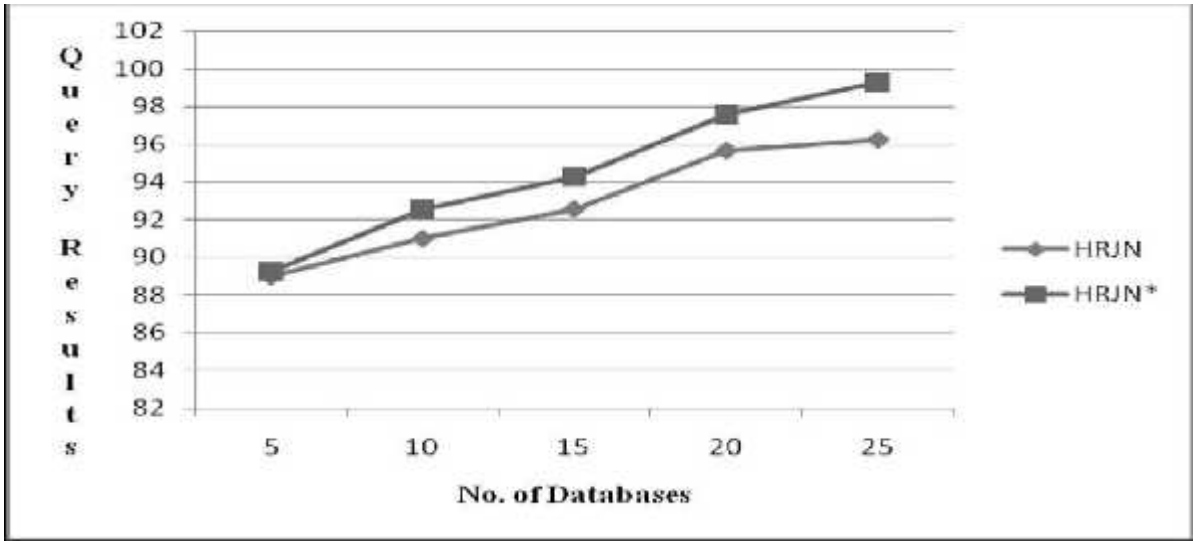

Fig. 5 A Searching Strategy to Adopt Multi-Join Queries Based on Top-K Query Model of Number of databases and Query time.

Fig. 5 shows compares the total time to report 50 ranked results, while compare the number of accessed disk pages and the extra space overhead, respectively.

For all selectivity values, HRJN shows the best performance. J has a better performance than HRJN for high selectivity values while HRJN performs better for low selectivity values.

The reason is that HRJN* combines the advantages of J* and HRJN. While HRJN* uses a score-guided strategy to navigate in the Cartesian space for a faster termination (similar to J*), it also uses the power of producing fast join results by using the symmetric hash join technique (similar to HRJN).

The CPU complexity of J* increases significantly increases. On the other hand, J* and HRJN* show better performance in terms of the number of accessed pages compare to HRJN (Fig 6), because of the score guided strategy they are using. HRJN_ is the most scalable in terms of the space overhead.

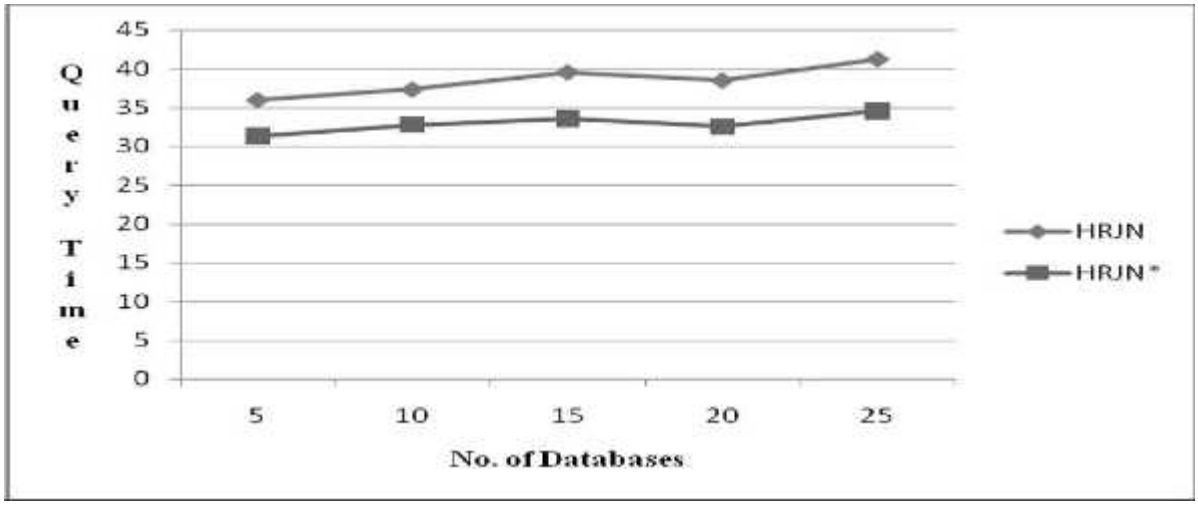

Fig. 6 A Searching Strategy to Adopt Multi-Join Queries Based on Top-K Query Model of Number of databases and Query Results.

The reason is that HRJN* combines the advantages of J* and HRJN. While HRJN* uses a score-guided strategy to navigate in the Cartesian space for a faster termination (similar to J*), it also uses the power of producing fast join results by using the symmetric hash join technique (similar to HRJN).

V. CONCLUSION

Top-k join queries in practical relational query processors. We introduce a new rank-join algorithm that is independent of the join strategy, along with its correctness proof. The proposed rank-join algorithm makes use of the ranking on the input relations to produce ranked join results on a combined score. The ranking is performed progressively during the join and hence, there is no need for a blocking sort operation after join. We present a physical query operator to implement rank-join based on ripple join; the hash rank join (HRJN).

We propose a new join strategy that is guided by the input score values. We apply the new strategy on the original HRJN algorithm and call the new operator HRJN*. We address exploiting available indexes on the join columns. We propose a general rank-join algorithm that utilizes these indexes for faster termination of the ranking process. We experimentally evaluate the proposed join operators and compare their performance with a recent algorithm to join ranked inputs. We conduct several experiments varying the number of required answers, the join selectivity, and the number of inputs in the pipeline.

REFERENCES

[1] H. Bast, A. Chitea, F.M. Suchanek, and I. Weber, "*ESTER:Efficient Search on Text, Entities, and Relations*," Proc. 30th nn.Int'l ACM SIGIR Conf. Research and Development in Information Retrieval (SIGIR '07), pp. 671-678, 2007.
[2] H. Bast and I. Weber, "*Type Less, Find More: Fast Autocompletion Search with a Succinct Index*," Proc. 29th Ann. Int'l ACMSIGIR Conf. Research and Development in Information Retrieval (SIGIR '06), pp. 364-371, 2006.
[3] H. Bast and I. Weber, "*The Complete Search Engine: Interactive,Efficient, and Towards IR & DB Integration*," Proc. ConfInnovativeData Systems Research (CIDR), pp. 88-95, 2007.
[4] R.J. Bayardo, Y. Ma, and R. Srikant, "Scaling up all Pairs Similarity Search," Proc. 16th Int'l Conf. World Wide Web (WWW '07), pp. 131- 140, 2007.
[5] K. Chakrabarti, S. Chaudhuri, V. Ganti, and D. Xin, "*An EfficientFilter for Approximate Membership Checking*," Proc. ACM SIGMODInt'l Conf. Management of Data (SIGMOD '08), pp. 805- 818, 2008.

An Adaptive Slot Reservation Frame for Efficient Contention Access in VeMAC-VANET

[1]K.Selvakumaran, [2]K.Saravanakumar
[1]M.E-CSE, [2]AP-CSE
V.S.B. Engineering College,
Karur, Tamilnadu, India.
[1]selvakumaranrk@gmail.com, [2]saravanakumar.mtech@gmail.com

***Abstract*— Vehicular ad hoc networks (VANETs) arehigh priority safety applications that need medium access control (MAC) protocol for efficient broadcast service. The existing work presented VeMAC, a novel multi channel TDMA MAC protocol for VANET supports efficient one-hop and multi-hop broadcast services on control channel using implicit acknowledgments and eliminating hidden terminal.The drawbacks of existing work allow a node to reserve only one slot in an information frame. Once a node has reserved a slot it ceases contending for other slots.**

The proposed work presented an Adaptive Slot Reservation Frame Scheme for improved contention access on control channel in VeMAC. Nodes are allowed to contend for more than one slot in a reservation frame according to priority criteria. The advantages of proposed work allow nodes to reserve a slot adaptively in the information frame as per priority. Simulation methodology is adopted to eliminate the artificial boundary effect of VeMAC.

Keywords—Ad hoc network, Five-Phase Reservation Protocol (FPRP), Contention Slot, Media Access Control (MAC)protocol.

I. INTRODUCTION

A mobile ad hoc network (MANET) consists of a number of mobile terminals connected with wireless links and is independent from any fixed infrastructure. MANETs can be established quickly and moved flexibly and therefore have wide applications in various types of communication, such as military and emergency. The media access control (MAC) protocol, which provides channel access control mechanisms to coordinate multiple nodes in a network, is an important part of ad hoc networks.

To date, many time division multiple access (TDMA)-based MAC protocols have been proposed. There are reservation-based protocols, such as the five-phase reservation protocol (FPRP) and the hop reservation multiple access (HRMA) protocol.

The reservation-based TDMA protocols can be classified into two categories: fixed allocation and dynamic allocation. Fixed allocation protocols make slot assignments at the scale of the whole network. They do not have the conflict problem but are not suitable for networks with dynamically changing topologies. In contrast, dynamic allocation protocols, such as FPRP, HRMA, evolutionary-TDMA (E-TDMA), and DRAND, use distributed algorithms to assign slots by coordinating nearby nodes. FPRP is a fully-distributed protocol with a low probability of conflict. Using dynamic slot assignments, FPRP has many advantages, such as being scalable with the network size, suitable for changing topology, and insensitive to node mobility. These merits make FPRP a very promising MAC layer protocol for MANETs.

In this algorithm, nodes compete for different time slots in a reservation cycle, making the number of transmission nodes in each slot nearly equal. In the authors modified the reservation mechanism to take into account different levels of urgency of the traffic. After the slot reservation cycle is completed, every node will maintain a table of slot assignments, which specifies which slots have been acquired by neighbor nodes. When the next reservation cycle starts, all nodes will contend for slots based on the prior information in the table, thereby improving the spatial channel utilization.

An improved FPRP algorithm was proposed, in which nodes use different initial probabilities for contention, according to different traffic loads. In this improved FPRP, the node that receives the collision report will check the report to decide whether it should continue to contend or stop immediately.

An improved FPRP (I-FPRP) protocol applying the pseudo-Bayesian broadcast algorithm is subsequently proposed and theoretically analyzed in section III. In section IV, we investigate various performance metrics in detail and critically study the pros and cons of FPRP and I-FPRP via simulation results.

II. RELATED WORK

The VeMAC framework is developed by Hassan Aboubakr Omar et al., (2011) [1] supports efficient one-hop and multi-hop broadcast services on the control channel by using implicit acknowledgments and eliminating the hidden terminal problem. The protocol reduces transmission collisions due to node mobility on the control channel by assigning disjoint sets of time slots to vehicles moving in opposite directions and to road side units. Analysis and simulation results in highway and city scenarios are presented to evaluate the performance of VeMAC and compare it with ADHOC MAC, an existing TDMA MAC protocol for VANETs. It is due to its ability to decrease the rate of transmission collisions, the VeMAC protocol can provide significantly higher throughput on the control channel than ADHOC MAC.

Location Division Multiple Access (LDMA) scheme is designed by R.Mangharam et al., (2007) [2] to suppress the broadcast storm problem and ensure bounded end-to-end delay across multiple hops. This scheme requires participating vehicles to time synchronize with the GPS time and receive the regional map definitions consisting of spatial cell resolutions and temporal slot schedules via an out-of-band FM/RDBS control channel. We use the Groove Net vehicular network virtualization platform with realistic mobility, car-following and congestion models to evaluate the performance of LDMA in simulation and on the road.

This paper is developed by J.W. Wang et al., (1999) [3] probability that m out of n boxes each have exactly one ball resulting from distributing k balls into n boxes. The solution to this problem is given by a set of recursive expressions. By translating these formulae into computer program, one can easily obtain the numerical results.

Our model is designed by M.I. Hassan et al., (2004) [4] validated using extensive simulations and we show that our model yields better predictive accuracy than other existing models. The model is then used to investigate the performance of a modified DCF that uses a fixed number of sequential retransmissions to improve the reliability of packet delivery. We find that with sequential retransmissions, the PDR improves at low vehicle density (i.e. low traffic load), but degrades at heavy loads where higher collisions induced by the retransmissions outweighs the benefit of repeated attempts.

III. AN ADAPTIVE SLOT RESERVATION FRAME FOR EFFICIENT CONTENTION ACCESS IN VEMAC-VANET

The protocol reduces transmission collisions due to node mobility on the control channel by assigning disjoint sets of time slots to vehicles moving in opposite directions and to road side units.

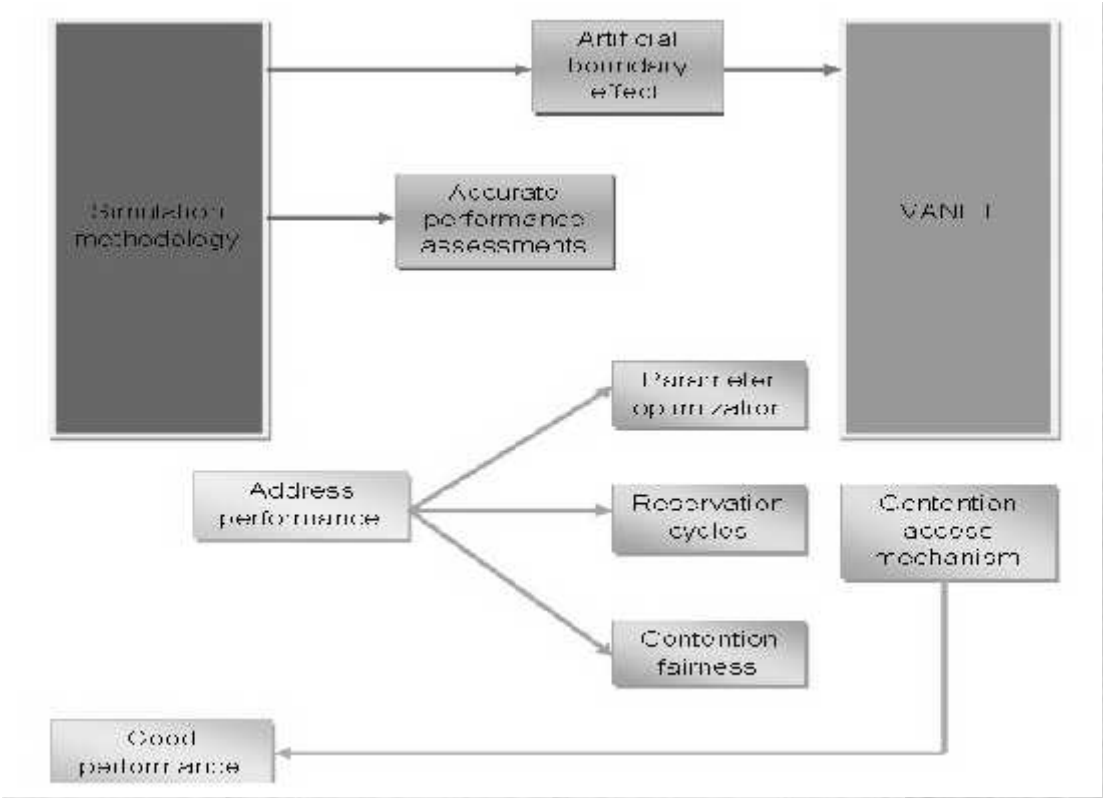

Fig.1Architecture Diagram of An Adaptive Reservation Frame for Efficient Contention Access in VeMAC-VANET

Analysis and simulation results in highway and city scenarios are presented to evaluate the performance of VeMAC and compare it with ADHOC MAC, an existing TDMA MAC protocol for VANETs. It is shown that, due to its ability to decrease the rate of transmission collisions, the VeMAC protocol can provide significantly higher throughput on the control channel than ADHOC MAC.

FPRP is proposed, in which nodes are allowed to contend for more than one slot in a reservation frame according to a certain probability/priority. Simulation results indicate that the proposed mechanism performs better than FPRP in time slot utilization and hence the network throughput under various scenarios.

Analysis and simulation results in highway and city scenarios are presented to evaluate the performance of VeMAC and compare it with ADHOC MAC, an existing TDMA MAC protocol for VANETs. It is shown that, due to its ability to decrease the rate of transmission collisions, the VeMAC protocol can provide significantly higher throughput on the control channel than ADHOC MAC.

FPRP is proposed, in which nodes are allowed to contend for more than one slot in a reservation frame according to a certain probability/priority. Simulation results indicate that the proposed mechanism performs better than FPRP in time slot utilization and hence the network throughput under various scenarios.

- Contention Access for VeMAC-VANET
- Adaptive Slot Reservation Frame
- Bayes Timeslot Probability
- VeMAC VANET Model
- Accessing Slots on Control and Service Channel
- Multi-hop Broadcast Services

A. CONTENTION ACCESS FOR VEMAC-VANET

Contention Mechanism, because nodes are allowed to contend for two slots, a node that has reserved a slot will continue to contend at the next slot with a reasonable probability until it gets two slots. Therefore, it will still update the number of contending nodes by detecting if there is an “idle,” “success,” or “collision” event. Clearly, the estimated number of contention nodes in the next slot will be different from that in FPRP due to the influence of second-round contention nodes. In what follows, we will first present the new contention algorithm in I-FPRP and then describe its reasonableness.

The Multi-hop pseudo-Bayesian algorithm used in FPRP is modified from the (single-hop) pseudo-Bayesian broadcast algorithm. The original pseudo-Bayesian algorithm only performs well in single-hop ALOHA networks, whereas the multi-hop pseudo-Bayesian extends itself to multi-hop networks to obtain efficient estimation on
the number of contention nodes within two hops. Following a similar procedure, we will first analyze the improved mechanism in single-hop networks and further extend it to multi-hop networks.

Each node has two transceivers: transceiver1 is always tuned to the cch, while transceiver2 can be tuned to any of the M schs. For a certain node x, the sch to which transceiver2 is currently tuned is denoted by sch(x). It is assumed that the transmission power levels on the cch and schs are fixed and known to all nodes. All channels are symmetric, in the sense that node x is in the communication range of node y if and only if node y is in the communication range of node x.

For a certain node x, the following two sets are defined:

1. Ncch(x): the set of one hop neighbors of node x on the cch, from/to which node x can receive/transmit packets on the cch;
2. Nm(x): the set of ‘expected’ one hop neighbors of node x on schm, m = 1; : : : ; M.

B. ADAPTIVE SLOT RESERVATION FRAME

An RS is composed of *M* RCs, each of which consists of a five-phase dialogue. If a node wants to reserve an IS, it contends in the RS. A slot is reserved in the RF and used in each IF until the next RF arrives to initiate the next round of reservation. In FPRP, a node that wants to make a reservation will first send a reservation request (RR) packet with probability *p* to its neighbors.

Two types of packets are used in the packing packet (PP) is sent by the nodes two hops away from the reservation node to inform nodes that are three hops away, and the elimination packet (EP) is sent with a probability of 0.5 to resolve a non isolated

deadlock (when there are two transmission nodes within one hop, and they cannot detect each other until one EP is received from one to the other). Further, nodes can always detect that they receive zero, one (success), or more (collision) packets, so they are aware of the success or failure events in each phase of FPRP.

Time is partitioned to frames. A frame consists of a fixed number S of constant-duration time slots. Each frame is partitioned into three sets of time slots: L, R, and F. The F set is associated with RSUs, while the L and R sets are associated with nodes moving in left and right directions respectively. Every node (i.e. vehicle or RSU) is equipped with a GPS receiver. Each vehicle can determine its direction using GPS, and synchronization among nodes can be performed using the 1PPS signal provided by any GPS receiver. The rising edge of this 1PPS is aligned with the start of every GPS second with accuracy within 100ns even for inexpensive GPS receivers. Consequently, this accurate 1PPS signal can be used as a common time reference among all nodes.

Each second contains an integer number of frames. Hence, at any instant, each node can determine whether the current time slot belongs to the L, R, or F set. The VANET has one control channel (cch), and M service channels (schs), denoted by sch1; sch2; : : : ; schM. The cch is mainly used for transmission of two kinds of information: high priority short applications (such as periodic or event driven safety messages), and control information required for the nodes to determine which time slots they should access on the cch and schs. The M schs are used for transmission of safety or non-safety related application messages.

C. BAYES TIMESLOT PROBABILITY

The pseudo-Bayesian algorithm assumes that the number of contention nodes during a slot can be approximated by a Poisson distribution with mean *v*. Moreover, each node keeps *v* as the best estimation for the number of contention nodes and broadcasts with probability $p=1/v$. To improve time slot utilization, we propose animproved contention mechanism for FPRP to allow the nodes to acquire two slots. The new mechanism keeps estimation about the number of nodes (within two hops) that contend for the second slot. Since every node can hear any successful reservation within two hops, nodes can know the number of slots reserved by other nodes within two hops.

Bayesian Algorithm:

1. A modified pseudo-Bayesian algorithm is chosen to compute the contention probability p in the RR phase.
2. In a multi-hop pseudo-Bayesian algorithm, a node needs to keep two estimated values: one is the number of nodes n_c that contend within two hops; the other is the number of nodes n_b within two hops that need reservations but cannot contend in the current slot due to a nearby successful reservation.
3. Some heuristic constants are used to capture the effect of a reservation success on the behavior of the nearby contenders.
4. Specifically, for nodes that are one hop away from the success node, a portion (R_1) of its neighboring contenders ceases to contend in the current slot.
5. Similarly, for nodes that are two and three hops away from the success node, this portion is R_2 and R_3, respectively.

D. VEMAC VANET MODEL

VANET consists is set of RSUs and set of vehicles moving in opposite directions on two-way vehicle traffic roads. If two vehicles are moving in opposite directions on a two-way road guaranteed that one vehicle is moving in a left direction, while the other vehicle is moving in a right one. VANET has one control channel and M service channels is used for transmission of two kinds of information and high priority short applications (such as periodic or event driven safety messages). Control information required for nodes to determine which time slots they should access on channel. Service channels are used for transmission of safety or non-safety related application messages.

Service provider is a node announces on channel for service offered on a specific service channel. User is a node receives the announcement for a service decides to make use of this service. Each node has two transceivers; transceiver1 is tuned to channel c. Transceiver2 is tuned to any service channel c. Transmission power levels on all channels are fixed and known to all nodes. All channels are symmetric node x and node y in the communication range between themselves. Each node is identified by a MAC address and a short identifier. ID is chosen by each node at random included in the header of each packet transmitted on channel.

Each node transmits a packet during its time slot even if the node has no data to include in high priority short applications field. Information in the header, AnS and AcSfields, is necessary for other nodes to decide which time slots they can access on the control channel and service channels. Two types of transmission collision on time slots on the channel are access collision is happen when two or more nodes within two hops of each other attempt to acquire same available time slot. Merging collision happens when two or more nodes acquiring same time slot become members of the same two-hop set (THS) due to node activation or node mobility.

In VANETs merging collisions happen among vehicles moving in same direction due to acceleration or deceleration, more likely to occur among vehicles moving in opposite directions or between a vehicle and a stationary RSU.

Let K denote the number of contending nodes, each of which needs to acquire a time slot on channel c0. We want to determine the average number of nodes which acquire a time slot within n frames, the probability that a specific node acquires a time slot within n frames, and the probability that all the nodes acquire a time slot within n frames. To simplify the analysis, the following assumptions are made:

1. All the contending nodes belong to the same set of THSs, with the same T0 and A sets, e.g. node w and node x in its final position.
2. The set of THSs to which the contending nodes belong does not change.
3. The set A is not augmented when a node fails to acquire a time slot after τ frames.
4. At the end of each frame, each node is aware of all acquired time slots during the frame, and updates the sets T0 and A accordingly, i.e. all nodes are within the communication range of each other.
5. At the end of each frame, all contending nodes are informed whether or not their attempts to access a time slot during this frame were successful. Based on this information, each colliding node randomly chooses an available time slot from the updated a set, and attempts to access this slot during the coming frame.

The delay that a high priority safety packet experiences on channel c0 depends on the value of s 0 as well as the duration of a time slot. Considering a maximum VeMAC packet size of 450 byte and a transmission rate of 12 Mbps, the packet requires a transmission time of 0.3ms. By adding guard periods and taking account of the physical layer overhead, such as the preamble and the physical layer header, a 0.35ms slot duration can be assumed. In terms of synchronization, this slot duration is suitable as it is much larger than the jitter of the 1PPS of GPS receivers which is usually in the order of nanoseconds.

E. ACCESSING SLOTS ON CONTROL AND SERVICECHANNEL

Access time slot assignment on channel in the header of each packet transmitted. Transmitting node includes set N(y) and time slot used by each node. Short IDs in set N(y) serve to decrease the overhead compared to including MAC address of each one-hop neighbor in the header of each transmitted packet.

Suppose node is just powered on and needs to acquire a time slot, starts listening to channel successive time slots. At the end of the slots node x can determine N(x) and the time slot used by each node. Since each node announces N (i) and time slot used by each node x determine the time slot used by each of its two-hop neighbors.

Consider node x has a MAC layer service data unit (MSDU) to be delivered to a certain destination on service channel. Service refers to the delivery of an MSDU on a certain service channel.

Node x announces information in the AnS field of its next packet transmitted on channel,

1. Reliability of service (i.e. acknowledged or not),
2. MAC address of intended destination y
3. Number of service channel
4. Priority of service

Once the provider announces for the serviceno further action is needed unless destination accepts service.

The assignment of time slots to nodes on the schs is performed by the providers in a centralized way. For the slot assignment without a hidden terminal problem, each node x should determine Um(x) defined as the set of time slots used on schm by all nodes which are expected to be within the two-hop neighborhood of node x on schm. This set represents the time slots that node x cannot use on schm, and will be used by the provider to assign time slots to nodes without causing any hidden terminal problem.When node x receives a packet on the cch from another node y indicating that sch(y) = m, if y2 Nm(x), node x adds to Um(x) the time slots used by each node j2 Nm(y); otherwise, node x does not update Um(x).

When a provider (R) has a service to offer on ansch, it announces the following information in the AnS field of the next packet transmitted on the cch: priority of the service, address (es) of the intended user(s), provider's main slot, and the sch on which the service will be offered. Based on the information announced by provider R on the cch, each node x2 Ncch(R) determines whether or not to make use of the announced service.

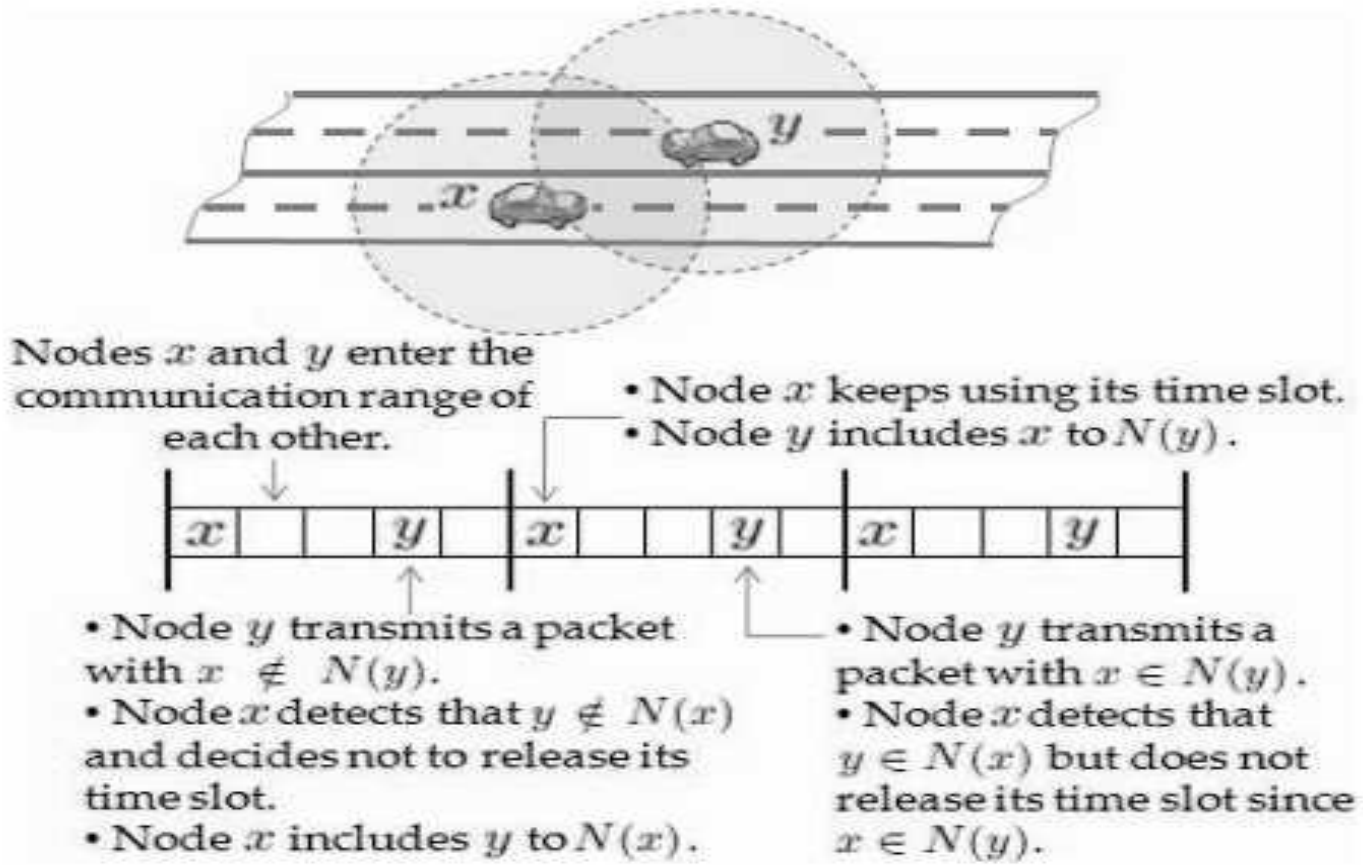

Fig.2 Slot Release Prevention Condition---Prevent Node x Unnecessary Time Slot Release

If node x decides to use the service by provider R on schm, it transmits the following information in the ACS field of the next packet transmitted on the cch: Um(x), address of provider R, and the number of time slots that node x needs. Once node x indicates its acceptance of the service, it tunes transceiver2 to schm and waits for the time slot assignment transmitted on the provider's main slot.

F. MULTI-HOP BROADCAST SERVICES

Efficient multi-hop broad- cast service presented for ADHOC MAC directly supported by VeMAC on channel. Node x transmits a broadcast packet on channel c; this packet needs to propagate throughout whole network. For each node which receives the broadcast packet as the set of one-hop neighbors of node i which did not receive the packet broadcast by node x.

Suppose node x is just powered on and needs to acquire a time slot on the cch. Node x starts listening to the cch for one complete frame. At the end of this frame, node x can determine Ncch(x) and the time slot used by each node i 2 Ncch(x). In addition, since each i 2 Ncch(x) announces Ncch(i) and the time slot used by each j 2 Ncch(i), node x can determine the time slot used by each of its two hop neighbors, j 2 Ncch(i); j =2 Ncch(x), 8i 2 Ncch(x). Hence, by listening to one complete frame, node x can determine the set of time slots used by all nodes within its two-hop neighborhood, denoted by Ucch(x). This set represents the time slots that node x cannot use on the cch, in order to avoid any hidden terminal problem. Given Ucch(x), node x determines the set of accessible time slots Vcch(x) (to be discussed) and then attempts to acquire a time slot by randomly accessing any time slot in Vcch(x), say time slot k. If no other node in the two-hop neighborhood of node x attempts to acquire time slot k, then no access collision happens. In this case, the attempt of node x is successful and all nodes i 2 Ncch(x) add node x to the sets Ncch(i) and record that node x is using time

slot k.

When node I receives the broadcast packet from node x listens to channel for successive time slots. At the end of this duration node I determine the sets N (j). Node i relays the packet if none of the previous three conditions is satisfied. By using this relaying procedure in most cases minimum set of relaying nodes needed to cover the whole network is selected.

IV. PERFORMANCE RESULTS AND DISCUSSION

The performances of FPRP and the proposed I-FPRP are simulated and compared. A new simulation methodology is adopted to eliminate the artificial "boundary effect" that occurs in simulations of finite-sized networks.

The performance of the protocols will be investigated from various aspects by changing the network parameters and protocol parameters. The performance measurement metrics are listed below,

- ✓ Protocol Overhead
- ✓ Packet Delay
- ✓ Gain Factor
- ✓ Reservation Cycles
- ✓ Number of nodes

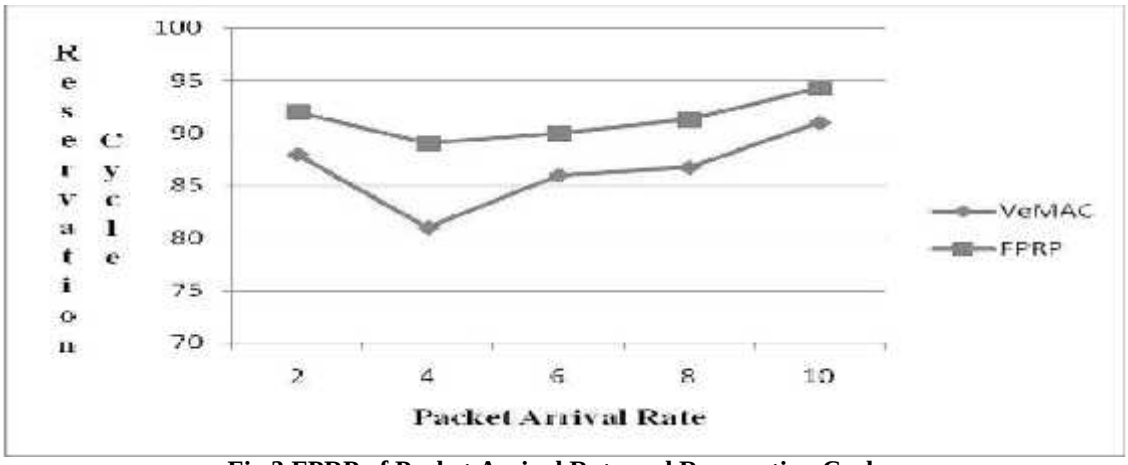

Fig.3 FPRP of Packet Arrival Rate and Reservation Cycle

Fig.3 shows I-FPRP adds extra reserved cycles in the remaining slots. Because nodes can contend for the second slot, with the increase of R_4, the reservation cycleswill increase as a logarithm function. Although extra reserved cycles do not lead to increased time delay because the RF frame includes a constant RC number in each slot, they do result in more power consumption.

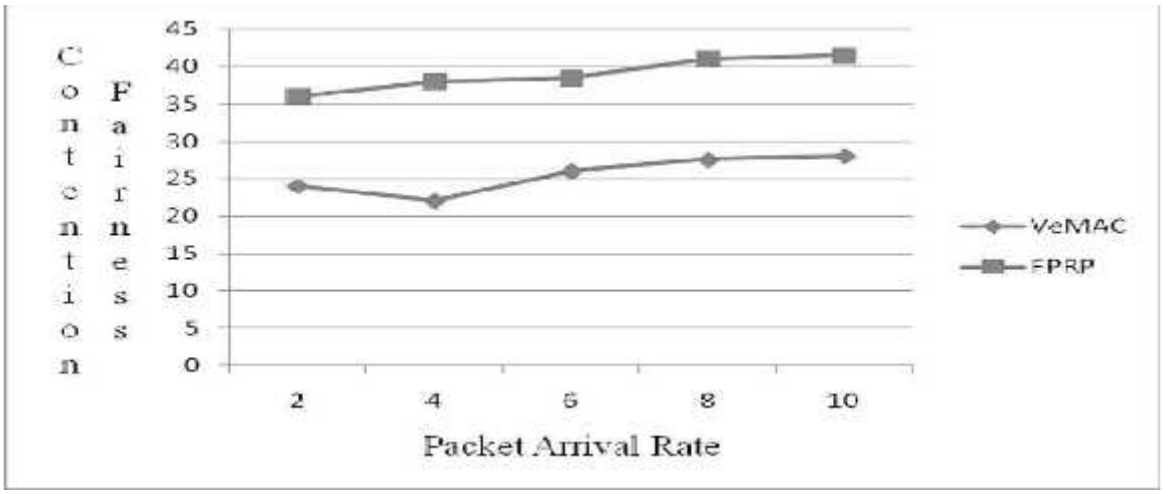

Fig.4 FPRP of Packet Arrival Rate and Contention Fairness

Fig.4 indicates that the failure ratio increases when either the traffic load, second contention probability R_4, or transmission range *R* increases.

V. CONCLUSION

The contention-based reservation mechanism in FPRP and showed that slots are not fully utilized because nodes can only contend for one slot in an information frame. An improved contention access mechanism based on a pseudo-Bayesian broadcast algorithm was subsequently proposed to allow nodes to contend for more slots with certain probabilities related to their traffic demands. Theoretical and simulation results show that the proposed mechanism can significantly improve the overall slot utilization and hence the throughput of MANETs, especially for networks with low spatial node densities. More importantly, such an improvement is achieved with an acceptable increase in the signaling overhead and a marginal and manageable deterioration to the overall user fairness. We conclude that the proposed I-FPRP makes a promising improvement to FPRP for high-throughput applications.

REFERENCES

[1] H.A. Omar, W. Zhuang, Li Li "*VeMAC: A TDMA-based MACProtocol for Reliable Broadcast in VANETs*", Mobile Hoc, 2011,pp. 190-201.

[2] R.Mangharam, R. Rajkumar, M. Hamilton "*Bounded-LatencyAlerts in Vehicular Networks*", University of Pennsylvania, 2007.

[3] J.H. Wen, J.W. Wang "*A recursive solution to an occupancyproblem resulting from TDM radio communication application*",Applied Mathematics and Computation 101(1-3), 1999.

[4] I. Hassan, L. Vu, T. Sakurai "*Performance Analysis of theIEEE 802.11 MAC Protocol for DSRC with and without Retransmissions*", the University of Melbourne, 2010.

[5] L. Kleinrock and F. Tobagi, "*Packet Switching in RadioChannels: Part I – Carrier Sense Multiple-Access Modes and Their Throughput-Delay Characteristics*," IEEE Trans.Communication, vol. 23, no. 12, Dec. 1975, pp. 1400-1416.

[6] IEEE Std 802.11, "*Wireless LAN Medium Access Control(MAC) and Physical Layer (PHY) Specifications*," IEEE, NewYork, 1999.

[7] B. Sharp, E. Grindrod, and D. Camm, "*Hybrid TDMA/CSMAProtocol for Self Managing Packet Radio Networks*," 4th IEEE Int.Conf. Universal Personal Communication, 1995, pp. 929-933.

Applying Computer Aided Designing for Steam Turbine Blade

Deepak Singh
Asst. Professor, Department of Mechanical Engineering
Kautilya Institute of Technology and Engineering, Sitapura,
Jaipur, India
singhdeep_77@rediffmail.com

Abstract- **Modern industries are using CAD models for the accurately representation of geometry for designing and manufacturing of turbines. The CAD model provide a more realistic analysis of performance of the product, this task included dimensional measurement and geometric modeling. This paper presented the procedure for how to achieve CAD model of turbine blade. The method discussed here is the latest profile developed for blades involves regularization and curve fittings using Bazier and B-spline curve generation . Weighting coefficients and nurbs are used for curvature surface of the model.**

Keywords- Cascade; Blade;

I INTRODUCTION

Turbine blade playas main role in absorbing the energy from the dynamics of fluid and converted into mechanical energy. These Blades are fabricated in the desired size and shape and assembled in a straight line or annular according to the designing of cascade. The designating of cascade is based on the database which contains a set of turbine cascades with their geometry and operating conditions. In general, there are two methods for blade profile design i.e. inverse method, and direct method. The inverse design is faster because it is based on the two-dimensional flow analysis to form the airfoil according to the airfoil pressure profile. However, the location of the profile control points is difficult to control and numbers of arcs are generally large. This makes it difficult to use the same curve definition routine for design and manufacturing. On the other hand, direct design may require more time in the aerodynamic design process, but can generate more accurate designs in the manufacturing process. In turbulent flow analysis is needed to evaluate the blade performance.

II. BLADE PROFILE

A turbo machine blade is usually a cantilever beam or plate is tapered and twisted with an airfoil cross-section. Typically a turbo machine has several stages, each stage with a stator and rotor. The function of stator is to guide the flow medium at an appropriate entry angle into rotor blades. The rotor blades are mounted on a disc at a stagger angle to the machine axis and they convert the thermal energy into mechanical energy in turbine. In turbine steam enters at high pressure and temperature in the first stage and expands while passing through the several stages before it is let out from the last Stage with low temperature and pressure after extracting as much as thermal energy as possible. Shape of the turbine is frustum conical type, small blades are assembled in first stage then size of blade increases progressively. Hence, the short blades in high pressure have high frequency to progressively lower up to the last stage long blades. The initial stages of the blades are designed with a variable degree of reaction. The design of these integrally shrouded blades results in an elastically pre-stressed blade ring after assembly that is characterized by an excellent damping behavior during operation. This robust and proven blade construction through long experience converts highly efficient three-dimensional airfoil designs. Within the blade path section interlocking labyrinth seals are applied. Since the overall efficiency of steam turbine power plants is very strongly related to the turbine blading performance, it is necessary to design each turbine blade path individually. It is very cumbersome method of design and can be easily achieved through application of Computer Aided Design (CAD).

CAD is very popular among the manufacturers due to many advantages like CAD has ability to create fast designing to meet today's tight design lead times. We can do fast modifications in developed parts in order to match the desired efficiency and performance levels in each particular application.

Developing the blades with CAD facilitate a highly standardized and flexible blading technology. This is essentially based upon the latest generation of highly efficient fully three-dimensional blading with compound lean and variable stage reaction. However, since not only the technology but also the quality and speed of the design process decide whether the overall performance and lead time requirements are met, the entire blade path design process has been automated within a very powerful design system. Design automation enables more

design cycles in a given time and hence leads to a much more efficient design process reaching a better optimum in a shorter period of time. Thus, from this automation significant cost and time savings due to accelerated and robust processes can be achieved, while at the same time a contract specific bladepath. design with optimum efficiencies is delivered to the customer. Different to the other elements of the steam turbine, the primary goal of standardization with regard to HP/IP blading has been to standardize the "way to the product" instead of the product itself. By using CAD we can create modular concept of bladepath construction from standard and proven elements (e.g. airfoils, roots, grooves, shrouds, extractions, locking devices). The composition of a single blade from root, shroud and airfoil is demonstrated.

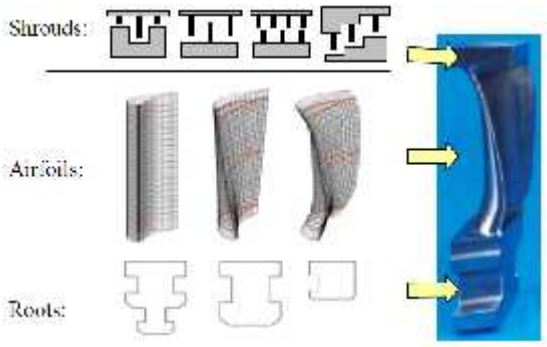

By assembly of each element with different types of another element exist for the various applications, so we may analysis of each type to measure advantages and disadvantages with respect to performance, mechanics and costs. Within the modular concept all these different types may be combined freely to give an optimum blade for the specific design boundary conditions such as aerodynamics, forces, materials and temperatures. Hence, cylindrical, twisted or bowed airfoils can be assembled with any of the roots or shrouds.

A. Shape of blade profile: The shape of a blade profile is function of a velocity triangle and an aerodynamic calculation. The shape of the blade profile must be defined through a suitable method with considering manufacturing point of view. It is very conveniently obtained through CAD systems by using vector graphic, because machine-tools are able to work with these inputs directly. Before determining CAD procedure for blade let we understand the geometry of the blade profile. The blade position inside the blade row is described by a few geometrically and aerodynamically angles, The geometrically parameters of the blade row has variable influence on their function. When we change the angle of blade profile inside blade row in the steam turbine it will affect the change of momentum of a jet of steam flowing over a curved vane. The steam jet, in moving over the curved surface of the blade, exerts a pressure on the blade owing to its centrifugal force. This centrifugal pressure is exerted normal to the blade surface and acts along the whole length of the blade. The resultant of these centrifugal pressures, plus the effect of change of velocity, is the motive force on the blade. Blade profile is made of airfoil by using aerodynamic properties and shape defined by mean camber line.

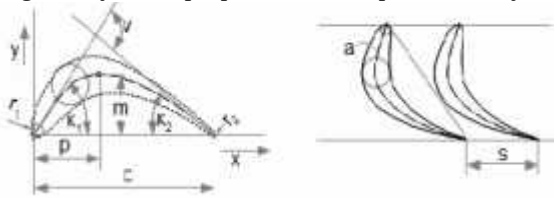

Description of the profile curves are shown in the figure.

As indicated in the fig. m is the maximum camber; p is the position of maximum camber; κ1, κ2 are the angles of the mean camber line (on the leading edge and the trailing edge the camber); c is the length of the chord line; s is the pitch. The blade profiles are generated by performing experiments on various blade profiles by changing their angles. The shape of the mean camber line usually has a shape of the circle, parabolic ,others geometric fundamentals curves or combination of two curves connected in the maximum camber point through together tangent. The terms and the signs of the blade profile geometry can be various. It depends on convention applied in the country. Therefore it is necessary wrote this convention with the descriptions of the shape of the blade profile. Here are used the terms and the sings by that are usually Fundamental geometric and aerodynamic angles of blade profiles are mentioned these are as shown in following figure

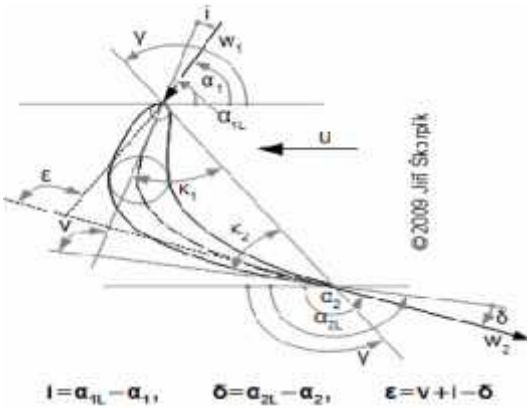

Y is angle of blade profile inside a blade row; α_{1L} is the blade inlet angle; α2L is the blade exit angle; i is the angle of attack (incidence); δ is the angle of deviation; ε is the angle of camber of flow; $\mathbf{w_1}$ the velocity of attack; $\mathbf{w_2}$ Others system of the angles be can use, for example the systems, which are shown in leaving velocity parameters (total pressure loss coefficient, exit flow angle, deviation angle).The pitch of a blade cascade is design from an appropriate density of the blade rows: Density of the blade row and comparative pitch is shown below

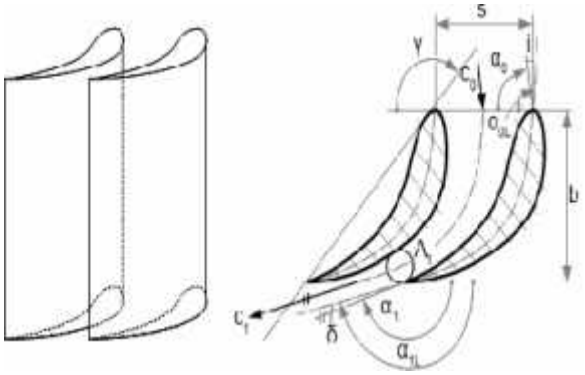

Creating **Geometry and aerodynamic characteristics of blade rows** The design approach is based on the definition of the cascade by the parameters with their geometry and operating conditions. That forms the artificial intelligence technique. For the geometrical representation of a Turbomachinery cascade a Bezier curve based approach has been used. The geometry of the Turbomachinery cascade is then completed by adding the pitch/chord ratio. The independent variables that define the cascade geometry are sixteen in total. These quantities will be the output values for the CAD. For each turbine cascade the database contains the above set of quantities for the geometrical representation, the operating conditions (inlet flow angle, exit Mach number) and the performance B- spline representation for heterogeneous representation for homogeneous object :ensor product solid representation has been widely used in CAD geometry design community.

III BLADE GEOMETRY

The geometry of a turbine profile with specified performance is generated with an innovative inverse design technique or direct design, based on total sixteen independent variables and are in a Cascade . These Variables are many dependent and independent variables. Important variables are Reynolds no., Mach number, Pitch chord ratio, Aspect Ratio, Blade Geometry and profile, Boundary layer and degree of turbulence, incidence. All these parameters have a broad range of variations , so a finite test program is obvious impossible. In the development or design of blade row some parameters are fixed by the given conditions and others parameters have marginal effect. Therefore, the variables involved can be reduced to a more practical and manageable member. In this paper our main focus will be concentrated on the blade geometry and profile. In the development of the blades mainly study the effect of blade profiles is important for the performance. In the Profile effects of leading and trailing edge shapes are important in designing of blades because of the high stresses in the blade are influenced by these factors.

The CAD is using the data stored in the database and then developed cascade geometry based on sixteen output values with a given in performance (total pressure loss coefficient, exit flow angle) during specified operating conditions.

In order to guarantee a homogeneous set of performance data in the database, the aerodynamic performance stored in the database for all the cascade configurations have been computed using the same Navier-Stokes method (with the same mesh density) that was also implemented into the optimisation procedure.

The additional set of cascades from the open literature have been geometrically parameterised using the same Bezier approach previously described. In order to obtain the set of geometrical parameters (fifteen) for the aerodynamic profile from the Cartesian co-ordinates available, an optimization technique has been set up as sketched The set of variables for the Bezier representation of a given reference profile are obtained by minimizing the distance between the co-ordinates of the actual profile and the reference co-ordinates. In the reference co-ordinates and the Bezier representation of the staggered turbine

To improve internal efficiency of steam turbines, reduced root diameter and increased number of stages is one of the important strategies for design. In order to accomplish this, optimization of parameters such as stage number, blade root diameter and the degree of reaction are required. After careful selection of optimized points, the combination of stage number and the degree of reaction that gives highest turbine efficiency is used for design.

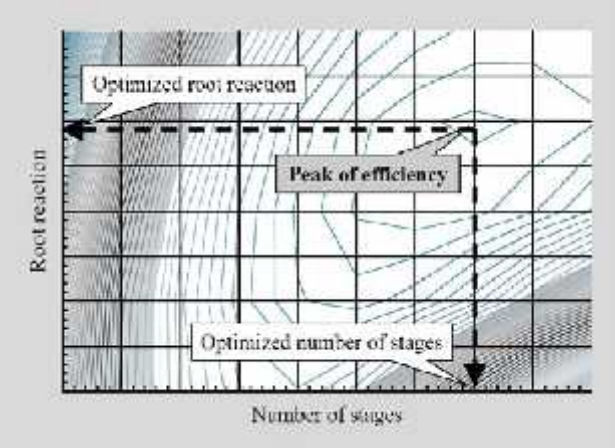

Contour lines represent the distribution of turbine efficiency and it is clear that peak of efficiency exists at certain combinations of stage number and degree of reaction.

To maximize efficiency, it is important that as many stages as possible are used in retrofit turbine within the limited bearing span. Deciding stages in the turbine efficiently is very easy by using CAD technology as an example before retrofit, the HP section was comprised of 6 stages. As a result of applying the improved design with the help of CAD, number of stages in HP section is increased to 11 stages after retrofit.
The IP section was comprised of 4 stages before retrofit. Due to the midpoint extraction, there was some restriction to increase the number of stages. However, by applying the latest CAD technology and improved design, it is possible to add two additional stages. In this case, one stage upstream and one stage downstream are added to maintain extraction pressure. Hence, after retrofit, number of stages in IP section is increased to 6 stages.
As a result of the optimized steam path design, following features are achieved for performance improvement:
1) Increased number of stages with increased stage reaction, reduced nozzle exit velocity and blade turning angle,
2) Higher aspect ratio blade and reduced root diameter resulting in reduced end-wall and leakage loss.
3) Axial entry dovetail design reduces the blade axial length to allow increased number of stages.

VI DESIGN OPTIMIZATION

3d blade design using CAD has been introduced to improve efficiency and minimize incident losses. We can develop steam turbine blade of optimised size base on the analysis using CAD softwares. An optimization of reaction blade design in the turbine stages is to make blade lengths comparatively smaller and to optimize degree of reaction, number of stages and blade root diameters. At the last stages upstream of fixed design LP stages. When the blade become longer and longer, the difference in ratio between flow velocity and blade rotating speed at hub and tip diameter respectively, becomes larger and larger. Thus the velocity vectors over the blade length change dramatically and it is no longer possible to find an optimized blade with a straight profile. With twisted 3D profile over the length of the blade, incident angles can be kept constant, thus avoiding

the corresponding incident losses. Additional effects are achieved in the shroud sealing, where the twisted blade profile gives a stronger support for the integral shroud plate, and an additional number of seal strips can be used to decrease the leakage losses still further**.** In addition, robust design on the bucket leading edge configuration based on statistical theory of design of experiment was carried out. As a result, it was observed that by optimizing the pitch-chord ratio, number of moving blade can be reduced by three-dimensional stage flow analysis. It can be observed that total pressure loss of cascade for optimized reaction blade decreases along almost the entire flow path. Also, it can be seen that the optimized profile reduces total pressure loss downstream from the trailing edge. The curve and surface of turbine blade in general have a Bezier or a B-spline curve representation. B-spline curve is applied for the blade simply to shorten the computational time. There is no technical difficulty to extend the methodology to nurbs volume.

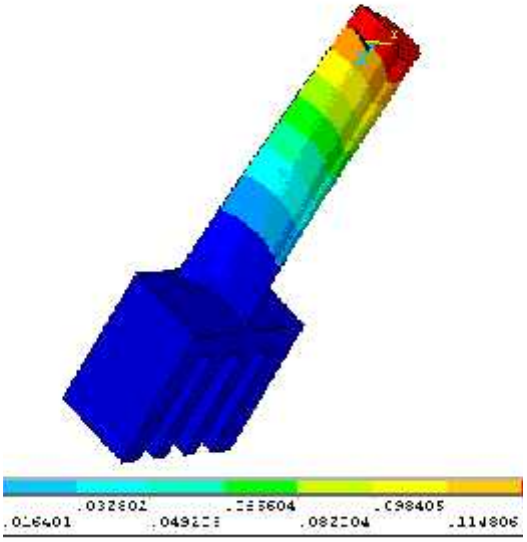

VARIATION OF GEOMETRY SHAPE AFTER APPLYING LOADS.

RESULTS OF FEM USING ANSYS

Structural analysis	
Material	**Stainless Steel**
Stress	339.07
displacement	0.147608
Thermal analysis	
Temperature	533
Thermal gradient	715.055
Thermal flux	11.727

Finite element results for free standing blades give a complete picture of structural characteristics, which can utilized for the improvement in the design and optimization of the operating conditions. Initially a Study on different materials performed to choose best for the optimized turbine blade.

The results of Testing of Different materials for turbine blade suggested best material as using cast iron with partially stabilized zirconium coating is more beneficial than previous materials, due to low stress displacement, good thermal strength, low cost and easy to manufacture.

V CONCLUSION

The blade with complicated airfoil construction is benefited designed by CAD technology which is allow the airfoil shape to be enhanced to the varying steam conditions between the base and tip of the blade. This design is a considerable advantage over the previous generation of the typical parallel-sided airfoil. In shorter blades, relatively large end-wall losses occur at the hub and shroud (secondary losses). Bowing the blades at the hub and shroud boundary improves the flow conditions at the end walls and minimizes losses. Longer blades are of twisted design depending on the hub-to-tip ratio, whereby each profile section is adapted to suit the local inlet and

exit angle conditions. The blade profiles themselves have also been improved using numerical optimization methods to provide better flow and strength properties.

REFERENCES

[1] S. Senoo et al., " Development of titanium 3600rpm-50inch and 3000rpm-60inch Last stage blede turbines,' Proceedings of IGTC 2011, IGTC2011-0249, pp. 1-8(2011).

[2] S.Senoo, " Development of design method for supersonic Turbine Aerofoils near the Tip of Long Blades in Steam Turbine Prat 1: Overall Configuration," Proceeding of ASME Turbo Expo 2012, GT2012-68218,pp 1-12(2012).

[3] Deckers, M., Doerwald, D. (1997). Steam Turbine Flow Path Optimizations for Improved Efficiency, Proceedings of owerGen Asia, Singapore.

[4] Simon V., Stephan, I., Bell, R.M., Capelle, U., Deckers, M Schnaus, J., Simkine, M. (1997). Axial Steam Turbines with Variable Reaction Blading, Advances in Turbine Material, Design and Manufacturing, Proceedings of the 4th International Charles Parsons Conference, pp. 46-60, London.

[5] Deckers, M., Hadden S.G.C., Pfitzinger, E.W., Simon, V. (2000). A Novel Bladepath Design System for Advanced Steam Turbines, Proceedings of the 4th European Conference on Turbomachinery – Fluid Dynamics and Thermodynamics 2000, Firenze, Italy.

[6] Jarrett, J.P., Dawes, W.N., Clarkson, P.J. (2002). Accelerating Turbomachinery Design, Proceedings of ASME Turbo Expo2002, Amsterdam, The Netherlands.

[7] Pfitzinger, E.W., Deckers, M., de Lazzer, A. (2003). Standardised Flexibility in Advanced Blading Technologies for Highly Efficient Steam Turbines, Proceedings of "XXXV. sraftwerkstechnisches Kolloquium 2003", Dresden, Germany.

[8] Schwarz, M.-A., Heine, W.-H., Wechsung, M., Tamme, R.(2003). Neue Dampfturbinengeneration für zukünftige GuD-Anwendungen, Proceedings of "XXXV. Kraftwerkstechnisches Kolloquium 2003", Dresden, Germany.

[9] Engelbert, C., Fadok, J.J, Fuller, R.A, Lüneburg, B. (2004). Introducing the 1S.W501GSingle-Shaft Combined- Cycle Reference Power Plant, Proceedings of ASME Power Baltimore, Maryland.

[10] Kern, T.-U., Wieghardt, K. (2000). The Application of HighTemperature 10Cr Materials in Steam Power Plants. VGB-ESKOM International Materials Conference, Pretoria, South Africa. Design And Materials For Modern Steam Turbines MW Helmut Pollak Ernst-Wilhelm fitzinger Norbert Thamm Mark-André Schwar (2010).

[11] Measurement-based updating of turbine blade CAD models: a case study MIHAILO RISTIC, DJORDJE BRUJIC and IAIN AINSWORTHINT. J. COMPUTER INTEGRATED MANUFACTURING, JUNE 2004, VOL. 17, NO. 4, 352–363 CAD-Based Parametric Cross-Section Designer for Gas Turbine Engine MDO Applications Christopher Dye1, Joseph B. Staubach2, Diane Emmerson3 and C. Greg Jensen4 Fluid Mechanics, Thermodynamics of Turbomachinery Fifth Edition, in SI/Metric units.

[12] S. L. Dixon, B.Eng., Ph.D. Senior Fellow at the University of Liverpool.

[13] BMWRolls-Royce GmbH, Dahlewitz, Germany A Parametric Blade Design System (Part I + II) Jürgen M. Anders and Jörg Haarmeyer Deros,

Homomorphic Encryption Schema for Privacy Preserving Mining of Association Rules

M.Sangeetha[1], P. Anishprabu[2], S. Shanmathi[3]
Department of Computer Science and Engineering
SriGuru Institute of Technology
Coimbatore, India.
Email: msangeetha2612@gmail.com[1], anishbtechit@gmail.com [2], shanmathi.shan@gmail.com[3]

***Abstract*-- Cloud computing and its model for IT services based on the internet and big data centers, the outsourcing of data and computing services .A company (data owner) lacking in expertise or computational resources can outsource its mining needs to a third party service provider (server). However, both the items and the association rules of the outsourced database are considered private property of the corporation (data owner). To protect corporate privacy, the data owner transforms its data and ships it to the server, sends mining queries to the server, and recovers the true patterns from the extracted patterns received from the server. The problem of outsourcing the association rule mining task within a business privacy-preserving framework. The comprehensive experiments on a very large and real transaction database demonstrate that our techniques are effective, scalable, and keep privacy.**

Index terms-- K-privacy, Privacy preserving, Outsourcing, Homomorphic Encryption, Association Rule Mining.

I . INTRODUCTION

Extraction of hidden predictive information from the large database is a new emerging technology in data mining. Data mining is the process of analyze data from dissimilar perspective and summarizing it into useful information that can be used to enlarge proceeds, cuts costs, or both. Data mining software is one of a number of analytical tools for analyzing data. It allows users to analyze data from many different extent or angles, classify it, and review the dealings identified. The actual data mining task is the automatic or semi-automatic analysis of large quantity of data to remove previously unknown interesting patterns such as groups of data records, unusual records and dependency.

This usually involves using database techniques such as spatial indices. These patterns can then be seen as a kind of summary of the input data, and may be used in further analysis or, for example, in machine learning and predictive analytics. results by a decision support system. In general, association rule mining is mostly used for market analysis applications.

II . PRIVACY PRESERVING SECURITY

Data mining is special technical term related with the discovery of new and interesting pattern of data from large data sets. The extraction of hidden predictive information from large databases is a new emerging technology having the huge potential for the help of companies to focus on the important information in the data warehouse. The tools of data mining predicts the future trends and behaviors. This future trends and behavior allow the businesses to make proactive analysis and decision making for the growth of different aspects of the companies. This data mining automates the system to search the relevant information from the databases of data warehouse of the given enterprise which maintains the data warehouse. The data mining tools can answer the business questions which are traditionally very complicated task and take too much time to analyze and produce the result. Most of the companies already collect and refine huge quantities of data.

A. *Security*

Data mining is the process of posing a series of proper queries to extract information from large quantities of data in the database. Data mining techniques can be functional to handle problems in database security. On the other hand, data mining techniques can also be employed to cause security problems. Data mining techniques include those based on rough sets, inductive logic programming, machine learning, and neural networks, among others. Essentially one arrives at some hypothesis, which is the information extracted, from examples and patterns observed. These patterns are observed from posing a series of queries; each query may depend on the response obtained to the previous queries posed.

B. *Issues*

The main model here is that private data is collected from a number of sources by a collector for the purpose of consolidating the data and conducting mining. The collector is not trusted with protecting the privacy, so data are subjected to a random perturbation as it is collected. Techniques have been developed for perturbing the data so as to preserve privacy while ensuring the mined patterns or other analytical properties are sufficiently close to the patterns mined from original data. This body of work was pioneered by and has been followed up by several papers since. This approach is not suited for corporate privacy, in that some analytical properties are disclosed.

Another related issue is secure multiparty mining over distributed datasets. Data on which mining is to be performed is partitioned, horizontally or vertically, and distributed among several parties. The partitioned data cannot be shared and must remain private but the results of mining on the union of the data are shared among the participants, by means of multiparty secure protocols. It do not consider third parties. This approach partially implements corporate privacy, as local databases are kept private, but it is too weak for our outsourcing problem, as the resulting patterns are disclosed to multiple parties.

C. *Privacy Preserving In Data mining*

Some people consider that data mining itself is ethically neutral. While the term "data mining" has no ethical implications, it is often associated with the mining of information in relation to peoples' behavior. To be precise, data mining is a arithmetical method that is applied to a set of information (i.e., a data set). associate these data sets with people is an extreme narrowing of the types of data that are available. Examples could range from a set of crash test data for customer vehicles, to the performance of a group of stocks. These types of data sets make up a great proportion of the information available to be acted on by data mining methods, and rarely have ethical concerns associated with them. However, the ways in which data mining can be used can in some cases and context raise questions regarding privacy, legality, and ethics. In particular, data mining government or commercial data sets for national security or law enforcement purposes, such as in the Total Information Awareness Program or in ADVISE, has raised privacy concerns.

III . **HOMOMORPHIC ENCRYPTION**

Homomorphic encryption is a form of encryption which allows specific types of computations to be carried out on ciphertext and obtain an encrypted result which decrypted matches the result of operations performed on the plaintext. For instance, one person could add two encrypted numbers and then another person could decrypt the result, without either of them being able to find the value of the individual numbers.Using such a scheme, any circuit can be homomorphically evaluated, effectively allowing the construction of programs which may be run on encryptions of their inputs to produce an encryption of their output. Since such a program never decrypts its input, it can be run by an untrusted party without revealing its inputs and internal state. The existence of an efficient and fully homomorphic cryptosystem would have great practical implications in the outsourcing of private computations, for instance, in the context of cloud computing.

The "homomorphic" part of a fully homomorphic encryption scheme can also be described in terms of category theory. If C is the category whose objects are integers (i.e., finite streams of data) and whose morphisms are computable functions, then (ideally) a fully homomorphic encryption scheme elevates an encryption function to a function from C to itself.

The utility of fully homomorphic encryption has been long recognized. The problem of constructing such a scheme was first proposed within a year of the development of RSA. A solution proved more elusive; for more than 30 years, it was unclear whether fully homomorphic encryption was even possible. During this period, the best result was the cryptosystem which supports evaluation of an unlimited number of addition operations but at most one multiplication.

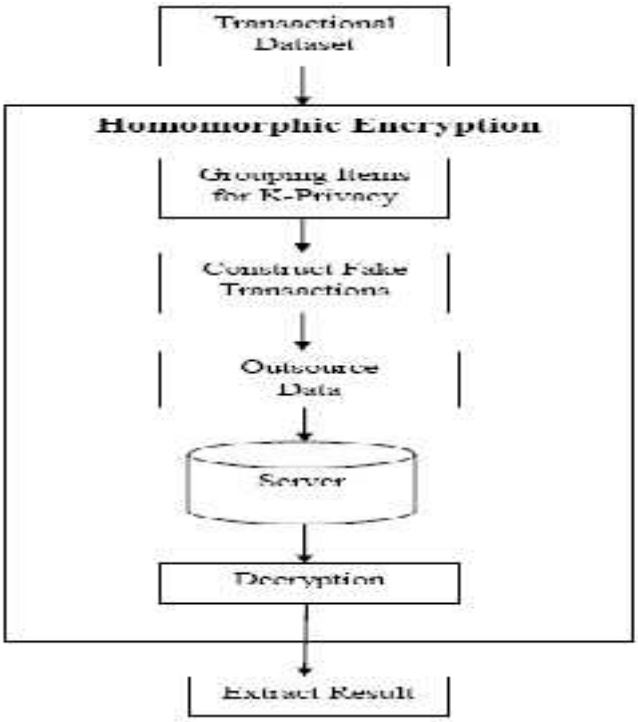

Fig 1.1 Architecture Diagram

IV . **RESULT**

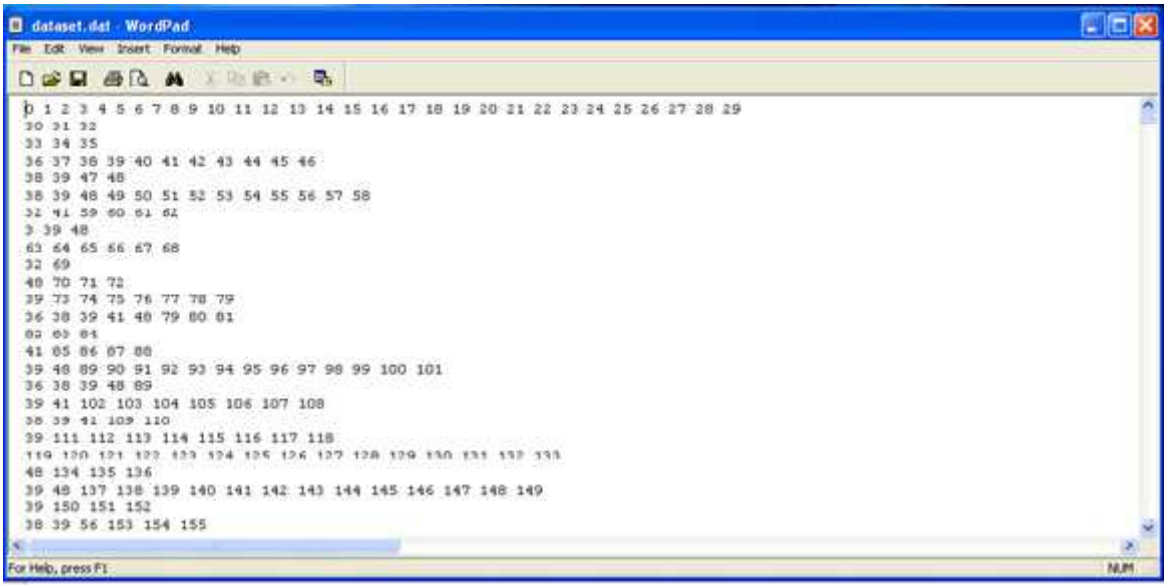

A. Dataset Collection and Encryption

A dataset (or data set) is a collection of data. Dataset is collected from Belgium trade market dataset. It contains the retail market basket data from an unidentified Belgian retail store. The data are provided 'as is'. Basically, any use of the data is allowed as long as the proper acceptance is provided and a copy of the work is provided.

B. Grouping Items For K-Privacy

Given the items support table, several strategy can be adopted to cluster the items into groups of size k. To start from a simple grouping method. To assume the item support table is sorted in descending order of support and refer to cipher items in this order as e1,e2, etc.

Grouping = Maximum support value – Minimum support value / No.of. groups

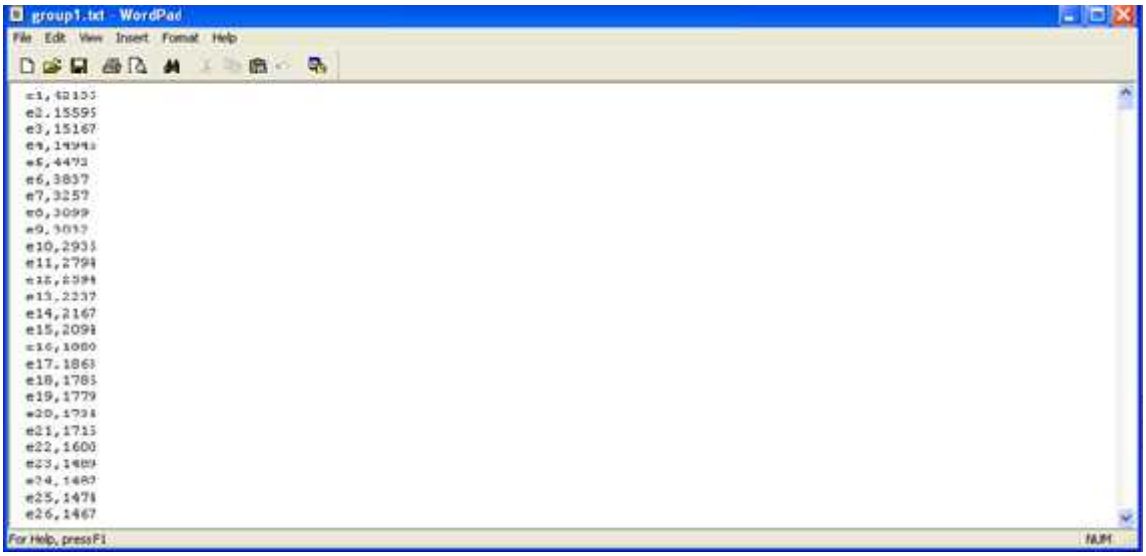

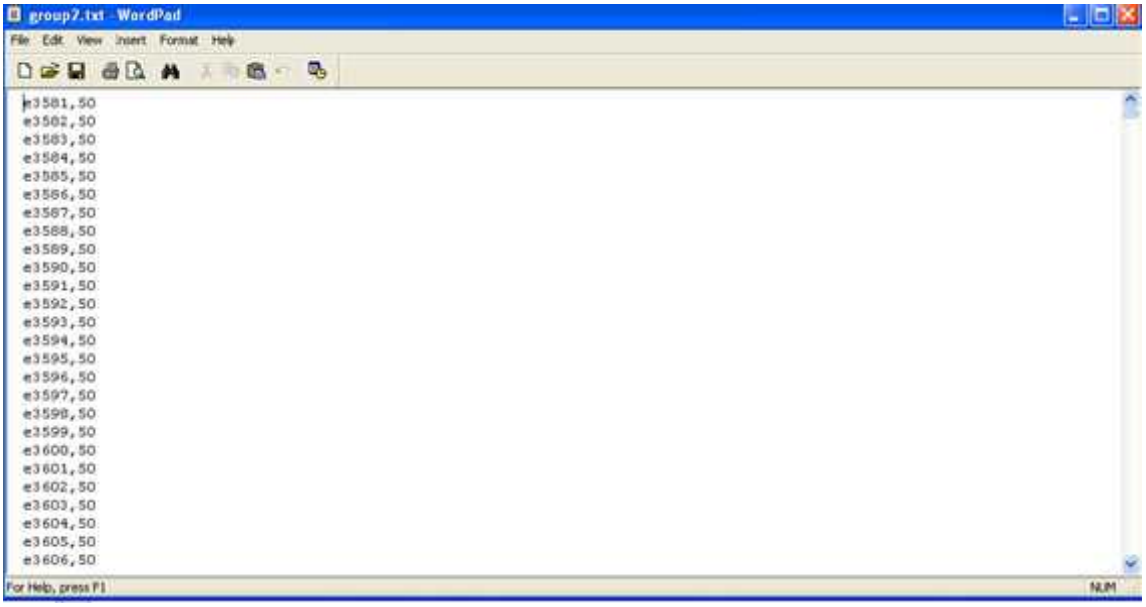

C. *Constructing Fake Transactions*

To add fake transactions for each and every transaction with the original transactional data. It will be in the form of noise.

D. *Decryption*

When the client requests the effecting of a pattern pulling out query to the server, then the server will provide the exact true patterns.

V .**CONCLUSION**

Security issues of the data-mining as- a-service paradigm. One of the main security issues is that the server has access to valuable data of the owner and may learn sensitive information from it. For example, by looking at the transactions, the server (or an intruder who gains access to the server) can learn which items are always copurchased. However, both the transactions and the mined patterns are the property of the data owner and should remain safe from the server.

Homomorphic Encryption scheme based association rule mining when new data is added to the transactional database, encryption schema was performed by whole data. Improve the security of the system by modifying the existing encryption schema. And, to reduce the time complexity by using this scheme then develop the encryption scheme which enables more security of the cloud outsourcing data in the transaction database. Analysis the encryption scheme to achieve the provable privacy guarantee of outsourced transaction database.

ACKNOWLEDGEMENT

The authors would like to thank the staff and students of SriGuru Institute of technology, friends and family members for their support and guidance in bringing this research article. The authors would also like to thank them for their valuable support.

VI . REFERENCES

[1] Fosca Giannotti, Laks V. S. Lakshmanan, Anna Monreale, Dino Pedreschi, and Hui (Wendy) Wang, "Privacy-Preserving Mining of Association Rules From Outsourced Transaction Databases," in IEEE Systems Journal,vol 7, No.3, September 2013.

[2] W. K. Wong, D. W. Cheung, E. Hung, B. Kao, and N. Mamoulis, "Security In Outsourcing Of Association Rule Mining," International Conference On Very Large Data Bases, 2007, pp. 111–122.

[3] L. Qiu, Y. Li, and X. Wu, "Protecting Business Intelligence And Customer Privacy While Outsourcing Data Mining Tasks," Knowledge Information System, vol. 17, no. 1, pp. 99–120, 2008.

[4] C. Clifton, M. Kantarcioglu, and J. Vaidya, "Defining Privacy For Data Mining," National Science Foundation. Workshop Next Generation Data Mining, 2002, pp. 126–133.

[5] I. Molloy, N. Li, and T. Li, "On The (In)Security And (Im)Practicality Of Data Mining, December 2009, pp. 872–877.

[6] F. Giannotti, L. V. Lakshmanan, A. Monreale, D. Pedreschi, and H. Wang, "Privacy-Preserving Data Mining From Outsourced Databases," SPCC2010 Conjunction with CPDP, 2010, pp. 411–426.

[7] R. Agrawal and R. Srikant, "Privacy-Preserving Data Mining," ACM SIGMOD International Conference Management Data, 2000, pp. 439–450.

[8] S. J. Rizvi and J. R. Haritsa, "Maintaining Data Privacy In Association Rule Mining," International Conference Very Large Data Bases, 2002, pp. 682– 693.

[9] M. Kantarcioglu and C. Clifton, "Privacy-Preserving Distributed Mining Of Association Rules On Horizontally Partitioned Data," IEEE Transaction on Knowledge Data Engineering, vol. 16, no. 9, pp. 1026–1037, September 2004.

[10] B. Gilburd, A. Schuster, and R. Wolff, "k- ttp: A New Privacy Model For Large Scale Distributed Environments," International Conference Very Large Data Bases, 2005, pp. 563–568.

M Sangeetha was born in Theni on 26th December 1990. She received her B.Tech.(IT) degree from Periyar Maniammai University, Thanjavur, Tamil Nadu in 2012. She is currently pursuing M.E. (CSE) degree in SriGuru Institute of Technology, Coimbatore, Tamil Nadu. She has Published research papers and articles in various international journals. She has presented a papers in various national and international conferences. She is interested in Secure Computing, Data mining and Audio mining.

P.Anishprabu was born in Namakkal on 14th May 1990. He received his B.Tech.(IT) degree from KSR College of Engineering, Tiruchengode, Tamil Nadu in 2011. He is currently pursuing M.E. (CSE) degree in SriGuru Institute of Technology, Coimbatore, Tamil Nadu.He has presented a papers in various conferences. He is interested in Data mining and Operating system.

S.Shanmathi was born in Tiruchengode on 8th Augest 1991. She received her B.E (CSE) degree from Sengundhar College of Engineering Tiruchengode, Tamil Nadu in 2012. She is currently pursuing M.E. (CSE) degree in SriGuru Institute of Technology, Coimbatore, Tamil Nadu. She has presented papers in various national conferences. Her areas of interest are Network Security, Datastructures and web designing.

Effective Load Balancing in Grid Environment

[1]Mr. D. S. Gawande, [2]Mr. S. B. Lanjewar, [3]Mr. P. A. Khaire, [4]Mr. S. V. Ugale

[1,2,3] Lecturer , CSE Dept, DBACER, Nagpur, India

[4] Lecturer, CSE Dept, GWCET, Nagpur, India

Abstract— **The computational grid is a new parallel and distributed computing paradigm that provides resources for large scientific computing applications. It typically consists of heterogeneous resources such as clusters that may reside in different administrative domains, be subject to different access policies and be connected by networks with widely varying performance characteristics. Many researchers have been proposed numerous scheduling and load balancing techniques for locally distributed multiprocessor systems. However, they suffer from significant deficiencies when extended to a grid environment. Computational grids have the potential for solving large-scale scientific computing applications. The main techniques that are most suitable to cope with the dynamic nature of the grid are the effective utilization of grid resources and the distribution of application load among multiple resources in a grid environment. In this paper contain short literature study on generic load balancing model, load balancing policies and propose scheduling and load balancing approach.**

Keywords: Grid computing, load balancer, Response Time

I. Introduction

The rapid development in computing resources has enhanced the performance of computers and reduced their costs. This availability of low cost powerful computers coupled with the popularity of the Internet and high-speed networks has led the computing environment to be mapped from distributed to Grid environments. In fact, recent researches on computing architectures are allowed the emergence of a new computing paradigm known as Grid computing. Grid is a type of distributed system which supports the sharing and coordinated use of geographically distributed and multi owner resources, independently from their physical type and location, in dynamic virtual organizations that share the same goal of solving large-scale applications. In order to fulfill the user expectations in terms of performance and efficiency, the Grid system needs efficient load balancing algorithms for the distribution of tasks. A load balancing algorithm attempts to improve the response time of user's submitted applications by ensuring maximal utilization of available resources. The main goal is to prevent, if possible, the condition where some processors are overloaded with a set of tasks while others are lightly loaded or even idle [2]. Although load balancing problem in conventional distributed systems has been intensively studied, new challenges in Grid computing still make it an interesting topic and many research projects are under way. This is due to the characteristics of Grid computing and the complex nature of the problem itself. Load balancing algorithms in classical distributed systems, which usually run on homogeneous and dedicated resources, cannot work well in the Grid architectures. Load balancing involves assigning job to a resource proportional to its performance, thereby minimizing the response time of a job. However, there are wide varieties of issues that need to be considered for a heterogeneous grid environment. For example, processing capacities of the resources may differ and their usable capacities may vary according to the load imposed upon them. Further, in grid computing, as resources are distributed in multiple domains in the Internet, not only the computational nodes but also the underlying network connecting them are heterogeneous. Therefore, in the grid environment it is essential to consider the impact of various dynamic characteristics on the design and analysis of scheduling and load balancing algorithms. Due to uneven job arrival patterns and unequal computing capacities, one resource may be overloaded while others may be underutilized. It is therefore desirable to dispatch jobs to idle or lightly loaded resources to achieve better resource utilization and reduce the mean job response time. The strategy proposed here is to perform scheduling and balancing the application load in the grid environment by taking resource heterogeneity, communication delay and network heterogeneity into consideration.

II. Literature Review

Previous related work [2] addresses the problem of scheduling and load balancing in a grid architecture where computational resources are dispersed in different administrative domains or clusters which are connected to the grid scheduler by means of heterogeneous communication bandwidths is considered. In this reference [14], the problem of transferring files that are generated during the execution of DAG workflows with interdependent tasks is addressed. The ineffectiveness of advanced file-transfer techniques in these cases is discussed, and a heuristic is proposed for dealing with the scheduling of interdependent and independent tasks that arrive on-line to be processes by grid infrastructure. The Best File-Transfer Time (BFTT) heuristic is proposed in this study as a means to circumventing the problem of reducing the time spent for transferring data files among different resources in the grid, while still ensuring good performance and/or good load balance among the resources. In addition, BFTT is implemented in this work in conjunction with the OLB algorithm, and a few tests for verifying its results are performed and discussed. One of the main load balancing methods mentioned in the reference [7] is dynamic decentralized approach. This approach considers the run time environment before distributing the jobs among the nodes of the grid. The dynamic decentralized approach is preferred because elements of the grid may vary in capacity or number during runtime and also be heterogeneous in nature giving rise to different loading conditions. In this paper we compare the different load balancing algorithms for the grid based on various metrics like communication overhead, load balancing time, scalability, fault tolerance, reliability and stability. [13]The GridSim toolkit provides a comprehensive facility for simulation of different classes of heterogeneous resources, users, applications, resource brokers, and schedulers. It can be used to simulate application schedulers for single or multiple administrative domains distributed computing systems such as clusters and Grids. Application schedulers in the Grid environment, called resource brokers, perform resource discovery, selection, and aggregation of a diverse set of distributed resources for an individual user. This means that each user has his or her own private resource broker and hence it can be targeted to optimize for the requirements and objectives of its owner. In contrast, schedulers, managing resources such as clusters in a single administrative domain, have complete control over the policy used for allocation of resources. This means that all users need to submit their jobs to the central scheduler, which can be targeted to perform global optimization such as higher system utilization and overall user satisfaction depending on resource allocation policy or optimize for high priority users.

III. Load Balancing In Grid Environment

A. Grid Topology

This is topological structure for a Grid computing Grid computing is a finite set of G clusters Ck, interconnected by gates gtk, k belongs to {0, ...,G − 1}, where each cluster contains one or more sites Sjk interconnected by switches SWjk and every site contains some Computing Elements CEijk and some Storage Elements SEijk, interconnected by a local area network[1]. This model is based on an incremental tree. First, for each site it creates a two-level subtree. The leaves of this subtree correspond to the computing elements of a site, and the root is a virtual node associated to the site. These sub trees, that correspond to sites of a cluster, are then aggregated to form a three-level sub-tree.

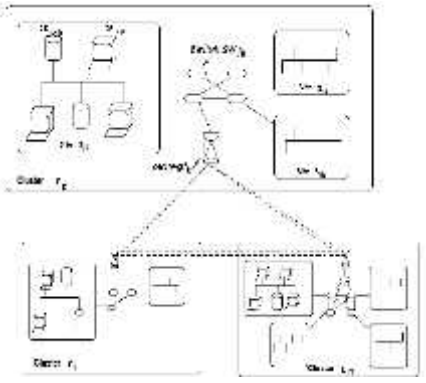

Figure 1: Grid Topology [1]

B. Load Balancing Policies

PoliciesLoad balancing algorithms can be defined by their implementation of the following policies [5]:

• Information policy: specifies what workload information to be collected, when it is to be collected and from where.

• Triggering policy: determines the appropriate period to start a load balancing operation.

• Resource type policy: classifies a resource as server or receiver of tasks according to its availability status.

• Location policy: uses the results of the resource type policy to find a suitable partner for a server or receiver.

• Selection policy: defines the tasks that should be migrated from overloaded resources (source) to most idle resources (receiver).

The main objective of load balancing methods is to speed up the execution of applications on resources whose workload varies at run time in unpredictable way. Hence, it is significant to define metrics to measure the resource workload. Every dynamic load balancing method must estimate the timely workload information of each resource. This is key information in a load balancing system where responses are given to following questions:

• How to measure resource workload?

• What criteria are retaining to define this workload?

• How to avoid the negative effects of resources dynamicity on the workload; and,

• How to take into account the resources heterogeneity in order to obtain an instantaneous average workload representative of the system? Several load indices have been proposed in the literature, like CPU queue length, average CPU queue length, CPU utilization, etc. The success of a load balancing algorithm depends from stability of the number of messages (small overhead), support environment, low cost update of the workload, and short mean response time which is a significant measurement for a user. It is also essential to measure the communication cost induced by a load balancing operation.

III. Proposed System

In grid environments, the shared resources are dynamic in nature, which in turn affects application performance. Workload and resource management are two essential functions provided at the service level of the Grid software infrastructure. To improve the global throughput of these environments, effective and efficient load balancing algorithms are fundamentally important. Load Balancing is one of the most important factors which can affect the performance of the grid application. All Load Balancing algorithms implement five policies. The efficient implementation of these policies decides overall performance of Load Balancing algorithm. The main objective of this thesis is to propose an efficient Load Balancing Algorithm for Grid environment. Main difference between existing Load Balancing algorithm and proposed Load Balancing is in implementation of two policies: Triggering Policy and Selection Policy. For implementation of Triggering Policy all existing Load Balancing algorithm use periodic approach, which is time consuming. The proposed approach uses activity based approach for implementing Triggering policy. For implementation of Selection Policy Proposed algorithm uses Job length as a parameter, which can be used more reliably to make decision about selection of job for migration from heavily loaded node to lightly loaded node.

IV. Experimental Environment

A. GridSim Simulation ToolKit

The simulation was carried out on the excellent grid simulation toolkit GridSim ToolKit 5.0 [13] which allows modeling and simulation of entities in grid computing systems-users, applications, resources, and resource load balancers for design and evaluation of load balancing algorithms. A heterogeneous grid environment by using various resource specifications was built. It proposes the method of creating a user job and different types of heterogeneous resources. The resources differ in their operating system type, CPU speed, RAM memory, MIPS rating.

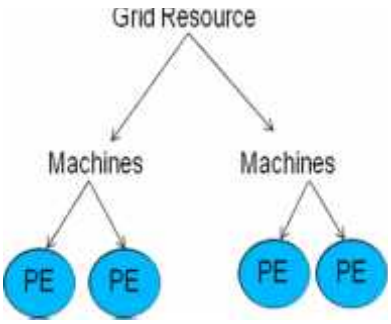

Fig. 2 GridSim Resource Hierarchy

In GridSim, application jobs are modeled as Gridlet objects that contains all information related to the job and the execution management. Details of the available Grid resources are obtained from Grid Information Service (GIS) entity that keeps track of the resources available in the grid environment. The experimental environment consisting of hierarchy of resources used for the evaluation of proposed algorithm is shown in figure 2. A grid resource (GS) maintains information about machines (LS) and each machine contains PEs running at different speeds.

B. Simulation Result

Number of grid resource, number of machine, number of processing element and MIPS is provide as a input to module 1 as shown in Figure 3.

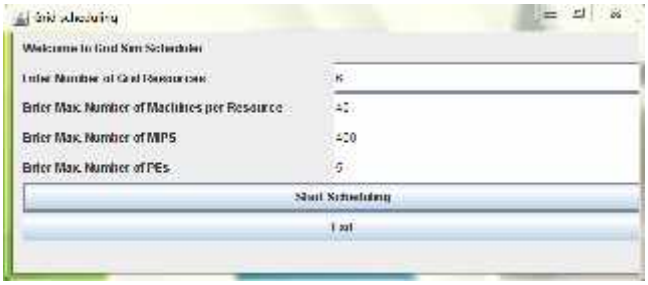

Figure 3 : Grid Implementation Input Frame

Gridlet/Tasks Creation

- Gridsim provide facility to create various tasks
- The tasks has various characteristics..
  - Gridlet id
  - Length
  - File size
  - Output size

GridletDataStorage class is used for creating various tasks and creating number of users. In Figure 4. show the result of creating gridlet or tasks and users.

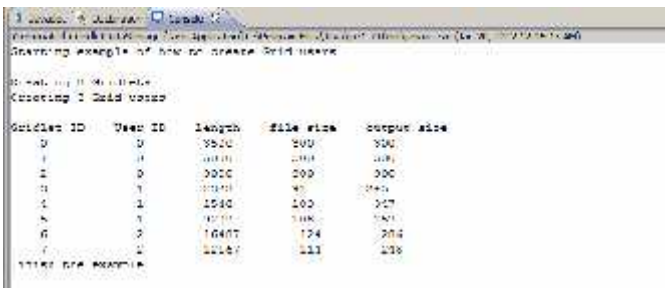

Figure 4: Result of creating gridlet and user

Here 8 Gridlets and 3 Grid users are created and each gridlet assign their properties. Tasks are randomly generated and divide among the resources and simulate by using gridsim simulator toolkit.

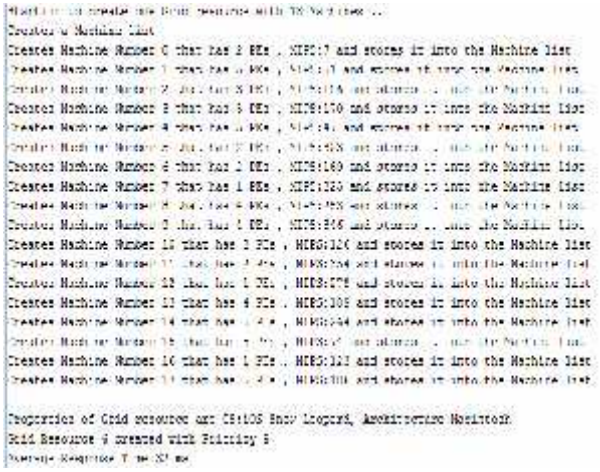

Figure 5: Image of creating grid Resource

In this image number of grid resource are created with properties and priority and store into machine list. Each grid resource having number of machines, PEs and MIPS is assign and each resource having different properties associated with it.

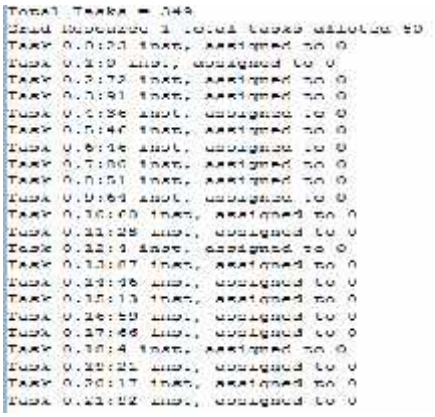

Figure 6: Image of Tasks Scheduling

In this image show that the number of tasks are assigned to resource with length of that tasks.

C. Performance Parameter

The following metrics were selected to evaluate the performance of the proposed model:

- Average Response Time: Response time rj of job j is the time period from the job arrival to the completion time of the job. i.e., the time spent in the resource queue plus the job service (execution) time.

The Average response time ART:

$$ART=1/N \sum_{j=1}^{N} rj$$

Where, N is the total number of processed jobs.

Here Average response time is used for analyze the system performance before load balancing or no load balancing and after load balancing by using proposed load balancing algorithm. Number of samples is collected by performing the simulation number of times and note down the Average response time, before load balancing

and after load balancing the system load. All time units are in milliseconds so the performance metrics are also measured in milliseconds.

Table 1: Average Response Time

No. of Tasks	No Load Balancing	Proposed Load Balancing
250	32	16
500	31	16
1000	35	15
1500	31	15
2000	47	32
2500	47	16

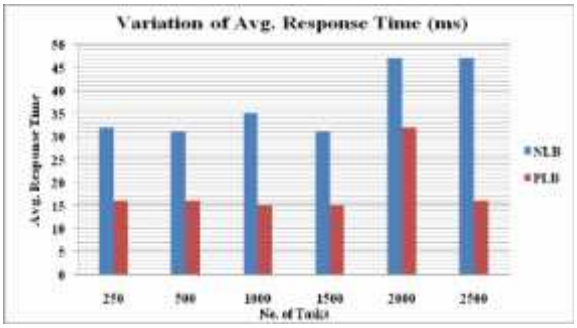

Figure 7: ART versus No. of Tasks

In the simulation, it is observed that Average response time with no load balancing is much higher than load balancing with proposed algorithm.

V. Conclusion

The proposed load balancing model takes into account the heterogeneity of the computational and network resources. i.e., the resources are with different processing capacity and network bandwidth. The load balancing policies at various levels of hierarchy are proposed to optimize various performance metrics. This thesis focuses on load balancing and presents factors due to which load balancing is initiated, and finally proposes an efficient load balancing algorithm for Grid environment.

Some of the limitations of this work and present some possible directions for future research. In this work, we assume that there is no precedence constraint among different jobs or different tasks of a job. Usually, the jobs are independent of each other in the grid, but different tasks of a job may have some precedence constraints. Hence, it is an interesting direction for future research. Such dependencies will not only make the problem extremely difficult to solve, but would also require estimating a very large number of parameters. In future we should also consider some fault tolerant measures to increase the reliability of our algorithm.

REFERENCES

[1].Belabbas Yagoubi and Yahya Slimani, "Dynamic Load Balancing Strategy for Grid Computing" Proceedings of World Academy of Science, Engineering and Technology Volume 13 May 2006 ISSN 1307-6884.

[2] Malarvizhi Nandagopal1 and Rhymend V Uthariaraj2 “Hierarchical Status Information Exchange Scheduling and Load Balancing For Computational Grid Environments” IJCSNS International Journal of Computer Science and Network Security, VOL.10 No.2, February 2010.

[3].S.Rips “Load Balancing Support for Grid-enabled Applications” NIC Series, Vol. 33, ISBN 3-00- 017352-8, pp. 97-104, 2006.

[4].Po-Cheng Chen,Cheng-I Lin,Sheng-Wei Huang,Jyh- Biau Chang, Ce-Kuen Shieh,Tyng-Yeu Liang, “A Performance Study of Virtual Machine Migration vs Thread Migration for Grid Systems”.

[5].S Kalaiselvi Supercomputer Education and Research Centre (SERC), Indian Institute of Science, Bangalore V Rajaraman Jawaharlal Nehru Centre for Advanced Scientific Research, Indian Institute of Science Campus, Bangalore “A Survey of Check-Pointing Algorithms for Parallel and Distributed Computers” vol. 25,Part 5,October 2000,pp.489±510.

[6] A. Abed, G. Oz, A. Kostin, Competition-Based Load Balancing for Distributed Systems, Proceedings of the Seventh IEEE International Symposium on Computer Networks (ISCN' 06),pp 230 – 235.

[7] D. Acker, S. Kulkarni, “A Dynamic Load Dispersion Algorithm for Load-Balancing in a Heterogeneous Grid System” Sarnoff Symposium IEEE, May 2007, pp 1- 5.

[8] Dobber, M., Koole, G., Mei, R.: Dynamic load balancing experiments in a Grid. In: Proceedings of IEEE International Symposium on Cluster Computing and the Grid, Cardiff, 2005.

[9] Kai Lu, Riky Subrata and Albert Y. Zomaya, “An Efficient Load Balancing Algorithm for Heterogeneous Grid Systems Considering Desirability of Grid Sites”, IEEE International Performance, Computing, and Communications Conference, 2006. IPCCC 2006. Vol 25Page(s):9 pp. – 320.

[10] Kimura, K., Ichiyosi, N.: Probabilistic analysis of the optimal efficiency of the multi-level dynamic load balancing schemes. In: Proceedings of the 6th Distributed Memory Computing Conference, Portland, (1991)

[11] Kameda, H., Li, J., Kim, C., Zhang, Y.: Optimal Load Balancing in Distributed Computer Systems. Springer, London (1997).

[12].Shahzad Malik, “Dynamic Load Balancing in a Network of Workstations”, 95.515F Research Report, November 29, 2000.

[13] Rajkumar Buyya1,∗,† and Manzur Murshed2 “GridSim: a toolkit for the modeling and simulation of

distributed resource management and scheduling for Grid computing” CONCURRENCY AND COMPUTATION: PRACTICE AND EXPERIENCE *Concurrency Computat.: Pract. Exper.* 2002; **14**:1175–1220 (DOI: 10.1002/cpe.710)

[14] Elaine C. Machtans1,2; Liria M. Sato2; Airton Deppman3”Improvement on Scheduling Dependent Tasks for Grid Applications” 2009 International Conference on Computational Science and Engineering

Economic Statistical Design of $\overline{X}$ Control Chart using Genetic Algorithm

Vaisakh P. S.
P. G. Scholar,
Department of Mechanical Engineering,
Mar Athanasius College of Engineering, Kothamangalam, Kerala, India
vaisakh.vps@gmail.com

Dileeplal J.
Associate Professor,
Department of Mechanical Engineering,
Mar Athanasius College of Engineering, Kothamangalam, Kerala, India
dileeplal@mace.ac.in

Abstract - **Control chart are widely used to establish and maintain statistical control of a process. In other words it is a tool used to monitor the processes and to assure that they remain "in control" or stable. The $\overline{X}$ control chart is preferred most in comparison to any other control chart technique if quality is measured on a regular scale. The design of a control chart involves the selection of the parameters like sample size (n), sampling interval (h), and control limits width (L). The design of a control chart also has an economic aspect as it involves the costs of sampling, inspection, checking for out of control signals, and cost of non-conforming units reaching the consumer. Economic-statistical design is basically a combination of economic and statistical design of control chart. In this type of design, the total cost of maintaining the control chart need to be minimized and at the same time Type-I and Type-II errors are not allowed to exceed their permissible level. In the present work, a genetic algorithm has been developed for the economic design of the $\overline{X}$ control chart (ESDCC-GA) under uniform and non-uniform sampling interval that gives the optimum values of the sample size, sampling interval and width of control limits such that the expected total cost per hour (ECT) is minimized. The results obtained are found to be better compared to that reported in the literature.**

Keywords - Control chart, economic statistical design, expected cost per hour, genetic algorithm.

I. INTRODUCTION

ISO, an international body for formulating standards, has defined quality as degree to which a set of inherent characteristics fulfils requirements. Degree refers to a level to which a product or service satisfies. So, depending upon the level of satisfaction, a product may be termed as excellent, good or poor quality product. Inherent characteristics are those features that are a part of the product and are responsible to achieve satisfaction. Requirements refer to the needs of customer, needs of organization and those of other interested parties (e.g. regulatory bodies, suppliers, employees, community and environment) or it is the expectations that may be stated, generally implied or obligatory (ISO 1802:1994).

Improving the quality of the output is a major factor for a successful and competitive business in the market. Statistical process control (SPC) is one of the best technical tools for improving product and service quality. SPC consists of methods for understanding, monitoring and improving process performance over time (Woodall, 2000). It is now realized that SPC is not just a collection of techniques, but a way of thinking about quality improvement, and it is regarded in many organizations as an important element of Total Quality Management (Caulcutt, 1995).

Control chart is one of the widely used statistical process control tools. It is used to statistically monitor the process through sampling inspection instead of 100% inspection. It only indicates whether the process is in-control or out-of-control but it cannot on its own rectify the process. It presents a graphic display of process stability or instability over time. One goal of using a control chart is to achieve and maintain process stability. Process stability is defined as a state in which a process has displayed a certain degree of consistency in the past and is expected to continue to do so in the future. This consistency is characterized by a stream of data falling within control limits based on plus or minus 3 standard deviations (3 sigma) of the centerline. (Hachicha and Ghorbel, 2012)

The main aim behind the idea of control charts is the need for perfection and elimination of non-conforming products. Control chart helps to differentiate between the inherent variation in a process and variation due to assignable causes. The inherent variation in a process is background noise due to several small unavoidable causes. Assignable causes are considerably larger fluctuations when compared to the background noise. Variation from an assignable cause can only be removed from the process through human intervention (Juran and Godfrey, 1998).

Control charts are classified by the type of quality characteristic they are supposed to monitor. Control charts can be broadly classified as control charts for variables and control charts for attributes.

One of the first control charts to receive attention is the $\overline{X}$ chart, devised by Walter Shewhart. The $\overline{X}$ chart provides an illustrative example for general control chart theory. The $\overline{X}$ control chart consists of a centre line (CL or μ_0), an upper control limit (UCL) and a lower control limit (LCL).

In $\overline{\overline{X}}$ control chart, the sample mean is compared with the upper and lower control limits of the control chart to decide whether the process is in-control or out-of-control. If a point falls within the upper and lower control limits, the process is referred to as "in control" whereas if it falls outside the control limits, the process is referred to as "out-of control". There are two possible errors: a process can be deemed in-control when in fact the process is out-of-control (Type II error), and vice versa (Type I error). When the process is judged to be out-of-control, there is an attempt to identify the special cause of variation which is called an assignable cause search. (Duncan, 1956)

Generally there are economic design of $\overline{X}$ control chart and economic statistical design of $\overline{X}$ control chart. In economic design of $\overline{X}$ control chart, the objective is to reduce the total cost of maintaining the control chart as minimum as possible. It is used to determine the values of various design parameters i.e. sample size (n), sampling interval (h), and control limit coefficient (L) that minimizes total expected cost. The statistical errors associated with control chart are Type-I error and Type-II error. These two errors are cannot be completely eliminated since 100% inspection is not carried out. In economic statistical design, the total cost of maintaining the control chart need to be minimized and at the same time Type-I and Type-II errors are not allowed to exceed their permissible level.

The remainder of this paper is organized as follows: Section II presents the problem description. The proposed genetic algorithm is explained in section III. Result and discussion are presented in section IV and section V gives the concluding remarks.

II. PROBLEM DESCRIPTION

The customer requirements and expectations are becoming increasingly high in terms of quality and cost in the present industrial environment. Accordingly the selection of control chart design parameters like n, h and L becomes a challenging job. The economic statistical design of $\overline{X}$ control chart is considered in this paper to determine the parameters of $\overline{X}$ control chart.

A. Mathematical model

The mathematical model for economic statistical design of the $\overline{X}$ control chart is adopted from Rahim and Banerjee cost's model proposed in 1993. In this model, the failure mechanism belongs to the gamma (λ, 2) distribution, and the sample mean $\overline{X}$ is normally distributed.

1) The cost model of uniform sampling interval (Rahim and Banerjee, 1993)

The objective function of the cost model is expressed mathematically as:

$$\text{Min } F(n, h, L) = \frac{E(C)}{E(T)} \quad (1)$$

$$\text{Subject to } \alpha \leq \alpha_U,\ 1-\beta \geq P_L, \text{ and} \quad (2)$$

$$n \geq 1 \text{ and integer},\ h \geq 0,\ L \geq 0 \quad (3)$$

Where E(T) and E(C) represent the expected cycle length and the total expected cost per cycle, respectively. The objective function that the type I error probability (α) and power (1-β) as subjected to the predetermined statistical constraints, including maximum value of type I error (α_U) and minimum value of power (P_L), is minimized by determining the sample size (n), sampling interval (h), and the control limits (L). This can be expressed mathematically as:

$$E(T) = h + (\alpha Z_0 + h)\frac{e^{-\lambda h}}{1-e^{-\lambda h}}\left(1 + \frac{\lambda h}{1-e^{-\lambda h}}\right) + \frac{h\beta}{1-\beta} + Z_1 \quad (4)$$

$$E(C) = (a+bn+\alpha Y+D_1 h)\frac{e^{-\lambda h}}{1-e^{-\lambda h}}\left(1 + \frac{\lambda h}{1-e^{-\lambda h}}\right) + \frac{a+bn}{1-\beta} + \frac{2D0}{\lambda} + D_1\left(\frac{\beta}{1-\beta} - \frac{\lambda}{2}\right) + W \quad (5)$$

$$\text{Where } \alpha = 2\emptyset(-L),\ \beta = 1-\left[\emptyset\left(\delta\sqrt{n} - L\right) + \emptyset\left(-\delta\sqrt{n} - L\right)\right] \quad (6)$$

2) The cost model of non-uniform sampling interval(Rahim and Banerjee, 1993)

The objective function of the cost model is expressed mathematically as:

$$\text{Min } F(n, h_1, h_2, L) = \frac{E(C)}{E(T)} \quad (7)$$

$$\text{Subject to } \alpha \le \alpha_{U,1}\text{-}\beta \ge P_{L,} \text{ and} \quad (8)$$

$$n \ge 1 \text{ and integer, } h_1 \ge 0, h_2 \ge 0, L \ge 0 \quad (9)$$

Where E(T) and E(C) represent the expected cycle length and the total expected cost per cycle, respectively. The objective function that the type I error probability (α) and power (1-β) as subjected to the predetermined statistical constraints, including maximum value of type I error (α_U) and minimum value of power (P_L), is minimized by determining the sample size (n), sampling interval (h_1, h_2, representing the intervals of drawing a sample initially and taking a sample after the first sample over the cycle length, respectively), and the control limits (L). This can be expressed mathematically as:

$$E(T) = h_1 + (\alpha Z_0 + h_2)\frac{e^{-\lambda h_1}}{1-e^{-\lambda h_2}}\left(1 + \lambda h_1 + \frac{\lambda h_2 e^{-\lambda h_2}}{1-e^{-\lambda h_2}}\right) + \frac{h_2\beta}{1-\beta} + Z_1 \quad (10)$$

$$E(C) = (a + bn + \alpha Y + D_1 h_2)\frac{e^{-\lambda h_1}}{1-e^{-\lambda h_2}}\left(1 + \lambda h_1 + \frac{\lambda h_2 e^{-\lambda h_2}}{1-e^{-\lambda h_2}}\right) + \frac{a+bn}{1-\beta} + \frac{2D_0}{\lambda} + D_1\left(\frac{h_2\beta}{1-\beta} - \frac{2}{\lambda}\right) + W \quad (11)$$

$$\text{Where } \alpha = 2\emptyset(-L), \ \beta = 1\text{-}\left[\emptyset\left(\delta\sqrt{n} - L\right) + \emptyset\left(-\delta\sqrt{n} - L\right)\right] \quad (12)$$

The parameters of the model are listed below.

Time parameters:

Z_0 = the expected search time associated with a false alarm

Z_1 = the expected search time and repair time if a failure is detected

Cost parameters:

D_0 = the expected cost per hour caused by the production of a nonconforming item when the process is in control

D_1 = the expected cost per hour caused by the production of a nonconforming item when the process is out of control

W = the expected cost of locating an assignable cause and repairing the process, including the cost of down time

Y = the expected cost of false alarms, including the costs of searching and down time if production ceases during the search

a = the fixed cost per sample

b = the cost per unit sample

III. METHODOLOGY OF PROPOSED GENETIC ALGORITHM

Genetic algorithms (GA) are the heuristic search and optimization techniques that mimic the process of natural evolution. Simplicity of operation and power of effect are two of the main attractions of the GA approach (Goldberg, 1989). GA can be applied to a wide range of problems (e.g. location, partitioning, and scheduling problems) and GA makes no assumptions about the functions to be optimized.

All that GA requires is a performance measure, some form of population representation, and operators that generate new population members. This general approach can be applied to many combinatorial optimization problems. Hence GA is adapted for the economic statistical design of $\bar{X}$ control chart in this study. Adaptation is made with respect to chromosome representation, population initialization, crossover operation, and mutation operation in the proposed GA.

1) Mechanism of the proposed genetic algorithm (ESDCC-GA)

The proposed genetic algorithm is shown in Figure 1

a. Initialization

Initialize population size (N), crossover rate (CR) and mutation rate (MR) for the proposed genetic algorithm.

b. Initial population generation and fitness evaluation

Initial population of size N is randomly generated under a constrained condition for uniform sampling interval and non-uniform sampling interval.

c. Chromosome structure and representation

Each individual in a population is called chromosome (C). In the current study the problem is to optimize the parameters of control chart for uniform (n, h, L) and non-uniform (n, h_1, $h_{2,}$ L) sampling interval scheme to reduce expected cost per hour (ECT). So each chromosome is coded with parameters of control chart. Chromosome representation in this case is phenotype, that is actual values of parameters are used to code all the genes in a chromosome. The structure of chromosome for uniform sampling interval is shown in Table 1 and

non – uniform sampling interval is shown in Table 2. The chromosome length (l) is set as equal to number of parameters.

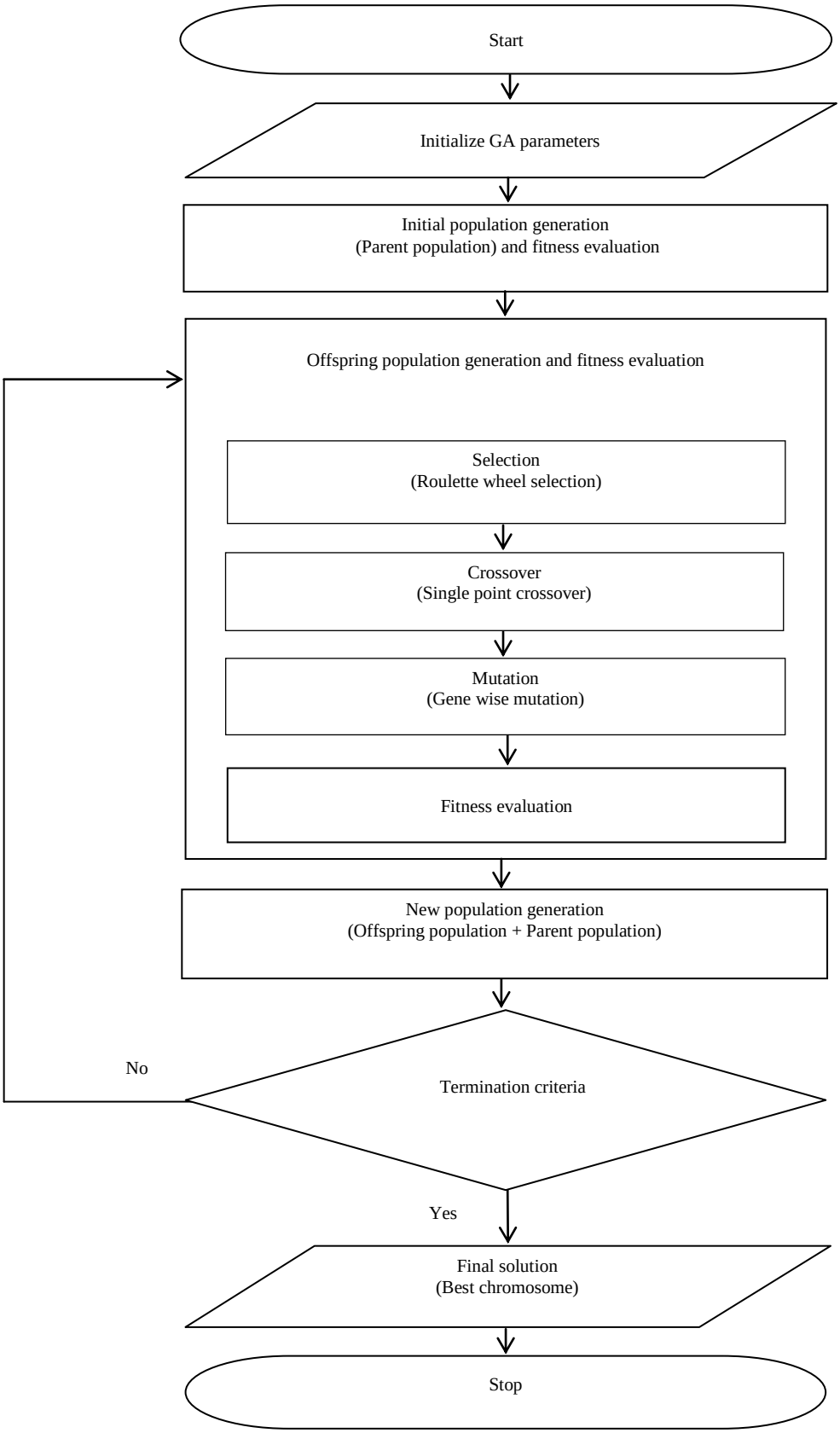

Figure 1 Proposed genetic algorithm

In the case of sample size, the generated gene value should be discrete, and for sampling interval and control limit, gene value is continuous for each chromosomes.
Gene value of each chromosome is generated using the following equation (Daniel and Rajendran, 2005).
Gene= rand ()* (upper_limit - lower_limit) + lower_limit;

Table 1 Chromosome structure for uniform sampling interval scheme

Chromosome, C		
g_1	g_2	g_3
n	h	L

Table 2 Chromosome structure for non-uniform sampling interval scheme

Chromosome, C			
g_1	g_2	g_3	g_4
n	h_1	h_2	L

d. Fitness evaluation

Every chromosome in the initial population is evaluated with respect to its fitness function, F = 1/ECT.

e. Offspring population generation and fitness evaluation

Offspring populations are generated by applying the following GA operators.

1 Selection - roulette wheel procedure
2 Crossover - single point crossover (based on crossover rate)
3 Mutation - gene wise mutation (based on mutation rate)

The fitness value of each chromosome in the offspring population is also calculated.

f. New population generation

The chromosomes in the offspring and parent populations are combined to generate a new population . The best N chromosomes, among the 2N chromosomes are chosen as the surviving chromosomes for the next generation (Parental chromosomes for the next generation).

g. Termination criteria and final solution

The total number of generation is taken as the termination criteria and GA gives the global best solution after termination criteria is satisfied.

IV. RESULTS AND DISCUSSION

A. Economic statistical design of $\bar{X}$ control chart under uniform sampling interval

In the computational experiment of uniform sampling interval, the population size was set to 80. The crossover probability and mutation probability were set to 0.7 and 0.2, respectively. Parameters are selected based on the pilot study. Generation number is selected based on the convergence analysis of each test problem. For uniform sampling interval, the initial population is randomly generated under the following constrained condition.

$1 \leqslant n \leqslant 3000$ (Sample size)
$0.1 \leqslant h \leqslant 100$ (Sampling interval)
$0.1 \leqslant L \leqslant 6$ (Control limit)

The values of time, cost, Gamma and shift parameters of the example test problem are as follows: $Z_0 = 0.25$ h; $Z_1 = 1.00$ h; $D_0 = \$50.00$; $D_1 = \$950.0$; W = \$1100.00; Y = \$500.00; a = \$20.00; b = \$4.22; $\delta = 0.50$; $\lambda = 0.05$; alphaUB = 0.05; and pLB = 0.9. After the experimental study, convergence point of the test problem is identified as 77901th generation and the generation number was set to 80000. The result obtained from ESDCC-GA is compared with the result obtained for same number of solutions (3921017) from PSO (Chih et. al) and it is shown in Table 3. The result shows that EDDCC-GA is better than PSO in terms of minimum ECT and is faster than PSO in terms of elapsed time for uniform sampling interval.

Table 3 Result of uniform sampling interval scheme by ESDCC-GA

Algorithm	n	h	L	α	1-β	ECT	Time (m)
ESDCC-GA	43	4.3879	1.9599	0.05	0.9063	178.0005	29.28
PSO	43	4.3364	1.9602	0.0499	0.9063	178.0085	48.82

B. Economic statistical design of $\bar{X}$ control chart under non-uniform sampling interval

In the computational experiment of non-uniform sampling interval, the population size was set to 80. The crossover probability and mutation probability were set to 0.7 and 0.2, respectively. Parameters are selected after conducting the pilot study. Generation number of each test problem under non-uniform sampling interval is selected based on convergence analysis. For non - uniform sampling interval, the initial population is randomly generated under the following constrained condition.

$1 \leqslant n \leqslant 3000$ (Sample size)
$0.1 \leqslant h1 \leqslant 100,\quad 0.1 \leqslant h2 \leqslant 40$ (Sampling interval)
$0.1 \leqslant L \leqslant 6$ (Control limit)

The values of time, cost, Gamma (λ, 2), and shift parameters of the example are as follows: $Z_0 = 0.25$ h; $Z_1 = 1.00$ h; $D_0 = \$50.00$; $D_1 = \$950.0$; $W = \$1100.00$; $Y = \$500.00$; $a = \$20.00$; $b = \$4.22$; $\delta = 0.50$; $\lambda = 0.05$; alphaUB = 0.05; and pLB = 0.9. In the computational experiments of non-uniform sampling interval, convergence point of the test problem is identified as 79946th generation and the generation number was set to 90000. The result obtained from ESDCC-GA is compared with the result obtained for same number of solutions (5062252) from PSO (Chih et. al) and it is shown in Table 4. The result shows that EDDCC-GA is better than PSO in terms of minimum ECT and is faster than PSO in terms of elapsed time for non uniform sampling interval.

Table 4 Result of non-uniform sampling interval scheme

Algorithm	n	h_2	h_2	L	α	1-β	ECT	Time (m)
ESDCC-GA	43	10.53	3.9081	1.9599	0.05	0.9063	173.803765	36.04
PSO	43	10.60	3.8589	1.9647	0.0494	0.9055	173.8344	72.38

C. Test problems

To demonstrate the efficacy of the proposed GA, 20 test problems from literature (Chih et. al) were solved using ESDCC – GA. The test problems considered in this study are shown in Table 5.

D. Result of test problems

The results of test problems by ESDCC-GA and PSO (Chih et. al) under uniform and non-uniform sampling interval are shown in Table 6 and Table 7 respectively. The result shows that ESDCC-GA takes lesser time than PSO (Chih et. al) for inspecting similar number of solutions in uniform and non-uniform sampling interval. The result indicates that ESDCC-GA is superior to PSO (Chih et. al) in terms of convergence speed for economic statistical design of $\bar{X}$ control chart.

The proposed GA is better than PSO in terms of minimum ECT and is faster than PSO in terms of elapsed time. Comparing the uniform and non-uniform sampling interval scheme, the expected cost per hour (ECT) is minimum in non-uniform sampling interval scheme.

V. CONCLUSION

This present study aimed to develop a genetic algorithm (ESDCC-GA) for economic statistical design of $\bar{X}$ control charts under uniform and non-uniform sampling interval. The proposed algorithm is designed to solve the constrained problem, which involves the simultaneous use of continuous and discrete decision variables. To verify the performance of the proposed GA, the numerical example of Rahim and Banerjee (1993) with a Gamma failure mechanism is illustrated in this paper.

The various test problems in the literature is also used to evaluate the proposed GA. The computational results demonstrated that proposed GA and PSO (Chih et. al) have the similar performance in terms of final solution quality for the economic statistical design of $\bar{X}$ control charts. However, the proposed GA (EDDCC-GA) is significantly faster and is better than PSO (Chih et. al) in terms of elapsed time. When inspecting similar number of solutions, EDDCC-GA takes lesser time than PSO (Chih et. al). A higher cost was saved in the non-uniform sampling scheme than the uniform sampling scheme regardless of which method was adopted. Meanwhile, no significant differences were observed between control chart parameters from EDDCC-GA and PSO (Chih et. al).

Table 5 Test problems

Problem No.	Z_0	Z_1	D_0	D_1	W	Y	a	b	δ	α_{UB}	p_{LB}	λ
1	0.025	0.1	25	475	550	250	10	2.11	0.25	0.01	0.85	0.025
2	0.025	0.1	25	475	1100	500	20	4.22	0.5	0.05	0.9	0.05
3	0.025	0.1	25	475	2200	1000	40	8.44	1	0.1	0.95	0.1
4	0.025	1	50	950	550	250	10	4.22	0.5	0.05	0.95	0.1
5	0.025	1	50	950	1100	500	20	8.44	1	0.1	0.85	0.025
6	0.025	1	50	950	2200	1000	40	2.11	0.25	0.01	0.9	0.05
7	0.025	10	100	1900	550	250	10	8.44	1	0.1	0.9	0.05
8	0.025	10	100	1900	1100	500	20	2.11	0.25	0.01	0.95	0.1
9	0.025	10	100	1900	2200	1000	40	4.22	0.5	0.05	0.85	0.025
10	0.25	0.1	50	1900	550	500	40	2.11	0.5	0.1	0.85	0.05
11	0.25	0.1	50	1900	1100	1000	10	4.22	1	0.01	0.9	0.1
12	0.25	0.1	50	1900	2200	250	20	8.44	0.25	0.05	0.95	0.025
13	0.25	1	100	475	550	500	40	4.22	1	0.01	0.95	0.025
14	0.25	1	100	475	1100	1000	10	8.44	0.25	0.05	0.85	0.05
15	0.25	1	100	475	2200	250	20	2.11	0.5	0.1	0.9	0.1
16	0.25	10	25	950	550	500	40	8.44	0.25	0.05	0.9	0.1
17	0.25	10	25	950	1100	1000	10	2.11	0.5	0.1	0.95	0.025
18	0.25	10	25	950	2200	250	20	4.22	1	0.01	0.85	0.05
19	0.5	0.1	100	950	550	1000	20	2.11	1	0.05	0.85	0.1
20	0.5	0.1	100	950	1100	250	40	4.22	0.25	0.1	0.9	0.025

Table 6 Result of test problem under uniform sampling interval scheme

Problem No.		**1**	**2**	**3**	**4**	**5**	**6**	**7**	**8**	**9**	**10**
GA	Convergence Point	76666	65126	73023	64956	82808	81671	82117	76667	78352	67187
	Generation Number	80000	70000	80000	70000	90000	90000	90000	80000	80000	70000
	Solutions inspected	3925996	3393136	3816918	3407686	4289034	4542012	4363175	3874998	3836693	3428670
	n	209	43	14	52	10	239	9	286	39	41
	h	12.1287	6.53722	5.16334	3.44407	4.39791	7.25411	2.01607	3.81182	4.31569	2.40646
	L	2.5758	1.95996	2.0968	1.95996	1.98869	2.57583	1.71844	2.57583	1.97777	1.92076
	α	0.01	0.05	0.03601	0.05	0.04674	0.01	0.08572	0.01	0.04795	0.05476
	1-β	0.85045	0.90637	0.95	0.95008	0.85972	0.90131	0.9	0.95074	0.87384	0.89987
	ECT	110.293	124.136	212.466	213.171	120.963	259.434	176.765	334.421	218.452	190.625
	Time (m)	40.5602	35.4594	39.4241	39.9938	41.5442	41.8979	41.8379	39.3925	39.8306	35.1188
PSO	Solutions inspected	3925996	3393136	3816918	3407686	4289034	4542012	4363175	384998	3836693	3428670
	n	210	43	14	52	10	240	9	286	39	41
	h	12.2792	6.65081	5.13963	3.3402	4.40073	7.2783	2.02334	3.75501	4.3125	2.40402
	L	2.57834	1.96014	2.09583	1.96033	1.98708	2.5786	1.7164	2.57619	1.97471	1.91979
	α	0.00993	0.04998	0.0361	0.04996	0.04691	0.00991	0.08609	0.00999	0.0483	0.05488
	1-β	0.85188	0.90635	0.9501	0.95004	0.88004	0.90229	0.90036	0.9507	0.87447	0.90004
	ECT	110.359	124.146	212.472	213.231	120.963	259.427	176.769	334.452	218.452	190.625
	Time (m)	52.5044	43.0607	61.7003	47.8221	59.1871	65.2915	62.0128	66.5141	59.9515	42.4805

Table 6 Result of test problem under uniform sampling interval scheme (Continued)

Problem No.		**11**	**12**	**13**	**14**	**15**	**16**	**17**	**18**	**19**	**20**
GA	Convergence Point	66789	73686	84124	58117	77680	75551	86264	74332	65123	81671
	Generation Number	70000	80000	90000	60000	80000	80000	90000	80000	70000	90000
	Solutions inspected	3366393	3809401	4371420	2896750	3989404	3924229	4289645	3742404	3243902	4561267
	n	15	208	18	144	35	169	59	14	17	138
	h	1.27861	12.9625	7.22725	19.1451	4.10507	8.4715	5.22212	2.47284	1.6928	10.8103
	L	2.57583	1.95997	2.57583	1.95997	1.64485	1.9623	2.1957	2.5758	2.6864	1.64485
	α	0.01	0.05	0.01	0.05	0.1	0.04	0.02811	0.01	0.00722	0.1
	1-β	0.90271	0.95008	0.95222	0.85084	0.90544	0.90148	0.95	0.8781	0.92459	0.9018
	ECT	235.193	364.356	139.278	272.858	254.426	294.623	90.2557	117.582	201.632	235.68
	Time (m)	38.6242	39.7378	46.0379	22.9571	37.8936	40.46	47.2025	33.4396	37.1808	43.1536
PSO	Solutions inspected	3366393	3809401	4371420	2896750	3989404	3924229	4289645	3742404	3243902	4561267
	n	15	209	18	144	35	169	59	14	17	138
	h	1.28831	13.2154	7.25323	18.4653	4.0838	8.4715	5.2575	2.47846	1.70304	10.7823
	L	2.57679	1.96	2.57872	1.96298	1.64517	1.96237	2.19245	2.57799	2.6843	1.64527
	α	0.00997	0.04976	0.00992	0.04965	0.09993	0.04972	0.0283	0.00994	0.00727	0.09991
	1-β	0.90255	0.95075	0.95194	0.85014	0.90538	0.90106	0.95034	0.87777	0.92489	0.90174
	ECT	235.199	364.849	139.283	273.004	254.427	294.735	90.2746	117.602	201.634	235.688
	Time (m)	46.4415	60.0953	61.4228	26.843	62.6017	59.2417	63.546	52.425	45.3988	63.8143

Table 7 Result of test problem under non-uniform sampling interval scheme

Problem No.		**1**	**2**	**3**	**4**	**5**	**6**	**7**	**8**	**9**	**10**
GA	Convergence Point	56794	71972	71357	67896	79952	73958	73958	72000	79951	62432
	Generation Number	60000	80000	80000	70000	90000	90000	80000	80000	80000	70000
	Solutions inspected	3541384	4495917	4537386	3954281	4970392	5054985	4395712	4549270	4426780	3975804
	n	209	43	14	52	10	239	9	286	38	40
	h_1	27.30075	13.62814	8.875577	6.789171	13.97242	14.65416	6.50242	7.25993	13.86627	7.238837
	h_2	10.40099	5.63661	4.29653	2.984342	4.048314	6.185903	1.873377	3.277038	3.925159	2.189877
	L	2.57583	1.959965	2.096802	1.959964	1.996788	2.57583	1.71844	2.575832	1.974716	1.917124
	α	0.01	0.05	0.036011	0.05	0.045848	0.01	0.085716	0.01	0.0483	0.055222
	1-β	0.850453	0.906374	0.95	0.950076	0.878089	0.901314	0.9	0.950738	0.865959	0.893462
	ECT	106.5418	120.9353	209.0958	207.3724	118.9528	252.3095	173.9508	324.4844	214.7907	186.2246
	Time (m)	25.6872	30.9271	31.0345	26.1945	35.7714	35.4539	37.5203	30.1581	32.5003	29.0492
PSO	Solutions inspected	3541384	4495917	4537386	3954281	4970392	5054985	4395712	4549270	4426780	3975804
	n	209	43	14	53	10	241	9	286	39	40
	h_1	26.18701	13.66926	8.993446	6.882441	13.9249	14.08294	6.376289	7.382344	13.93939	7.347877
	h_2	10.96082	5.724924	4.206441	3.040485	4.038741	6.161699	1.860838	3.139819	3.990992	2.174579
	L	2.577271	1.960872	2.096268	1.965662	2.00214	2.588259	1.717832	2.576188	1.986138	1.922985
	α	0.009958	0.049894	0.036058	0.049338	0.04527	0.009646	0.085827	0.00999	0.047018	186.2294
	1-β	0.850117	0.906223	0.950055	0.952973	0.877004	0.901957	0.900107	0.950702	0.872097	0.054482
	ECT	106.6491	120.9449	209.1115	208.1076	118.9533	252.7861	173.9574	324.6389	214.7918	0.892381
	Time (m)	47.33	54.61	56.6563	46.4123	70.946	76.7032	54.0317	82.4915	56.6679	46.8512

Table 7 Result of test problem under non-uniform sampling interval scheme (Continued)

Problem No.		**11**	**12**	**13**	**14**	**15**	**16**	**17**	**18**	**19**	**20**
GA	Convergence Point	67507	71986	71990	72456	79648	74298	82457	70000	80000	80000
	Generation Number	70000	80000	90000	80000	90000	80000	90000	67234	75345	76479
	Solutions inspected	3962218	4605403	5074088	4523146	5024789	4534782	5121748	392476	4487415	4612481
	n	15	208	18	144	35	169	67	15	17	138
	h_1	3.755649	26.09059	17.85138	29.0862	7.9063	12.998	14.631	7.5664	4.4	24.194
	h_2	1.175287	11.28959	6.559405	13.8705	3.4683	6.5424	4.8716	2.386	1.5227	9.4628
	L	2.57583	1.959966	2.575829	1.96	1.644	1.96	2.4478	2.5758	2.6989	1.644
	α	0.01	0.05	0.01	0.05	0.01	0.05	0.014	0.01	0.007	0.1
	1-β	0.902711	0.950075	0.952224	0.8507	0.9053	0.9014	0.95	0.9027	0.9228	0.9017
	ECT	230.5957	352.6095	138.0564	265.8333	251.9064	282.5949	89.1105	115.7021	198.8551	230.4388
	Time (m)	30.0996	32.195	35.752	33.45	36.12	32.78	36.478	28.367	33.147	34.128
PSO	Solutions inspected	3962218	4605403	5074088	4523146	5024789	4534782	5121748	392476	4487415	4612481
	n	15	209	18	145	35	169	62	15	17	139
	h_1	0.1	26.68258	17.888	29.1032	7.8979	13.0407	14.8415	7.5292	4.3771	23.987
	h_2	1.283045	11.26566	6.5765	13.918	3.4691	6.5984	4.772	2.2545	1.558	9.3645
	L	2.577229	1.967786	2.575	1.96	1.63	1.96	2.2554	2.568	2.6651	1.6449
	α	0.00996	0.049093	0.01	0.05	0.01	0.05	0.024	0.01	0.0071	0.09
	1-β	0.90247	0.950161	0.9522	0.8507	0.90541	0.90142	0.9503	0.8782	0.9213	0.9507
	ECT	238.8497	353.2209	139.1245	267.0124	252.3654	282.9012	89.8742	115.7841	199.1245	230.784
	Time (m)	53.3333	63.3	66.412	60.124	69.321	58.651	71.23	52.198	59.34	61.147

REFERENCES

[1] Ben-Daya M. and Rahim M. A., "Effect of maintenance on the economic design of x-control charts", European Journal of Operational Research, vol. 120 (1), pp. 131–143, 2000.

[2] Cai D. Q., Xie M., Goh T. N. and Tang X. Y., "Economic design of control chart for trended processes", International Journal of Production Economics, vol. 79, pp. 85 -92, 2001.

[3] Caulcutt R., "The rights and wrongs of control charts", Applied Statistics, vol. 44 (3), pp. 279–288, 1995.

[4] Chen Y. S. and Yang Y. M., "An extension of Banerjee and Rahim's model for economic design of moving average control chart for a continuous flow process", European Journal of Operational Research, vol. 143, pp. 600–610, 2002.

[5] Chen Y. S. and Yang Y. M., "Economic design of $\overline{X}$ control charts with Weibull in-control times when there are multiple assignable causes", International Journal of Production Economics, vol. 77, pp. 17–23, 2002.

[6] Chen H. and Cheng Y., "Non-normality effects on the economic–statistical design of $\overline{X}$ charts with Weibull in-control time", European Journal of Operational Research, vol. 176, pp. 986–998, 2007.

[7] Chen F. L. and Yeh C. H., "Economic statistical design of non-uniform sampling scheme $\overline{X}$ control charts under non-normality and Gamma shock using genetic algorithm", Expert Systems with Applications, vol. 36, pp.9488–9497, 2009.

[8] Chou C. Y., Chen C. H., Liu H. R. and Huang X. R., "Economic-statistical design of multivariate control charts for monitoring the mean vector and covariance matrix", Journal of Loss Prevention in the Process Industries, vol. 16, pp. 9–18, 2003.

[9] Duncan A. J., "The economic design of $\overline{X}$ chart used to maintain current control of a process", Journal of the American Statistical Association, vol. 51, pp. 228-242, 1956.

[10] Girshick M. A., and Rubin H. A., "Baye's approach to a quality control model", Annals of Mathematical Statistics, vol. 23, pp. 114-125, 1952.

[11] Lin S. N., Chou C. Y., Wang S. L. and Liu H. R., "Economic design of autoregressive moving average control chart using genetic algorithms", Expert Systems with Applications, vol. 39, pp. 1793–1798, 2012.

[12] M. A. Rahim, P. K. Banerjee, "A generalized economic model for the economic design of control charts for production systems with increasing failure rate and early replacement", Naval Research Logistics, vol. 40, pp. 787–809, 1993.

[13] Morteza Behbahani, Abbas Saghaee and Rassoul Noorossana, "A case-based reasoning system development for statistical process control: case representation and retrieval", Computers & Industrial Engineering, vol. 63, pp. 1107–1117, 2012.

[14] Pei-Hsi Lee, Chau-Chen Torng and Li-Fang Liao, "An economic design of combined double sampling and variable sampling interval X control chart", International Journal of Production Economics, vol. 138, pp. 102–106, 2012.

[15] Vijaya V. B., Murty S. S. N., "A simple approach for robust economic design of control charts", Computers & Operations Research, vol. 34, pp. 2001 – 2009, 2007.

[16] Wafik Hachicha, Ahmed Ghorbel, "A survey of control-chart pattern-recognition literature (1991–2010) based on a new conceptual classification scheme", Computers & Industrial Engineering, vol. 63, pp. 204–222, 2012.

[17] Weiler H., "On the most economical sample size for controlling the mean of a population", Annals of Mathematical Statistics, vol. 23, pp. 247-254, 1952.

[18] Woodall W. H., "Conflicts between Deming's philosophy and the economic design of control charts", Frontiers in Statistical Quality Control, vol. 3, pp. 242-248, 1987.

[19] Woodall, W. H., "Controversies and contradictions in statistical process control", Journal of Quality Technology", vol. 32 (4), pp. 341–378, 2000.

[20] Yan K. C., Hung C. L., "Multi-criteria design of an $\overline{X}$ control chart", Computers & Industrial Engineering, vol. 46, pp. 877–891, 2004.

[21] Yan-Kwang Chena, Kun-Lin Hsieh, Cheng-Chang Chang (2007), "Economic design of the VSSI $\overline{X}$ control charts for correlated data", International Journal of Production Economics, vol. 107, pp. 528–539.

Misbehavior Report Authentication Intrusion Detection System in MANETs

[1]M.Geetha [2]N.Senthilkumar
[1]PG scholar, [2]Assistant Professor
ECE department
VivekanandhaCollege of Engineering For Women
Mail id: geethasharthi@gmail.com, senthilsuguna@gmail.com

Abstract **- Mobile Ad hoc Network is a collection of wireless mobile nodes forming a network without using any existing infrastructure. MANET is a collection of mobile nodes prepared with both a wireless-transmitter and receiver that communicate with each other via bi-directional wireless links either directly or not directly. A new intrusion detection system named Enhanced Adaptive Acknowledgement (EAACK) specially designed for MANETs. By the implementation of Misbehavior Report Authentication(MRA) scheme, EAACK is able of detecting malicious nodes despite the existence of false misbehavior report and compared it against other popular mechanisms in different scenarios during simulation. The results will demonstrate positive performances next to Watchdog, TWOACK and AACK in the cases of receiver collision, limited communication power and false misbehavior statement. EAACK demonstrates higher malicious behavior detection rates in certain circumstance while does not greatly affect the network performances.**

Keywords – Mobile Ad hoc Network, Enhanced Adaptive Acknowledgement (EAACK), Misbehavior Report Authentication (MRA), TWO Acknowledgement (TWOACK), Adaptive Acknowledgement (AACK).

.

I. Introduction

Due to their natural mobility and scalability, wireless networks are always preferred since the rest day of their creation. Due to the improved technology and reduced costs, wireless networks have increase much more preferences over wired networks in the past a lot of decades.

By definition, Mobile Ad hoc Network (MANET) is a collection of mobile nodes equipped with both a wireless transmitter and a receiver that communicate with each other via bidirectional wireless links either directly or indirectly. Industrial remote access and control via wireless networks are becoming more and more popular these days. One of the major advantages of wireless networks is its ability to allow data communication between different parties and still maintain their mobility. However, this communication is limited to the range of transmitters. This means that two nodes cannot communicate with each other when the distance between the two nodes is beyond the communication range of their own. MANET solves this problem by allowing intermediate parties to relay data transmissions. This is achieved by dividing MANET into two types of networks, namely, single-hop and multi hop. In a single-hop network, all nodes within the same radio range communicate directly with each other. On the other hand, in a multi

hop network, nodes rely on other intermediate nodes to transmit if the destination node is out of their radio range.

In contrary to the traditional wireless network, MANET has a decentralized network infrastructure. MANET does not require a fixed infrastructure; thus, all nodes are free to move randomly [10], [12]. MANET is capable of creating a self-configuring and self-maintaining network without the help of a centralized infrastructure, which is often infeasible in critical mission applications like military conflict or emergency recovery. Minimal configuration and quick deployment make MANET ready to be used in emergency circumstances where an infrastructure is unavailable or unfeasible to install in scenarios like natural or human-induced disasters, military conflict, and medical emergency situations [9], [7].

Owing to these unique characteristics, MANET is becoming more and more widely implemented in the industry [5]. However, considering the fact that MANET is popular among critical mission applications, network security is of vital importance. Unfortunately, the open medium and remote distribution of MANET make it vulnerable to various types of attacks. For example, due to the nodes' lack of physical protection, malicious attackers can easily capture and compromise nodes to achieve attacks. In particular, considering the fact that most routing protocols in MANETs assume that every node in the network behaves cooperatively with other nodes and presumably not malicious [5], attackers can easily compromise MANETs by inserting malicious or non cooperative nodes into the network. Furthermore, because of MANET's distributed architecture and changing topology, a traditional centralized monitoring technique is no longer feasible in MANETs. In such case, it is crucial to develop an intrusion-detection system (IDS) specially designed for MANETs.

Advantages of Mobile Ad Hoc Networks

Having discussed the general issues in MANETs, the reason behind their popularity and their benefits will now be discussed.

Low cost of deployment: As the name suggests, ad hoc networks can be deployed on the fly, thus requiring no expensive infrastructure such as copper wires, data cables, etc.

Fast deployment: When compared to WLANs, ad hoc networks are very convenient and easy to deploy requiring less manual intervention since there are no cables involved.

Dynamic Configuration: Ad hoc network configuration can change dynamically with time. For the many scenarios such as data sharing in class-rooms, etc., this is a useful feature. When compared to configurability of LANs, it is very easy to change the network topology.

In the next section, mainly focus on discussing the background information required for understanding this research topic.

II. Related Work

As discussed before, due to the limitations of most MANET routing protocols, nodes in MANETs assume that other nodes always cooperate with each other to relay data. This

assumption leaves the attackers with the opportunities to achieve significant impact on the network with just one or two compromised nodes. To address this problem, IDS should be added to enhance the security level of MANETs. If MANET can detect the attackers as soon as they enter the network, we will be able to completely eliminate the potential damages caused by compromised nodes at the first time. IDSs usually act as the second layer in MANETs, and they are a great complement to existing proactive approaches [8]. In this section, mainly describe three existing approaches, namely, Watchdog [4], TWOACK [5], and Adaptive Acknowledgment (AACK) [3].

1) Watchdog that aims to improve throughput of network with the presence of malicious nodes. In fact, the watchdog scheme is consisted of two parts, namely Watchdog and Pathrater. Watchdog serves as an intrusion detection system for MANETs. It is responsible for detecting malicious nodes misbehaviors in the network. Watchdog detects malicious misbehaviors by promiscuously listens to its next hop's transmission. If Watchdog node overhears that its next node fails to forward the packet within a certain period of time, it increases its failure counter.

Whenever a node's failure counter exceeds a pre-defined threshold, the Watchdog node reports it as misbehaving. In this case, the Pathrater cooperates with the routing protocols to avoid the reported nodes in future transmission. Many following researches and implementations have proved that the Watchdog scheme to be efficient. Furthermore, compared to some other schemes, Watchdog is capable of detecting malicious nodes rather than links. These advantages have made Watchdog scheme a popular choice in the field. Many MANET IDSs are either based on or developed as an improvement to the Watchdog scheme. Watchdog scheme fails to detect malicious misbehaviors with the presence of Ambiguous collisions, Receiver collisions, Limited transmission power, False misbehavior report, Partial dropping.

2) TWOACK is neither an enhancement nor a Watch-dog based scheme. Aiming to resolve the receiver collision and limited transmission power problems of Watchdog, TWOACK detects misbehaving links by acknowledging every data packets transmitted over each three consecutive nodes along the path from the source to the destination. Upon retrieval of a packet, each node along the route is required to send back an acknowledgement packet to the node that is two hops away from it down the route. TWOACK is required to work on routing protocols such as Dynamic Source Routing (DSR).The working process of TWOACK is demonstrated in Figure 1 node A first forwards packet 1 to node B, and then node B forwards Packet 1 to node C. When node C receives Packet 1, as it is two hops away from node A, node C is obliged to generate a TWOACK packet, which contains reverse route from node A to node C, and sends it back to node A. The retrieval of this TWOACK packet at node A indicates the transmission of Packet 1 from node A to node C is successful. Otherwise, if this TWOACK packet is not received in a predefined time period, both nodes B and C are reported malicious.

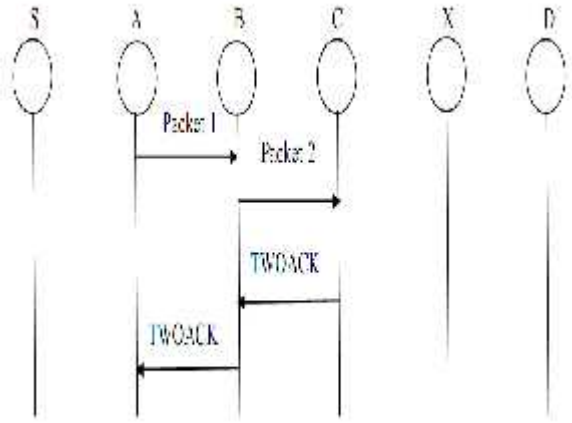

Figure 1.TWOACK

TWOACK scheme successfully solves the receiver collision and limited transmission power problems posed by Watchdog. However, the acknowledgement process required in every packet transmission process added a significant amount of un-wanted network overhead. Due to the limited battery power nature of MANETs, Such redundant transmission process can easily degrade the life span of the entire network.

3) AACK is based on TWOACK Acknowledgement (AACK) similar to TWOACK,AACK is an acknowledgement-based network layer scheme which can be considered as a combination of a scheme call ACK (identical to TWOACK) and an end-to-end acknowledgement scheme called ACK. Compared to TWOACK, AACK significantly reduced network overhead while still capable of maintaining the same network throughput. Source node S will switch to TACK scheme by sending out a TACK packet. The concept of adopting a hybrid scheme in AACK greatly reduces the network over-head, but both TWOACK and AACK still suffer from the problem that they fail to detect malicious nodes with the presence of false misbehavior report and forged acknowledgement packets.

Both TWOACK and AACK still suffer from the problem that they fail to detect malicious nodes with the presence of false misbehavior report and forged acknowledgment packets. In fact, many of the existing IDSs in MANETs adopt an acknowledgment-based scheme, including TWOACK and AACK. The functions of such Detection schemes all largely depend on the acknowledgment packets. Hence, it is crucial to guarantee that the acknowledgment packets are valid and authentic.

III. Problem Definition

My proposed approach EAACK is designed to deal with three of the six weaknesses of Watchdog scheme, namely, false misbehavior, limited transmission power, and receiver collision. In this section discuss these three weaknesses in detail.

In the case of receiver collisions, demonstrated in Figure 2, after node A sends Packet 1 to node B, it tries to overhear if node B forwarded this packet to node C; meanwhile, node X is forwarding packet 2 to node C. In such case, node A overhears that node B has successfully, forwarded Packet 1 to node C, but failed to detect that node C did not receive this packet due to a collision between Packet 1 and Packet 2 at node C.

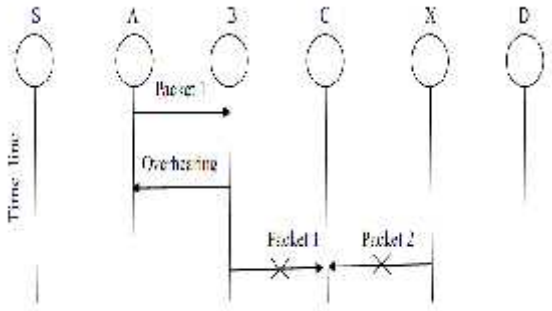

Figure 2.Receiver collision

In the case of limited transmission power, in order to preserve its own battery resources, node B intentionally limits its transmission power so that it is strong enough to be overheard by node A but not strong enough to be received by node C, as shown in Figure 3.

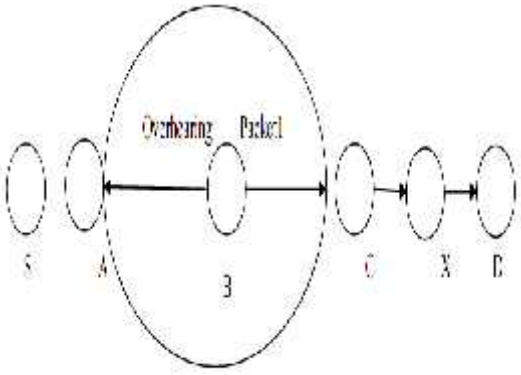

Figure 3.Limited Transmission power

For false misbehavior report, although node A successfully overheard that node B forwarded Packet 1 to node C, node a still reported node B as misbehaving as shown in Figure 4. Due to the

open medium and remote distribution of typical MANETs, attackers can easily capture and compromise one or two nodes to achieve this false misbehavior report attack.

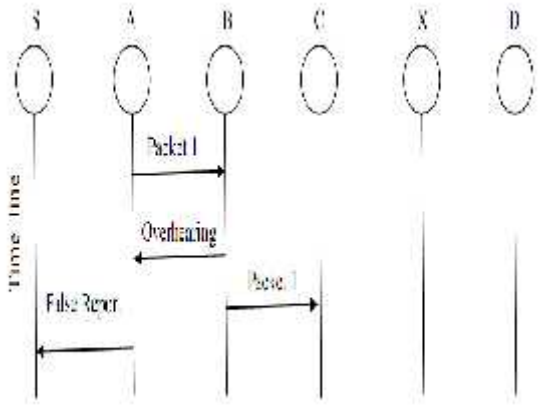

Figure 4.False misbehavior report

IV. Scheme Description

In this section, describe my proposed EAACK scheme in detail. The approach described in this research paper is based on our previous work [12], where the backbone of EAACK was proposed and evaluated through implementation. In this paper, extend it with attacker from forging acknowledgment packets.

My proposed approach EAACK is designed to tackle three of the six weaknesses of Watchdog scheme, namely, false misbehavior, limited transmission power, and receiver collision. EAACK is consisted of three major parts, namely, ACK, secure ACK (S-ACK), and misbehavior report authentication (MRA).

1. *A. ACK*

ACK is basically an end-to-end acknowledgement scheme. It acts as a part of the hybrid scheme in EAACK, aiming to reduce network overhead when no network misbehavior is detected. In Figure 5 in ACK mode, node S first sends out an ACK data packet ad1 P to the destination node D.

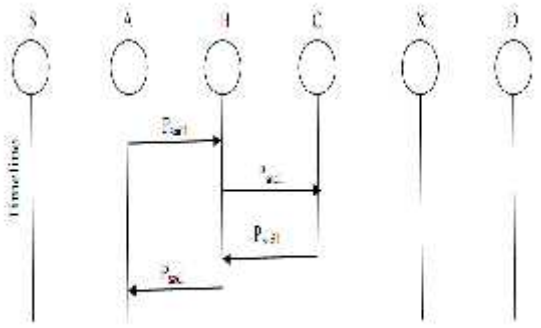

Figure 5.ACK

If all the intermediate nodes along the route between node S and node D are cooperative and node D successfully receives Pad1, node D is required to send back an ACK acknowledgement packet ak1 P along the same route but in a reverse order. Within a predefined time period, if node S receives ak1 P, then the packet transmission from node S to node D is successful. Otherwise, node S will switch to S ACK mode by sending out an S-ACK data packet to detect the misbehaving nodes in the route.

2. B. S-ACK

S-ACK scheme is an improved version of TWOACK scheme. The principle is to let each three consecutive nodes work in a group to detect misbehaving nodes. For each three consecutive nodes in the route, the third node is required to send an S-ACK acknowledgement packet to the first node. The intention of introduce

S-ACK mode is to detect misbehaving nodes in the presence of receiver collision or limited transmission power. As demonstrated in Figure 6 in S-ACK mode, the three consecutive nodes (i.e. F1, F2 and F3) work in a group to detect misbehaving nodes in the network. Node F1 first sends out S-ACK data packet P_{sad1} to node F2. Then node F2 forwards this packet to node F3.

When node F3 receives P_{sad1}, as it is the third node in this three node group, node F3 is required to send back an S-ACK acknowledgement packet P_{sak1} to node F2. Node F2 forwards P_{sak1} back to node F1. If node F1 does not receive this acknowledgement packet within a predefined time period, both nodes F2 and F3 are reported as malicious.

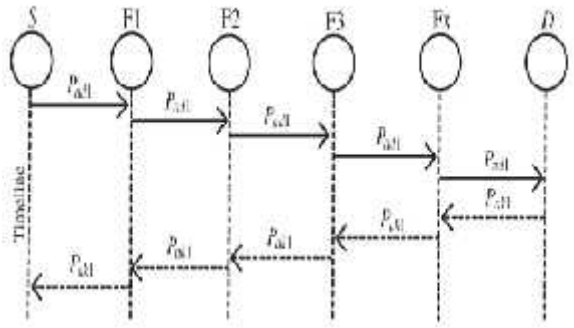

Figure 6.S-ACK

Moreover, a misbehavior report will be generated by node F1 and sent to the source node S. Nevertheless, unlike the TWOACK scheme, where the source node immediately trusts the misbehavior report, EAACK requires the source node to switch to MRA mode and confirm this misbehavior report. This is a vital step to detect false misbehavior report in our proposed scheme.

3. C.MRA

The Misbehavior Report Authentication (MRA) scheme is designed to resolve the weakness of Watchdog when it fails to detect misbehaving nodes with the presence of false misbehavior report. False misbehavior report can be generated by malicious attackers to falsely report that innocent nodes as malicious. This attack can be lethal to the entire network when the attackers break down sufficient nodes and thus cause a network division. The core of MRA scheme is to authenticate whether the destination node has received the reported missing packet through a different route. To initiate MRA mode, the source node first searches its local knowledge base and seeks for alternative route to the destination node.

If there is none other exists, the source node starts a DSR routing request to find another route. Due to the nature of MANETs, it is common to find out multiple routes between two nodes. By adopting an alternative route to the destination node, circumvent the misbehavior reporter node. When the destination node receives an MRA packet, it searches its local knowledge base and compare if the reported packet was received. If it is already received, then it is safe to conclude this is a false misbehavior report and whoever generated this report is marked as malicious.

Otherwise, the misbehavior report is trusted and accepted. By the adoption of MRA scheme, EAACK is capable of detecting malicious nodes despite the existence of false misbehavior report.

V. Conclusion

Packet dropping attack has always been a major threat to the security in MANETs. In this work a novel IDS named EAACK protocol specially designed for MANETs and compared it against other popular mechanisms in different scenarios through simulation. The results described positive performances against Watchdog, TWOACK and AACK in the cases of receiver collision and limited Transmission power and false misbehavior report.

Furthermore, in an effort to prevent the attackers from initiating a forged acknowledgement attacks, extended to incorporate digital signature in proposed scheme. Although it generates more routing overhead in some cases, as demonstrated in experiment, it can vastly improve the networks packet delivery ratio when the attackers are smart enough to forget acknowledgement packets. This trade-off is worthwhile when network security is of top priority. In order to seek the optimal digital signature algorithms in MANETs, implemented both DSA and RSA scheme in our simulation.

REFERENCE

[1] R. H. Akbani, S. Patel, and D. C. Jinwala, "DoS attacks in mobile ad hoc Networks: A survey," in Proc. 2nd Int. Meeting ACCT, Rohtak, Haryana, India, 2012, pp. 535–541.

[2] K. Al Agha, M.-H. Bertin, T. Dang, A. Guitton, P. Minet, T. Val, and J.-B Viollet, "Which wireless technology for industrial wireless sensor networks? The development of OCARI technol," IEEE Trans. Ind. Electron., vol. 56, no. 10, pp. 4266–4278, Oct. 2009.

[3] T. Anantvalee and J. Wu, "A Survey on Intrusion Detection in Mobile Ad Hoc Networks," in Wireless/Mobile Security. New York: Springer-Verlag, 2008.

[4] Ashish Kumar, Vidya Kadam, Subodh Kumar, Shital Pawar, "An Acknowledgement – Based Approach for the Detection of Routing Misbehavior in MANETS" International Journal of advances in Embedded Systems, vol.1, Issue.1, 2011.

[5] V. C. Gungor and G. P. Hancke, "Industrial wireless sensor networks: Challenges, design principles, and technical approach," IEEE Trans. Ind.Electron., vol. 56, no. 10, pp. 4258–4265, Oct. 2009.

[6] Jun Yao, Salil S. Kanhere,, "Improving QoS in High-Speed Mobility Using Bandwidth Maps,"ieee transaction On mobile computing, vol. 11, no. 4, April 2008.

[7] N. Kang, E. Shakshuki, and T. Sheltami, "Detecting misbehaving nodes In MANETs," in Proc. 12th Int. Conf. iiWAS, Paris, France, Nov. 8–10,2010, pp. 216–222.

[8] Liqun Hou and Neil W. Bergmann, "Novel Industrial Wireless Sensor Networks for Machine Condition Monitoring and Fault Diagnosis," IEEE Trans. Ind. Electron., vol. 61, no. 10, pp. 4266–4278, Oct. 2012.

[9] J. G. Rocha, L. M. Goncalves, P. F. Rocha, M. P. Silva, and S. Lanceros-Mendez, "Energy harvesting from piezoelectric materials fully integrated in footwear," *IEEE* Trans. Ind. Electron. vol. 57, no. 3, pp. 813–819,Mar. 2010.

[10]T. Sheltami, A. Al-Roubaiey, E. Shakshuki, and A. Mahmoud, "Video Transmission enhancement in presence of misbehaving nodes in MANETs,"Int. J. Multimedia Syst., vol. 15, no. 5, pp. 273–282, Oct. 2009.

[11] A. Singh, M. Maheshwari and N. Kumar. "Security and Trust Management in MANET", in Communications in Computer and Information Science, vol. 147, part 3, pp. 384-387. Springer, 2011.